

**POLYMERISATION OF CYCLODEXTRINS AND MULTIWALLED CARBON
NANOTUBES FOR USE IN WATER PURIFICATION**

BY

KETULO LACKSON SALIPIRA

Dissertation:-

Submitted in fulfilment of the requirement for the degree of

MASTER OF TECHNOLOGY

in

Chemistry

in the

FACULTY OF SCIENCE

at the

UNIVERSITY OF JOHANNESBURG

Supervisor : Dr B B Mamba

Co-supervisor: Dr R W Krause

Co-supervisor: Mr S H Durbach

November 2006

DECLARATION

I hereby declare that this dissertation, which I submit for the qualification of

Master of Technology in Chemistry

to the University of Johannesburg, Department of Chemical Technology is, apart from the recognized assistance of my supervisors, my own work and has not previously been submitted to any other institution before for a research diploma or degree.

_____ on this _____ day of _____
Candidate

_____ on this _____ day of _____
Supervisor

_____ on this _____ day of _____
Co-supervisor

_____ on this _____ day of _____
Co-supervisor

DEDICATION

I dedicate this work to my wife Ellen, my children (Francis, Flora, Paul and Nyasha), my mother Emily and my late father, Lackson Salipira.

ACKNOWLEDGEMENTS

I wish to sincerely acknowledge the people and organisations listed below for their valuable contribution towards the success of this project:

- ❖ Dr B.B. Mamba, Dr R.W. Krause, Dr T.J. Malefetse and Mr S.H. Durbach (my supervisors) for the moral and technical support.

- ❖ Fellow students (Makhotso M. Khitsane, Edward Nxumalo, Soraya Malinga, Thabile Manyatsi, Thobile Dlamini, Phathu Letsoalo, Thembinkosi Ndzimandze, Mphilisi Mahlambi, Sikulungile Mkhize, Sandile, Heena, Armstrong and all I might have forgotten) for the company and support.

- ❖ Sabelo D Mhlanga of University of Witwatersrand, School of Chemistry, for help with DSC and TGA analysis.

- ❖ Mr Abe Seema of the University of Witwatersrand, Biology Department, Microscopy Unit, for help with TEM and SEM analysis.

- ❖ The University of Johannesburg and National Research Foundation (NRF) for the financial support.

- ❖ Special thanks are due to my wife and parents for their support during the period of my study. May the Lord God reward you for all you have done.

- ❖ Finally I wish to thank The Lord Almighty who has made it possible for me to come this far. To Him be the glory and honour.

PRESENTATIONS AND PUBLICATIONS

The work presented in this dissertation has been published and submitted in part to peer-reviewed journals and presented in conferences as shown below.

Conference presentations

1. Salipira K.L., Mamba B. B., Krause R. W., Malefetse T.J., Durbach S.H. *Cyclodextrin polyurethanes with carbon nanotubes for the removal of organic pollutants*. Oral presentation, International Congress of Nanotechnology (ICNT), San Francisco, USA. 30 October - 4 November 2005.
2. Salipira K. L., Mamba B. B., Krause R. W., Malefetse T.J., Durbach S.H. *Cyclodextrin polyurethanes with carbon nanotubes for the removal of organic pollutants*. Poster presentation, International Congress of Nanotechnology (ICNT), San Francisco, USA. 30 October - 4 November 2005.
3. Rui W.M. Krause, Bhekie B. Mamba and Ketulo Salipira. *Water Treatment by combination of iron nanoparticles and cyclodextrin polymers*. Oral presentation, 10th Annual Green Chemistry and Engineering Conference, Capital Hilton, Washington, DC, USA. 26-30 June 2006.
4. B.B. Mamba, R.W. Krause. T.J. Malefetse, S. Durbach, K.L. Salipira. *Cyclodextrin polyurethanes polymerized with multiwalled carbon nanotubes for the removal of organic pollutants in water*. Oral presentation, 2nd Water Research Showcase, University of Pretoria. 6 October, 2006.

5. B.B. Mamba, R.W. Krause, T.J. Malefetse, S.H Durbach, K.L. Salipira. *Cyclodextrin polyurethanes polymerized with multiwalled carbon nanotubes for the removal of organic pollutants in water*. Oral presentation, SACI, University of Kwazulu Natal, Durban, 3-8 December 2006.

Publications

1. Salipira K. L., Mamba B. B., Krause R. W., Malefetse T. J., Durbach S. H. *Cyclodextrin polyurethanes with carbon nanotubes for the removal of organic pollutants*. International Congress of Nanotechnology (ICNT) Proceedings, 2005.
2. Salipira K.L., Mamba B. B., Krause R. W., Malefetse T. J., Durbach S. H. *Carbon nanotubes and cyclodextrin polymers to remove organic pollutants*. Environmental Chemistry Letters (2006). Published online.
3. B.B. Mamba, R.W. Krause, T.J. Malefetse, S. Durbach, L.M. Cele, K.L. Salipira. *Cyclodextrin polyurethanes polymerized with multiwalled carbon nanotubes for the removal of organic pollutants in water*. Submitted for publication, Water and Environmental Journal.
4. B.B. Mamba, R.W. Krause, T.J. Malefetse, S. Durbach, L.M. Cele, K.L. Salipira. *Cyclodextrin polyurethanes polymerized with multiwalled carbon nanotubes: synthesis and characterization*. In preparation for submission to Macromolecules.

ABSTRACT

Organic compounds are some of the major pollutants of water worldwide. They can be toxic or carcinogenic even at low concentrations. The non-reactivity of these species makes it difficult to destroy or remove them from water using the current treatment techniques such as chlorination, activated carbon (AC) or zeolites filtration and reverse osmosis. This is particularly true when pollutants are present at parts per billion (ppb) levels or lower. Reasonably inexpensive yet effective methods for the removal of these organic pollutants to below ppb levels are therefore required.

Insoluble cyclodextrin polymers have demonstrated the ability to remove organic species from water. However, they are only effective at low concentration levels of organic pollutant (ppb level). In addition, the structural integrity of these polymers may somewhat be compromised after prolonged use. Multiwalled carbon nanotubes (MWNTs) have also been reported to efficiently absorb some organic molecules such as dioxins and polychlorinated dibenzo-furans, but large quantities of high purity MWNTs are currently too expensive to be used exclusively in water treatment.

This project featured an investigation into the use of cross-linked β -cyclodextrin polyurethanes copolymerized with functionalized MWNTs as absorbents for organic pollutants. It is not known yet whether these polymers remove organic pollutants by absorption, adsorption or both until characterization using techniques such as circular dichroism is performed. The term absorption will be used in this dissertation. A summary of our findings is presented as follows:

- ❖ Multiwalled carbon nanotubes were synthesized using the nebulized spray pyrolysis technique. The MWNTs were obtained in high yields with an average of 0.76 g per run.

- ❖ Acid functionalization using a mixture of sulphuric and nitric acids successfully introduced the -COOH and -OH groups onto the walls of the nanotubes. This was evident from a comparative study of the functionalized and unfunctionalized MWNTs using infrared spectroscopy.
- ❖ Further evidence to the success of this functionalization was obtained by Raman analysis of the functionalized MWNTs. This characterization confirmed that there was a relative increase in the intensity ratio of the disordered peak, D, after functionalization. This increase was attributed to a change in the MWNT structure due to the introduction of the -COOH and -OH groups onto the walls of the nanotube.
- ❖ B-cyclodextrin (β -CD) polymers containing functionalized MWNTs were successfully prepared using the bifunctional linkers, hexamethylene diisocyanate (HMDI) and toluene 2,4-diisocyanate (TDI). These polymers were prepared in relatively high yields.
- ❖ Scanning electron microscopy (SEM) analyses of the polymers showed that the surface of the polymers resembled those of a sponge. However, this was only pronounced for the native β -CD/HMDI (without MWNTs) and 1% MWNTs (β -CD/HMDI) polymers. The sponginess of the polymers diminished with an increase in the percent loading of the MWNTs. It is not clear at this stage if this was a processing phenomenon or a function of the incorporated MWNTs.
- ❖ Characterization of the polymers using the Brunauer-Emmett-Teller (BET) technique showed that incorporation of MWNTs at 1 to 5% loading generally increased the surface area of the native polymers. For example, the surface area increased from 2.52 m²/g for the native CD/HMDI polymers to 6.82 m²/g for a 1% MWNT (CD/HMDI) polymer.

- ❖ Thermal gravimetric analyses (TGA) and differential scanning calorimetry (DSC) results demonstrated that inclusion of MWNTs to the native β -CD polymers improved their thermal stability. This was probably attributed to the high degree of cross-linking of the polymers after the incorporation of 1 to 5% functionalized MWNT. On the other hand, the TGA analysis showed that incorporation of MWNTs slowed the decomposition process of the native β -CD polymers. This further confirmed the assertion that the MWNTs increased the stability of the native polymers.
- ❖ Polymers containing MWNTs showed an outstanding performance in their ability to remove *p*-nitrophenol and trichloroethylene in model water samples. These novel polymers were able to remove *p*-nitrophenol present at concentration levels of 10 mg/L with an absorption efficiency of 99% compared to granular activated carbon and native cyclodextrin polymer that removed only 49 and 62% of the pollutant respectively.
- ❖ These novel polymers have also demonstrated the ability to remove trichloroethylene to non-detectable levels (detection limit <0.01ppb) as compared to 55 and 70% removal when granular activated carbon and native cyclodextrin polymers respectively, were used in the same application.
- ❖ Recycling studies using *p*-nitrophenol have shown that polymers containing MWNTs could be regenerated up to twenty-five times while still maintaining a high absorption efficiency. The average removal was 98% for polymers containing MWNTs while native β -CD polymers removed an average of 56% from a 10 mg/L *p*-nitrophenol solution.
- ❖ Incorporation of MWNTs to the native β -CD polymers increased the structural stability of the polymer. This was evident when polymers with

MWNTs lost only 5% of the initial mass after nine cycles compared to the native β -CD polymers that had lost 17% of its mass after nine cycles.

In summary, this study yielded useful results that may have an impact in future water treatment applications.

TABLE OF CONTENTS

	<u>Page Number</u>
Declaration	i
Dedication	ii
Acknowledgement	iii
Presentations and publications	iv
Abstract	vi
Table of contents	x
List of figures	xv
List of tables	xviii
List of abbreviations	xix
CHAPTER ONE	
INTRODUCTION	1
1.1 Background	1
1.2 Justification	2
1.3 Objectives	2
1.4 Outline of the dissertation	3
CHAPTER TWO	
LITERATURE REVIEW	5
2.1 Introduction	5
2.2 Selected types of organic contaminants	5
2.2.1 Dioxins	5
2.2.2 Endocrine disrupting compounds (EDCs)	6
2.2.3 Natural organic matter (NOM)	7
2.2.4 Drinking water disinfection by-products	7

2.2.5	Polyaromatic hydrocarbons (PAHs)	8
2.2.6	Polychlorinated biphenyls (PCBs)	9
2.2.7	Non aqueous phase liquids (NAPLs)	10
2.2.7.1	Dense non-aqueous phase liquids (DNAPLs)	11
2.2.7.2	Light non aqueous phase liquids (LNAPLs)	12
2.3	Current water treatment methods	12
2.4	Carbon nanotubes	13
2.4.1	Introduction	13
2.4.2	Synthesis of carbon nanotubes	14
2.4.2.1	Catalytic chemical vapour deposition	14
2.4.2.2	Laser ablation method	14
2.4.2.3	Arc-discharge method	14
2.4.2.4	Nebulized spray pyrolysis	15
2.4.3	Carbon nanotube purification	16
2.4.4	Potential application of carbon nanotubes	16
2.4.5	Functionalization of carbon nanotubes	17
2.5	Cyclodextrins (CDs)	17
2.5.1	Structure of cyclodextrins	18
2.5.2	Cyclodextrin inclusion chemistry	20
2.5.3	Reactivity of CDs	20
2.5.4	Cyclodextrin nanoporous polymers	21
2.6	Summary	22

CHAPTER THREE

EXPERIMENTAL METHODS 23

3.1	Introduction	23
3.2	Chemicals and materials	23
3.3	General experimental and characterization techniques	23
3.3.1	Nebulized spray pyrolysis	23
3.3.1.1	Synthesis of MWNTs using nebulized spray pyrolysis	23

3.3.2	Commercial multiwalled nanotubes	24
3.3.3	Transmission electron microscopy	25
3.3.3.1	Sample preparation and analysis using TEM	25
3.3.4	Functionalization of MWNTs	26
3.3.5	Solubility tests of functionalized MWNTS	27
3.3.6	Infrared spectroscopy	28
3.3.7	Raman spectroscopy	29
3.3.8	Polymerization of functionalized MWNTs with CD	29
3.3.9	Scanning electron microscopy	30
3.3.10	Brunauer-Emmett-Teller (BET) analysis	31
3.3.11	Differential scanning calorimetry	31
3.3.12	Thermal gravimetric analysis (TGA)	32
3.3.13	Trichloroethylene absorption tests	32
3.3.14	GC-MS analysis	34
3.3.15	Procedure for removal of <i>p</i> -nitrophenol using polymers	35
3.3.16	Analysis of <i>p</i> -nitrophenol using UV-Visible spectroscopy	36
3.3.17	Recycling tests for polymers	37

CHAPTER FOUR

RESULTS AND DISCUSSION 38

4.1	Introduction	38
4.2	Synthesis of MWNTs by nebulized spray pyrolysis	38
4.3	Functionalization of MWNTs	39
4.4	Transmission electron micrographs of raw commercial and NSP CNTs	40
4.5	Transmission electron micrographs of functionalized commercial and synthesized nanotubes	42
4.6	Solubility tests of functionalized MWNTs	43
4.7	Characterization of MWNTs by IR spectroscopy	45
4.8	Raman spectroscopy	48

4.9	Polymerization of β -CD with carbon nanotubes	50
4.10	Physical properties of the β -CD and nanotube polymers	54
4.11	Characterization of polymers using infrared spectroscopy (IR)	55
4.12	Characterization of polymers by scanning electron microscopy	56
4.13	BET analysis of the polymers	60
4.14	Thermal analysis of the polymers	62
4.14.1	Differential scanning calorimetry analysis of polymers	62
4.14.2	Thermal gravimetric analysis	63
4.15	Comparison of polymers on the absorption of <i>p</i> -nitrophenol	64
4.16	Comparison of absorption efficiencies of polymers prepared from commercial and NSP MWNTs	67
4.17	Absorption tests of polymers incorporated with carbon nanofibers	68
4.18	Comparison of <i>p</i> -nitrophenol absorption with time	69
4.19	Gas Chromatography-Mass Spectrometry (GC-MS) analysis for trichloroethylene (TCE) absorption	71
4.20	Recycling tests of polymers	75

CHAPTER FIVE

CONCLUSIONS AND RECOMMENDATIONS 80

5.1	Conclusions	80
5.2	Recommendations for further work	83

APPENDICES 85

Appendix A		86
Preparation of trichloroethylene standards		

Appendix B	
List of selected priority organic pollutants	87
Appendix C	88
Selected IR spectra of MWNT incorporated β -CD polymers	
<i>References</i>	90

LIST OF FIGURES

<u>Figure</u>	<u>Description</u>	<u>Page Number</u>
Figure 2.1:	Structures of dioxins	6
Figure 2.2:	Structures of poly-aromatic hydrocarbons	8
Figure 2.3:	Structures of polychlorinated biphenyls	10
Figure 2.4:	Structure of trichloroethylene	11
Figure 2.5:	Structures of carbon nanotubes	13
Figure 2.6:	1,4-Linkage between glucose units	18
Figure 2.7:	Schematic representation of cyclodextrin units	18
Figure 2.8:	Schematic representation of inner and outer CD surfaces	19
Figure 2.9:	Schematic representation of host-guest complex formation	20
Figure 3.1:	Schematic diagram for producing MWNTs by NSP	24
Figure 3.2:	Structure of carbon nanofiber	27
Figure 3.3	Demonstration of SPE technique	34
Figure 4.1a:	Raw Commercial MWNTs	40
Figure 4.1b:	Raw NSP MWNTs	41
Figure 4.1c:	NSP MWNTs functionalized at 45-50 ⁰ C	42
Figure 4.1d:	NSP MWNTs functionalized by reflux at 95 ⁰ C	42
Figure 4.2a:	Picture of functionalized and raw MWNTs mixed with water	43
Figure 4.2b:	Picture of functionalized and unfunctionalized MWNTs suspended in DMF	44
Figure 4.3a:	IR spectrum of NSP MWNTs before functionalization	45
Figure 4.3b:	IR spectrum of NSP MWNTs after functionalization	46
Figure 4.4a:	IR spectrum of raw commercial MWNTs	47
Figure 4.4b:	IR spectrum of functionalized commercial MWNTs	47
Figure 4.5a:	Comparison of Raman spectra of functionalized and unfunctionalized lab-synthesized MWNTs	48

Figure 4.5b: Raman spectra of raw and functionalized commercial MWNTs	49
Figure 4.6a: IR spectrum of HMDI showing isocyanate band at start of reaction	51
Figure 4.6b: IR spectrum of HMDI showing disappearance of isocyanate band at end of reaction	51
Figure 4.7a: IR spectrum showing reduction of isocyanate band during MWNTs polymerization	52
Figure 4.7b: IR spectrum showing disappearance of isocyanate band during MWNTs polymerization	53
Figure 4.8: IR spectrum of polymerized nanotubes	54
Figure 4.9a: IR spectrum of a 1% MWNT (β -CD/HMDI) polymer	55
Figure 4.9b: IR spectrum of a 1% MWNT (β -CD/TDI) polymer	56
Figure 4.10a: SEM of native β -CD/HMDI polymer	57
Figure 4.10b: SEM of 1% MWNT (β -CD/HMDI) polymer	57
Figure 4.10c: SEM of 3% MWNT (β -CD/HMDI) polymer	58
Figure 4.10d: SEM of 4% MWCNT (β -CD/HMDI) polymer	58
Figure 4.10e: SEM of 5% MWCNT (β -CD/HMDI) polymer	58
Figure 4.11a: SEM of a 1% MCNT (β -CD/TDI) polymer	59
Figure 4.11b: SEM of a 2% MWNT (β -CD/TDI) polymer	59
Figure 4.11c: SEM of a 3% MWNT (β -CD/TDI) polymer	60
Figure 4.12: DSC curves of native and nanotube included polymers	62
Figure 4.13: Superimposed TGA graphs of native β -CD/HMDI polymer, 1% MWNT (β -CD/HMDI) polymer and 5% MWNT (β -CD/HMDI) polymer	63
Figure 4.14: Removal of <i>p</i> -nitrophenol from water by HMDI polymers with time.	70
Figure 4.15a: GC-MS chromatogram of 50 μ g/L TCE before contact with polymer	71

Figure 4.15b: GC-MS chromatogram of 50 $\mu\text{g/L}$ TCE after passing through a 1% MWNT ($\beta\text{-CD/HMDI}$) polymer	72
Figure 4.15c: GC-MS chromatogram of 50 $\mu\text{g/L}$ TCE after passing through a 5% MWNT ($\beta\text{-CD/HMDI}$) polymer	72
Figure 4.16a: GC-MS chromatogram of TCE before contact with the polymers	73
Figure 4.16b: GC-MS chromatogram of residual TCE after passing through $\beta\text{-CD}$ polymer	74
Figure 4.16c: GC-MS chromatogram after passing through 5% MWNT ($\beta\text{-CD/HMDI}$) polymer	74
Figure 4.17a: Results of recycling of a 1% MWNT ($\beta\text{-CD/HMDI}$) polymer	75
Figure 4.17b: Results of recycling using $\beta\text{-CD/HMDI}$ polymer	76
Figure 4.18a: SEM of 1% MWCNT ($\beta\text{-CD/HMDI}$) polymer before recycling	77
Figure 4.18b: SEM of 1% MWCNT ($\beta\text{-CD/HMDI}$) polymer after recycling	77
Figure 4.19a: IR spectrum of a 1% MWNT ($\beta\text{-CD/HMDI}$) polymer after recycling	78
Figure 4.19b: IR spectrum of a 1% MWNT ($\beta\text{-CD/HMDI}$) polymer before recycling	78

LIST OF TABLES

<u>Table</u>	<u>Description</u>	<u>Page Number</u>
Table 2.1:	Physical characteristics of α -, β - and γ -cyclodextrins	19
Table 4.1:	Mass of synthesized MWNTS from the four runs	39
Table 4.2a:	Yield of MWNTs after reflux for 30 minutes at 95 ⁰ C	39
Table 4.2b:	Yield of MWNTs oxidized at 45-50 ⁰ C for 24 hrs	39
Table 4.3:	Physical properties of β -CD polymers	54
Table 4.4:	BET results for native and MWNT included polymers	60
Table 4.5:	Comparison of surface area versus percent <i>p</i> -nitrophenol absorbed	61
Table 4.6a:	Average <i>p</i> -nitrophenol removed by HMDI polymers	65
Table 4.6b:	Average <i>p</i> -nitrophenol absorbed by TDI polymers	65
Table 4.6c:	Comparison of surface area and absorption efficiency of the polymers	67
Table 4.7:	Absorption efficiencies of polymers containing commercial and NSP MWNTs	68
Table 4.8:	Comparison of absorption efficiencies between MWNT included polymers and CNFs included polymers	69

LIST OF ABBREVIATIONS

α -CD	Alpha Cyclodextrin
β -CD	Beta Cyclodextrin
γ -CD	Gamma Cyclodextrin
$\mu\text{g/L}$	Micrograms per litre
AC	Activated Carbon
b.p.	Boiling point
BET	Brunauer-Emmett-Teller
CCD	Charge coupled device
CDs	Cyclodextrins
CNFs	Carbon nanofibers
CNTs	Carbon nanotubes
CVD	Chemical vapour deposition
DBPs	Disinfection By-Products
DCM	Dichloromethane
DNAPLs	Dense Non-Aqueous Phase Liquids
DSC	Differential Scanning Calorimetry
EDCs	Endocrine disrupting compounds
EEC	European economic community
EI	Electron Ionization
FTIR	Fourier transform Infrared spectrometer
GAC	Granular Activated Carbon
GC/MS	Gas Chromatography / Mass Spectrometry
HMDI	Hexamethylene diisocyanate
IARC	International agency for research on cancer
IR	Infra red
KHz	Kilo-Hertz
LLE	Liquid-liquid Extraction
LNAPLs	Light non-aqueous phase liquids

m.p.	Melting point
m/z	Mass to charge ratio
mbar	millibars
MHz	Mega-Hertz
MWNTs	Multiwalled carbon nanotubes
NOM	Natural Organic Matter
NSP	nebulized spray pyrolysis
PAHs	Polyaromatic hydrocarbons
PCBs	Polychlorinated biphenyls
PCDD	Polychlorinated dibenzo- <i>p</i> -dioxin
POP	Persistent Organic Pollutant
ppb	Parts per billion
ppt	Parts per trillion
Rpm	Revolutions per minute
SEM	Scanning Electron Microscopy
SPE	Solid Phase Extraction
SWNTs	Singlewalled carbon nanotubes
TCDDs	Tetrachlorodibenzo- <i>p</i> -dioxine
TCE	Trichloroethylene
TDI	Toluene 2,6-diisocyanate
TEM	Transmission electron microscopy
TGA	Thermogravimetric Analysis
THMs	Trihalomethanes
TIC	Total Ion Count
WRC	Water Research Commission

CHAPTER ONE

INTRODUCTION

1.1 Background

Water is an important resource for our daily activities such that there would be no life without it. It is used in a number of household applications and in industrial processes. This resource is however being constantly polluted with organic and inorganic compounds from domestic utilization, manufacturing industries and also run off from rain.¹

Methods of water treatment are available but their effectiveness is limited by diversity and varying chemical properties of the organic contaminants. Very often these methods lack the ability to remove organic contaminants to safe levels.² For example, many organic species are inert and cannot be removed using ion exchange methods. Reverse osmosis fails to completely remove the organic pollutants because the membrane is not perfectly semi-permeable and a small concentration leaks through the permeate side. Activated carbon (AC) on the other hand fails to reduce many organic pollutants to parts per billion levels. Therefore, a reasonably cheap but effective method for the removal of these organic pollutants to the safe and acceptable levels of parts per billion (ppb) is required.

Insoluble cyclodextrin polyurethanes have demonstrated the ability to remove organic species from water to the desired low concentration levels of parts per billion (ppb). Further studies of these polymers at our laboratories demonstrated that they can be recycled at least eighteen times while still maintaining high absorption efficiency although they lose some polymer material.³ Two limitations of these nanoporous polymers (called native CD polymers) are that they are effective at low organic contaminant concentration only and that the polymer seems to break down during recycling.

Multiwalled carbon nanotubes are very strong and have been reported to efficiently absorb dioxins, polychlorinated dibenzo-furans, biphenyls and some

inorganic pollutants.⁴ However, they are too expensive to be used on their own for this application.

1.2 Justification

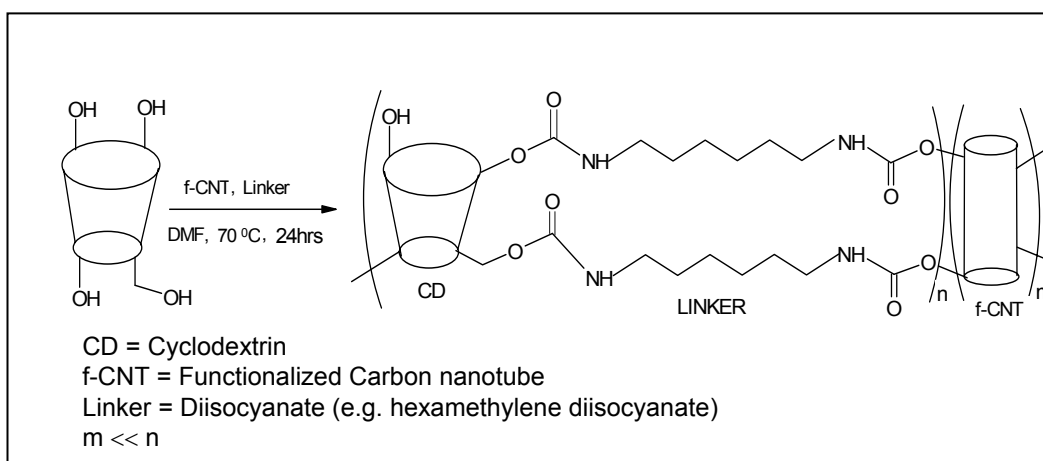
Although cyclodextrin polyurethanes are effective at low organic concentrations, the structural integrity of the polymers is somewhat compromised after prolonged recycling. Carbon nanotubes are ideal materials to use in combination with cyclodextrin polymers. Individually they have demonstrated an ability to absorb specific organic molecules at higher concentrations while remaining chemically inert. In addition, the strength given to the polymer by the carbon nanotubes⁵ is expected to provide the added stability over existing polymers. It is envisaged that this will be particularly useful in the improvement of recycling and recovery of the material. Addition of carbon nanotubes to the polymers is also expected to improve the absorption efficiency even when the organic pollutant is present at higher concentrations.

1.3 Objectives

The objectives of this research are as follows:

- To synthesize cyclodextrin polyurethanes containing a small percentage of carbon nanotubes using bifunctional linkers such as hexamethylene diisocyanate (HMDI) and toluene-2,4-diisocyanate (TDI).
- To characterise the new nanotube containing polymers using techniques such as thermal analysis, infrared spectroscopy (IR) and scanning electron microscopy (SEM).
- To test the ability of these polymers in the removal of organic pollutants and to conduct recyclability tests of the nanotubes incorporated polymers.

A schematic diagram of the polymerization of CNTs with selected linkers is shown in **Scheme 1.1**.



Scheme 1.1: Polymerization reaction of cyclodextrin and carbon nanotubes

1.4 Outline of the dissertation

Below is an outline of this dissertation:

Chapter 1 (Introduction):- This chapter gives an insight into the research work that was carried out and its importance. Also presented in this chapter is the problem statement, the justification and the objectives of the study.

Chapter 2 (Literature review):- In this chapter, a review of literature pertaining to carbon nanotubes and cyclodextrins, and their applications to water related problems is presented.

Chapter 3 (Methodology):- All analytical methods and experimental procedures that were used in this research project are discussed in detail in this chapter.

Chapter 4 (Results and discussion):- Results obtained from this study are presented in this chapter, together with their interpretation.

Chapter 5 (Conclusions):- Based on the results obtained with respect to the initial objectives and hypothesis, conclusions are drawn and highlighted in this last and final chapter.

Selected chromatograms and spectral data appear in the **Appendix section**.

CHAPTER TWO

LITERATURE REVIEW

2.1 Introduction

This chapter focuses on the literature associated with organic pollutants. The presence and dangers of these pollutants and techniques aimed at removing them from the water systems are discussed. The chapter concludes with a review of carbon nanotubes and cyclodextrins, which form the core of this study.

2.2 Selected types of organic contaminants

Some organic pollutants are classified as persistent organic pollutants (POPs). They are classified as POPs because they are highly stable and degrade slowly in the environment.⁶ This class of organic compounds pose the greatest risk to human health since they linger in the environment and they can cause damage even when present at low concentrations. Recent suggestions are that their effects may even be felt through several generations. Examples of POPs include endocrine disrupting compounds such as trichloroethylene and tetrachloroethylene, pentachlorophenol and dioxins. Endocrine disrupting compounds are particularly important because they are usually toxic to human beings and animals by mimicking naturally produced hormones or interfering with the normal functions and development of organisms.⁷ A selected number of organic compounds together with their toxic properties are discussed briefly in the following subsections.

2.2.1 Dioxins

Polychlorinated dibenzo-*p*-dioxins (PCDDs), commonly called dioxins, are organic compounds that consist of two benzene rings joined together by two oxygen atoms (**Figure 2.1**). They are introduced to the environment by, among other methods, combustion of organic compounds associated with municipal, medical and hazardous waste.⁸ Recently, some dioxins were

reported to be produced by photodegradation of triclosan, a common disinfectant used in anti-bacterial soap.⁹

Dioxins are fat soluble and can bioaccumulate in organisms *via* dietary sources.¹⁰ Thus, their presence in the environment even at low concentrations is a cause for concern due to their relative toxic potency to humans and the environment. Tetrachlorodibenzo-*p*-dioxin (2,3,7,8-TCDD) is known to be the most toxic dioxin.¹¹ Besides causing cancer, TCDD also affects the immune systems and male reproductive system. Structures of some common dioxins are shown in **Figure 2.1**. One promising way of removing these dioxins is by use of MWNTs. It is for this reason that MWNTs were selected as polymer composites for use in the removal of organic pollutants including dioxin.

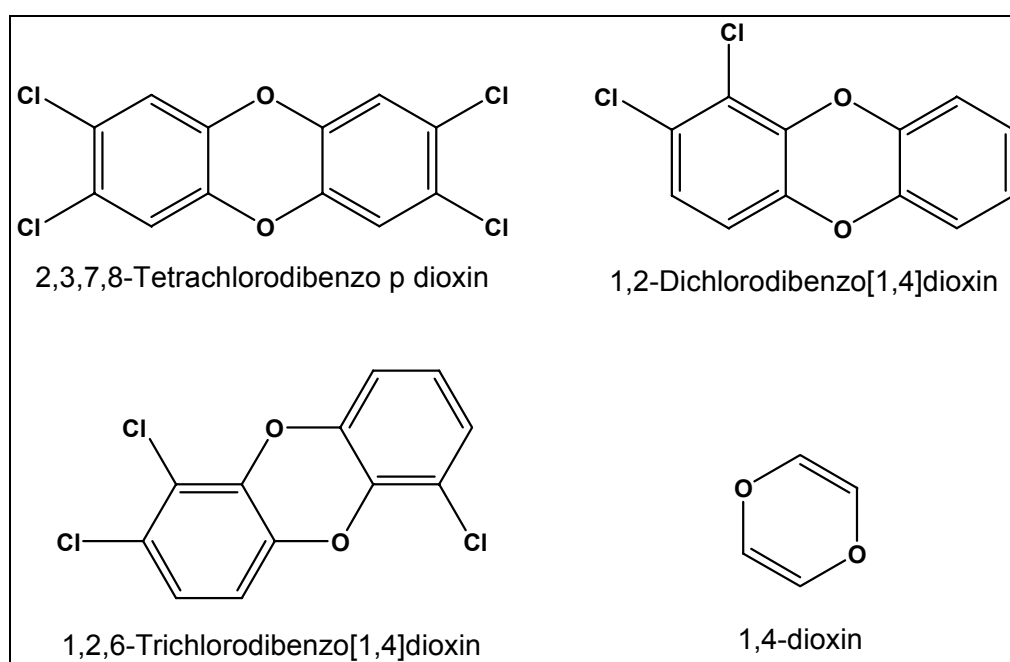


Figure 2.1: Structures of dioxins

2.2.2 Endocrine disrupting compounds (EDCs)

The endocrine system is one of the important systems in the human and animal bodies. Through an array of hormones, the endocrine system is responsible for the control of development, growth, reproduction and behaviour of organisms.¹² Some synthetic and natural chemical compounds tend to mimic these body hormones and in the process disrupt the normal

functions of the body, hence the name “endocrine disrupting compounds” (EDCs). Endocrine disrupting compounds can interfere with a growing foetus when present even in small quantities and they have also been associated with interrupted sexual behaviour and a decrease in the quality of the human semen.^{13,14,15} Some examples of the EDCs are alkyl phenols, chlorinated hydrocarbons, polychlorinated biphenyls (PCBs), bisphenol A, dioxins, natural and synthetic steroid sex hormones.^{14,15} The New Water Framework Directive (76/464/EEC)¹⁶ considers most of the EDCs as priority contaminants. Endocrine disrupting compounds are wide-spread in water systems in South Africa¹⁷ and they have been highlighted as one of the country’s priority organic pollutants. Therefore, measures to eliminate them from these systems are highly sought.

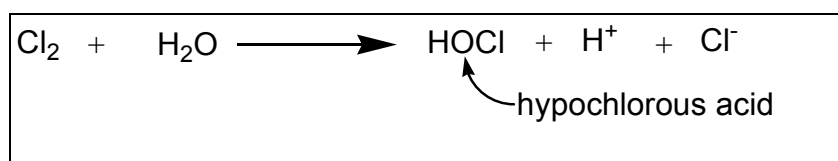
2.2.3 Natural organic matter (NOM)

Natural organic matter (NOM) is a name given to a group of substances that emanate from decomposing plants and animals.¹⁸ They are found in waters such as lakes, rivers and man-made water reservoirs. Examples of NOM include amino acids, organic acids and the humic substances (fulvic acid, humic acid and humin).^{14,19} Most of these humic substances have high molecular weights and, as a result have low solubility in water. Besides causing bad odour, taste and imparting colour to drinking water, NOM can also regulate the formation of disinfection by-products (DBPs).²⁰ This is discussed in more detail in the next section. The removal of NOM from drinking water sources is therefore necessary to prevent the formation of colour, odour, persistent and toxic organic contaminants.

2.2.4 Drinking water disinfection by-products

These are by-products formed during the reaction of NOM and disinfection chemicals, including chlorine. Chlorine is a popular and common disinfectant used by water service providers. In particular, chlorine is used to destroy microorganisms such as bacteria that may cause water borne diseases.²¹ During the treatment process, chlorine reacts with water to form hypochlorous acid (**Scheme 2.1**). The hypochlorous acid further reacts with the NOM such

as humic and fluvic acids to form DBPs. Some examples of DBPs are CHCl_3 , CH_2Cl_2 and CHBr_3 .^{14,21} These halogenated compounds are not readily degradable and are also known to cause liver damage and cancer. Dibromomethane for example is known to be extremely genotoxic to mammalian cells. It is therefore crucial that NOM and its by-products be removed from drinking water.



Scheme 2.1: Formation of hypochlorous acid

2.2.5 Polyaromatic hydrocarbons (PAHs)

Polyaromatic hydrocarbons (PAHs), also known as polynuclear aromatic hydrocarbons, are a group of organic compounds containing more than one aromatic ring fused together (**Figure 2.2**).²² They consist of only carbon and hydrogen atoms and have no other functional groups.^{22,23} Sources of PAHs are crude oil and coal. They can also be produced from incomplete combustion of organic compounds during household and industrial processes.^{22,23} PAHs are relatively insoluble in water but dissolve completely in fats and oils, a property that can allow for bioaccumulation in some organisms. Examples of PAHs include naphthalene, pyrene, benzo[a]pyrene, benzo[a]anthracene and chrysene, just to mention a few (**Figure 2.2**). PAHs have a wide range of exposure routes which include inhalation, ingestion and dermal contact.²⁴ They can be quickly absorbed by the gastro-intestinal tract of mammals. In the body, PAHs are often metabolised to epoxides which, being mutagenic and carcinogenic, can cause liver, intestine, pancreas and skin cancer. PAHs have also shown considerable toxicity to fish in the presence of UV radiation due to their tendency to undergo photooxidation when exposed to UV light. Some examples of PAHs that have been found to cause cancer and mutagenicity in human beings are benzo[a]pyrene and

benzo[a]anthracene. Efforts should therefore be made to remove PAHs from the drinking water.

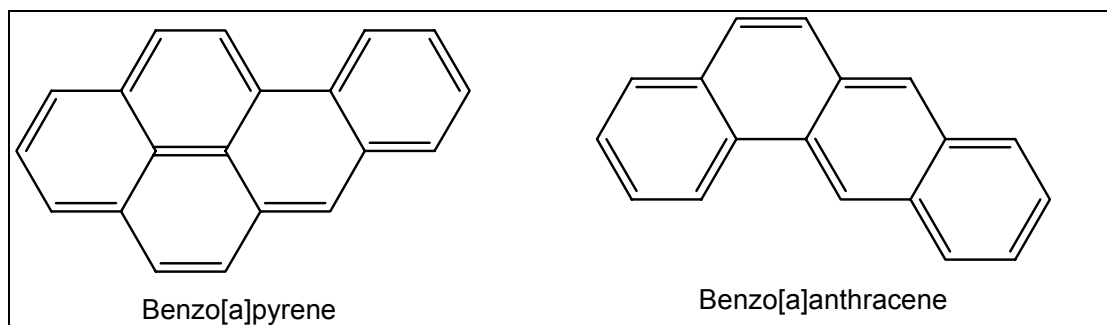


Figure 2.2: Structures of polycyclic aromatic hydrocarbons

2.2.6 Polychlorinated biphenyls (PCBs)

Polychlorinated biphenyls (PCBs) are environmental pollutants often found in water systems. They are produced by progressive chlorination of biphenyls and they exist as a mixture of varying chlorine substituents.²⁵ PCBs are used as ingredients in hydraulic fluids, plasticizers, adhesives and transformers.²⁵ Typical structures of PCBs are depicted in **Figure 2.3**. These compounds are highly lipophilic and do not degrade easily when in the environment.²⁶ PCBs are toxic organic contaminants and are persistent in the environment. Their high solubility in fats enables them to bioaccumulate high up in the food chain. This may cause the pollutant to exceed toxic threshold levels and hence trigger biochemical and physiological disturbances in the body.⁶

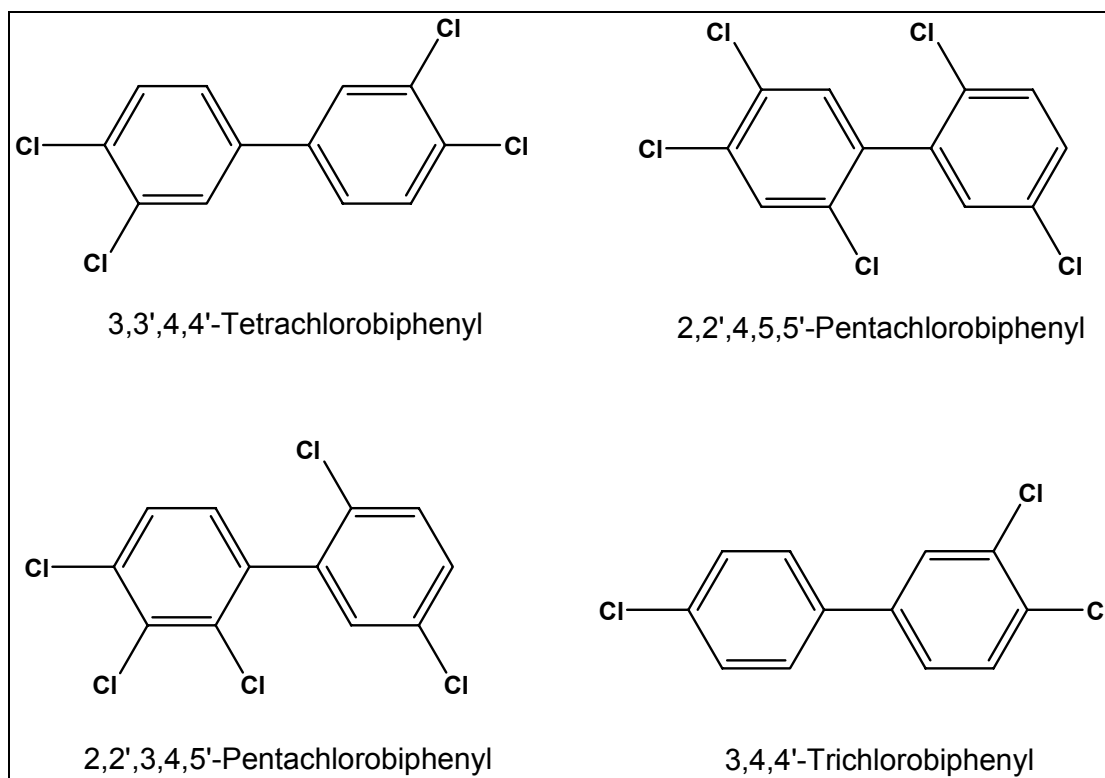


Figure 2.3: Structures of polychlorinated biphenyls

Some PCBs portray endocrine disrupting activity by mimicking sex steroid hormones thus causing developmental disorders and carcinogenesis.²⁷ Long time exposure or ingestion of PCBs has also been reported to cause liver damage and cancer. In aquatic animals, PCBs reduce the percentage of eggs that can hatch and even the survival of the hatchlings, resulting in the extinction of some species.²⁸ Although their use is slowly declining, PCBs are still a threat because of their toxicity especially when they are not detected and removed from the water supplies.

2.2.7 **Non-aqueous phase liquids (NAPLs)**

Pollutants can also be classified by their density, which helps to determine appropriate treatment regimes. There are two types of non-aqueous phase liquids namely: dense non-aqueous phase liquids (DNAPLs) and light non-aqueous phase liquids (LNAPLs).

2.2.7.1 Dense non-aqueous phase liquids (DNAPLs)

Dense non-aqueous phase liquids are a group of organic compounds that are denser than water. These compounds whether completely insoluble or slightly soluble in water, often form a separate layer below the water surface and eventually percolate through the soil and find their way into the underground water system. Due to their wide spread use, DNAPLs are major sources of soil and groundwater contaminants.²⁹ Some DNAPLs pose a serious problem to human health and the environment due to their toxicity. Difficulties in removing these compounds from the environment create further complications.³⁰ Examples of DNAPLs (**Figure 2.4**) include polychlorinated biphenyl (PCBs), coal tar, fluorine, dichlorobenzene, tetrachloroethylene and trichloroethylene (TCE).³¹ TCE was chosen as a model pollutant because it is a DNAPL, an EDC and a chlorinated hydrocarbon. A discussion on the properties and effects of TCE to the environment are presented below.

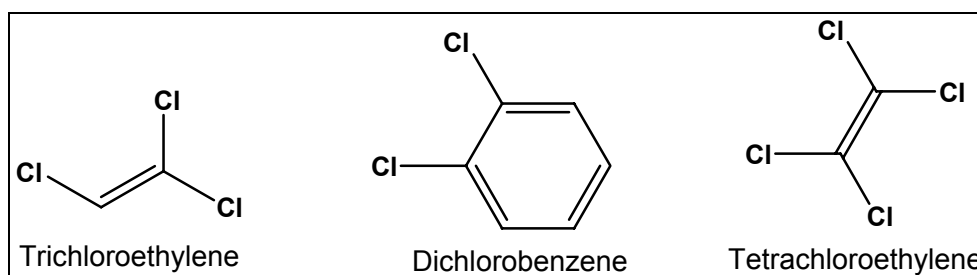


Figure 2.4: Structure of trichloroethylene

Trichloroethylene (TCE), also known as triclene or vitran (**Figure 2.4**), is a chlorinated aliphatic organic pollutant. It is a colourless and non-flammable liquid which is slightly soluble in water (1.07g/dm^3 at 20°C).³² It is denser than water (1.465 g/cm^3 at 20°C) and is classified as a DNAPL. Trichloroethylene is produced by, among other methods, direct chlorination of ethylene dichloride and it is used in the automotive industry as a solvent to remove grease, oils, fats and waxes from metals.³³ The textile industry uses TCE to scour cotton wool and other fabrics while the chemical industry uses TCE as starting material for the synthesis of other derivatives.

Due to its widespread use, TCE is a prevalent contaminant in most occupational environments. The effects of TCE exposure in humans have not been fully understood although some studies have linked TCE to health problems like cancer, spontaneous abortions and heart defects.³⁴ Exposure to high concentrations by inhalation results in central nervous system depression.³⁵ Laboratory tests on rats and mice have shown that TCE induces the formation of tumours in the lungs and liver. In a study in the USA, the presence of TCE in drinking water has been associated with the spread of leukaemia in women and children. Hence, the International Agency for Research on Cancer (IARC) has considered TCE as one of the probable carcinogens. The structure of TCE is shown in **Figure 2.4**.

2.2.7.2 Light non aqueous phase liquids

Unlike the DNAPLs, light non-aqueous phase liquids (LNAPLs) are less dense than water and therefore float on water. Their presence in water can cause adverse effects to humans and aquatic life as some have been confirmed to be carcinogenic. Benzene, toluene, xylenes and ethylene are examples of LNAPLs.³⁶ Some priority organic pollutants are listed in **Appendix B**.

2.3 Current water treatment methods

As mentioned earlier, there are currently a number of technologies used by municipalities and water service providers to remove organic pollutants from water. These include ion exchange, reverse osmosis, activated carbon and zeolites filtration. Unfortunately, these techniques are very expensive to use when removing organic compounds in water below regulatory approval i.e. ppb levels. Activated carbon and zeolites for example have limited affinity towards organic compounds and therefore fail to remove them to below required levels while reverse osmosis requires a lot of water and this makes the treatment technique expensive. The failure by most of these techniques to remove organic pollutants to the required levels is attributed to the diversity and varying chemical properties of the organic pollutants, most of which render these organic pollutants unreactive.

Carbon nanotubes and cyclodextrin polyurethanes have individually demonstrated the ability to remove organic contaminants from water, although neither are currently used for water treatment, partly because they have problems that limit their use individually. Since carbon nanotubes have been reported to absorb organic pollutants at high concentration, cyclodextrin polyurethanes containing a small percentage of carbon nanotubes were expected to absorb a wide range of organic pollutants, increase absorption efficiency and improve polymer strength. A discussion on nanotubes and cyclodextrin polyurethanes is presented in the following sections.

2.4 Carbon nanotubes

2.4.1 Introduction

Carbon nanotubes (CNTs) were discovered by Iijima³⁷ in 1991. They are hollow nano-sized tubes that resemble graphene sheet rolled into a tube.^{38,39} There are two main types of CNTs, namely: single-walled nanotubes (SWNTs) and multiwalled nanotubes (MWNTs). Single-walled nanotubes are only made up of one layer while MWNTs are made up of more than one layer that form concentric tubes. The structures of the two main types of nanotubes are shown in **Figure 2.5**.

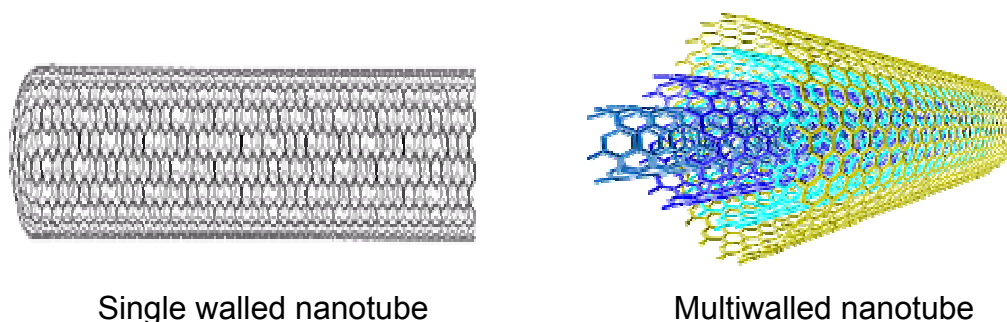


Figure 2.5: Structures of main types of carbon nanotubes⁴⁰

These nanotubes, have since their discovery attracted much attention from researchers because of their thermal, electrical, mechanical and adsorption properties.⁴¹ Long *et al* reported that MWNTs can efficiently remove dioxins and other related compounds more effectively than activated carbon.

2.4.2 Synthesis of carbon nanotubes

Carbon nanotubes are synthesized, by among others, the following four common methods: (1) Arc-discharge, (2) Catalytic Chemical Vapour Deposition (CVD), (3) Laser ablation⁴⁰ and (4) Nebulized Spray Pyrolysis (a form of CVD). These methods are discussed briefly and individually in the sections that follow.

2.4.2.1 Catalytic chemical vapour deposition

This method uses gases such as methane, carbon monoxide and acetylene as the source of carbon. The substrate containing the catalyst (Fe, Ni or Co) on which the nanotubes grow is placed in an oven or tube-furnace at 650 - 900⁰C. As the selected gas is passed through, it is converted into reactive carbon atoms which diffuse into the substrate. The carbon atoms then recombine and grow into nanotubes. This method, depending on the conditions, produces both SWNTs and MWNTs with yields ranging from 20-100%. However, carbon nanotubes prepared through this method do have amorphous carbon and catalyst metal particles and may require special treatment before the nanotubes are used.

2.4.2.2 Laser ablation method

The laser ablation method is similar to the arc-discharge (**Section 2.4.2.3**); both methods use graphite rods as the carbon source. There is, however, one difference between the two methods. While arc-discharge uses a high temperature to vaporize the positive graphite rod, the laser method employs a pulse or continuous laser to vaporize the graphite rod into carbon atoms. Singlewalled nanotubes are mostly produced by this method. This method is, however, expensive since it requires high power and expensive lasers.

2.4.2.3 Arc-discharge method

In this method, carbon nanotubes are produced by vaporization of graphite rods placed end to end in an arc-discharge chamber. The rods are usually separated by a distance of 1 mm in an enclosure or chamber filled either with

an inert gas such as helium or argon. Non-inert gases such as nitrogen and hydrogen can also be used.⁴² The chosen gas is generally regulated at low pressures between 50 and 700 mbar. Upon application of a direct current (50 to 100 A) driven by a direct voltage of 20 V, a high temperature arc-discharge is created between the two electrodes. This discharge vaporizes the positive carbon rod and the carbon vapour forms hot plasma, which is deposited on the negative electrode. The deposit eventually forms tubular structures called carbon nanotubes. Variation of temperature and pressure is believed to have an effect on the diameter of the tubes produced by this method.⁴³ Although the arc-discharge is considered as a simpler way of producing nanotubes, this technique produces a mixture of single and multiwalled nanotubes depending on the catalyst used. In addition, these nanotubes are often contaminated with amorphous carbon and catalytic metal particles. Hence, purification of CNTs before use is essential.

2.4.2.4 Nebulized spray pyrolysis

Nebulized spray pyrolysis (NSP) is one of the methods used in the synthesis of multiwalled nanotubes. It is a form of chemical vapour deposition method but the difference is in the introduction of the catalyst and carbon sources.⁴⁴ In NSP, the catalyst e.g. ferrocene is mixed together with a carbon source. The carbon source is normally a hydrocarbon solvent such as toluene or benzene.⁴⁵ The mixture is atomized to generate a spray by means of an ultrasonic atomizer at frequencies between 100 kHz and 10 MHz. This forms a spray which is carried through a heated quartz tube placed in the oven by an inert carrier gas such as argon. The advantage of this technique over the normal CVD method is that the nanotubes produced are well aligned and the diameter and quality of nanotubes can be controlled by varying synthesis parameters. Furthermore, the NSP produces nanotubes with little or no amorphous carbon impurities compared to ordinary CVD technique and other synthetic methods. It is also easy to scale up to industrial production. Considering all these attributes, it was considered worth doing a comparative study on the absorption efficiencies of polymers previously prepared by

incorporating multiwalled carbon nanotubes from CVD technique with those from NSP of ferrocene and toluene.

2.4.3 Carbon nanotube purification

Carbon nanotubes produced by CVD contain traces of metal catalysts such as Fe, Co and Ni.^{46,47} These need to be removed before nanotubes are used for any application. One method used for their purification is through thermal oxidation in air prior to the removal of the metal catalyst by sonication in hydrochloric acid.^{46,47} Alternatively, the carbon nanotubes can be heated under reflux in a sodium hydroxide solution for 2 days to remove the alumina support. Subsequent stirring in HCl for 5 hrs removes the metal catalyst.⁴⁸ These methods are harsh and do often introduce some functionality onto the CNTs.

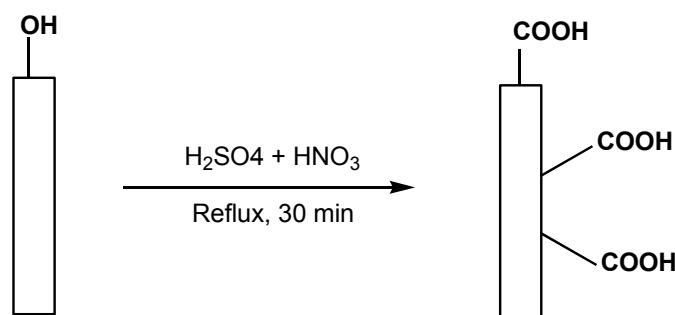
2.4.4 Potential application of carbon nanotubes

Carbon nanotubes have attracted huge interest from researchers since their discovery; they have been found to possess excellent thermal, mechanical and electrical properties. Extensive studies are underway to explore the use of nanotubes as nanosensors, electronic devices and gas storage devices. Studies have also been carried out on other applications such as the removal of dioxins from combustion compounds associated with municipal, medical and hazardous waste incinerators. Yang *et al* have also reported that MWNTs outclass activated carbon in the removal of dioxins and other related compounds such as polychlorinated dibenzo-furans and biphenyls from water. Based on this property, this research seeks to investigate the use of nanotubes as polymer composites for use in the absorption of organic pollutants in water. It has also been reported that MWNTs can improve structural stability especially when used as polymer reinforcements.^{49,50} It is therefore envisaged that inclusion of MWNTs to the native β -CD/HMDI polymers (without MWNTs) would increase polymer strength. Carbon nanotubes however require modification of their surfaces in order for them to be suited for such an application.

2.4.5 Functionalization of carbon nanotubes

Raw carbon nanotubes (both single and multiwalled) have very few functional groups. Most of the few functional groups that are present are as a result of the purification process imposed on the newly synthesized CNTs. The purification process is aimed at removing catalyst particles and amorphous carbon as discussed in **Sections 2.4.3**. Because of the few functional groups, CNTs are unreactive and hence, not suitable for direct use in various applications. It is therefore necessary to functionalize carbon nanotubes before they are used for most applications.

Several methods are used for the functionalization of carbon nanotubes. These include wet oxidation with a mixture of concentrated nitric and sulphuric acid, ball milling, and hydrothermal functionalization.^{46,47} In this study, acid functionalization (**Scheme 2.2**) was used. This process introduces the carboxyl and hydroxyl groups which would then take part in the polymerization of functionalized CNTs with cyclodextrin monomers using bifunctional linkers.



Scheme 2.2: Carbon nanotube functionalization procedure

2.5 Cyclodextrins

Cyclodextrins (CDs), discovered in 1891 by Villers,⁵¹ can be described as cyclic oligomers formed by the joining together of glucose units *via* α -1, 4-linkages.^{52,53} They are formed naturally through the hydrolysis of starch by the action of cycloglycosyl transferase (CGTase) and α -amylase bacteria. **Figure 2.6** demonstrates the α -1,4-linkage in CDs.

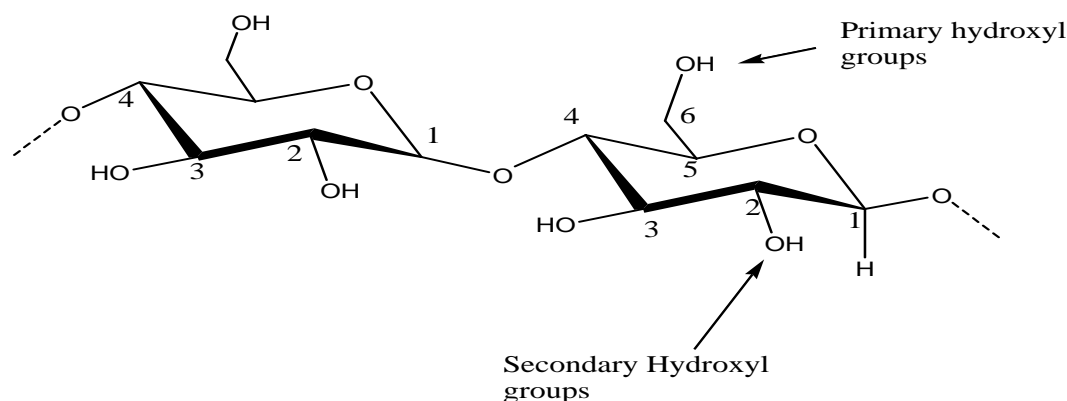


Figure 2.6: 1,4-Linkage between glucose units

2.5.1 Structure of cyclodextrins

Although CDs with between nine and fourteen glucopyranose units have been reported, there are three most common types of CDs on which a lot of research has been conducted.⁵⁴ These are alpha-CD (α -CD), beta-CD (β -CD) and gamma-CD (γ -CD). They comprise 6, 7, and 8 glucopyranose units, respectively. **Figure 2.7** is a diagrammatic representation of the α -, β - and γ -CDs.

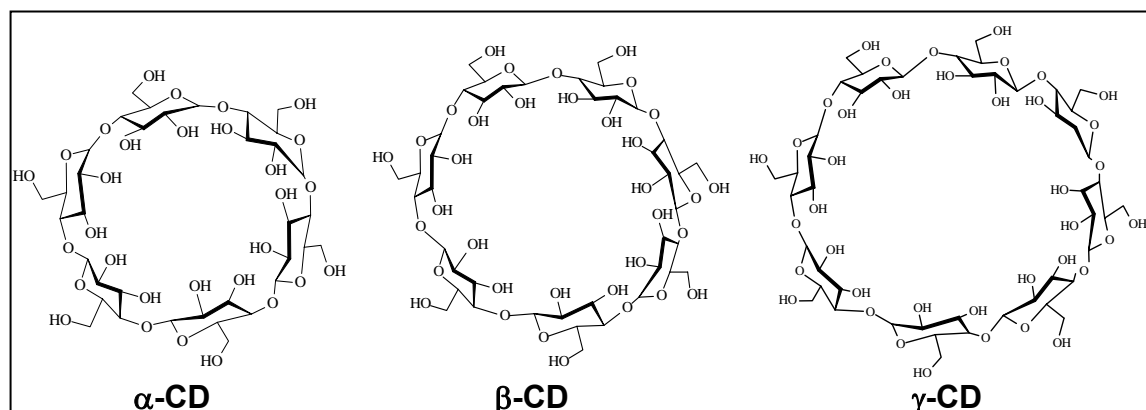


Figure 2.7: Diagrammatic representation of cyclodextrin units

The structure of cyclodextrins resembles that of a bottomless bucket with one end wider than the other. The narrow end is occupied by primary hydroxyl groups while the secondary groups occupy the wider end. These “buckets” have a depth of about 8 Å and a diameter of between 5-10 Å, depending on the number of glucose units forming the ring. The inner cavity of cyclodextrins is non-polar and hydrophobic while the exterior is hydrophilic. This

characteristic comes about because of the way the glucose units in a CD are arranged.⁵⁵ The inner cavity is occupied by hydrogen and carbon atoms, which accounts for the hydrophobicity of the interior cavity. The outer cavity is occupied by the primary and secondary hydroxyl groups; the presence of these OH groups gives the outer sphere its hydrophilic nature.^{55,56} **Figure 2.8** shows the schematic representation of the inner and outer surfaces of the CD. Physical properties of the α -, β -, and γ -CDs are summarised in **Table 2.1**.

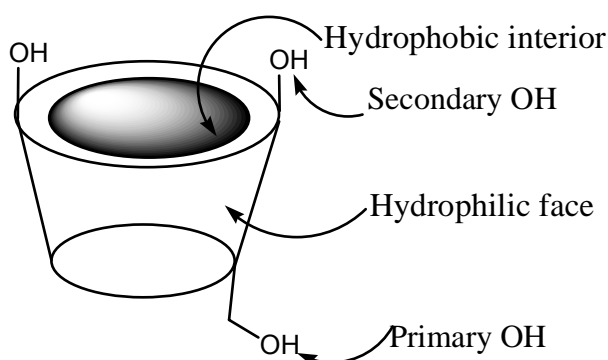


Figure 2.8: Schematic representation of inner and outer CD surfaces

Table 2.1: Physical characteristics of α -, β - and γ -cyclodextrins

Parameter	α -CD	β -CD	γ -CD
Number of glucose units	6	7	8
Molecular weight (g/mol)	972.85	1134.99	1297.14
Solubility in H ₂ O [g/cm ³]	14.5	1.85	23.2
Acid constant [pKa]	12.33	12.2	12.08
Inner diameter [nm]	0.45 - 0.57	0.62 - 0.78	0.79 - 0.95
Outer diameter [nm]	1.37	1.53	1.69
Height [nm]	0.79	0.79	0.79
Cavity volume [nm ³]	0.174	0.262	0.472

2.5.2 Cyclodextrin inclusion chemistry

The hydrophobic nature of CD cavities and the non-polar characteristics of most organic compounds allow for the hydrophobic-hydrophobic attraction between the CDs and the guest organic molecules that results in the formation of inclusion complexes. No covalent bonds are formed in the formation of these complexes; it is just an attraction between the guest and the host owing to their polarities.^{56,57} Other factors which play a role in the formation of inclusion complexes are the size of the guest molecule and the type of CD used. The α -, β - and γ -CDs have different cavity volumes (0.174, 0.262 and 0.472 nm³, respectively) and, as a result, would accommodate organic compounds of different sizes. **Figure 2.9** is a schematic representation of host-guest complex formation.

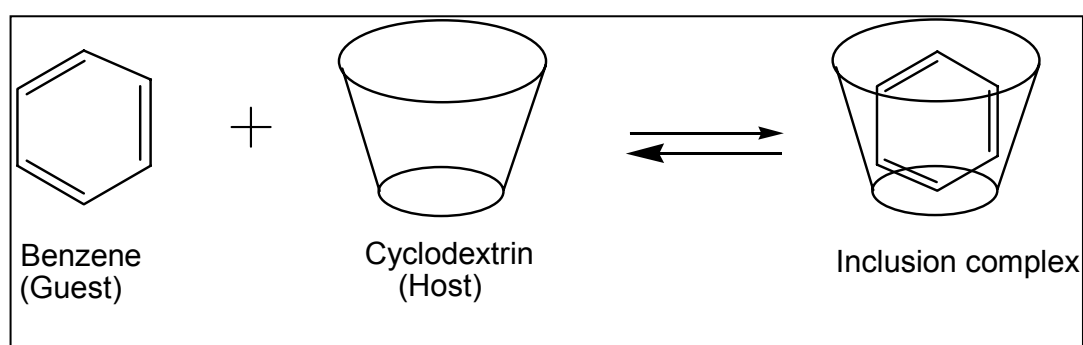


Figure 2.9: Schematic representation of host-guest complex formation

In spite of this good attribute, cyclodextrins are soluble in water. This property limits the direct use of CDs in the *removal* of organic contaminants from water. Hence, converting cyclodextrins to insoluble polymers while maintaining a high affinity for the organic compounds is desired if they are to be used in water treatment applications

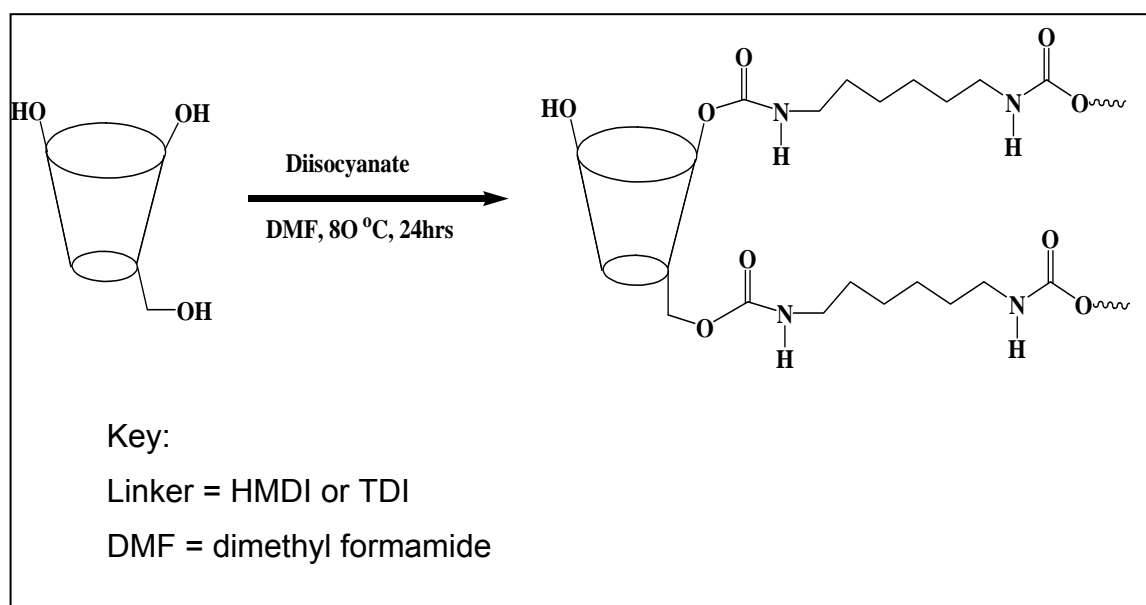
2.5.3 Reactivity of CD

The presence of hydroxyl groups on the exterior cavity of the CD makes them reactive. This may allow for the introduction of other groups by way of functionalizing or polymerizing the CD with other desired groups for specific applications. The secondary groups are situated on the wider end of the CD

cavity at carbons 2 and 3 while the primary is situated on carbon 6 at the narrow end of the cavity. The primary hydroxyl groups are the most accessible, hence often more reactive.

2.5.4 Cyclodextrin nanoporous polymers

As described in **Section 2.5.2**, CDs are soluble in water, a property that limits their direct use in water treatment exercises. Therefore, it is vital to convert these CDs to polymers that are insoluble in water. One way in which this can be done is to exploit the hydroxyl groups present on the CD ring, which can react with linkers. For instance, the polymerization of CD monomers with bifunctional linkers such as hexamethylene diisocyanate (HMDI) and 2, 4-toluene diisocyanate (TDI) in a 1:8 molar ratio of CD to linker can produce polymers, which are granular solids, powders or films. The final form of these polymers depends on the reaction conditions used during their preparation. Thus polymerization in this way results in the formation of highly cross-linked nanoporous materials consisting of a cyclodextrin moiety and the complementary bifunctional linker, as shown in **Scheme 2.3**.



Scheme 2.3: Polymerization of cyclodextrins with linker

2.6 Summary

From the literature cited in the preceding sections, it is clear that organic pollutants still pose a serious threat to human life and the environment in general. Their effects will become even more devastating if novel technologies that are capable of removing them in water systems to ppb levels are not developed. CD nanoporous polymers have demonstrated the ability to remove organic pollutants but their effectiveness has only been proven at very low concentration levels (ng/L). CNTs, on the other hand, have demonstrated an ability to remove dioxins, dibenzofurans and biphenyls better than the currently used activated carbon. However, CNTs are very expensive to be used independently for this application. It is anticipated that the incorporation of CNTs to the CD polymers could enhance the capacity of the CDs to remove a wide range of predominantly organic pollutants to acceptable levels.

CHAPTER THREE

EXPERIMENTAL METHODS

3.1 Introduction

Experimental techniques that were used in the execution of this research project are discussed in this chapter. Most of the techniques are standard and where necessary, modifications to these standard procedures were done in order to suit the application that was required.

3.2 Chemicals and materials

While most of the chemicals used in this project were of reagent grade, some were purified as required. Solvents obtained at high purity from suppliers were used as they were unless otherwise mentioned, or were dried and deoxygenated by distillation over sodium under argon gas. All reactions unless otherwise stated were performed under argon. Two types of multiwalled nanotubes were used in this study. The first was a commercial sample purchased from Sunnano Co Ltd while the other was synthesized in our laboratory by the nebulized spray pyrolysis technique.

3.3 General experimental and characterization techniques

In this section, methods that were used for producing nanotubes and characterizing the MWNT functionalized polymers are described.

3.3.1 Nebulized spray pyrolysis

This is a form of chemical vapour deposition for the synthesis of carbon nanotubes. A detailed procedure is described in 3.3.1.1 below.

3.3.1.1 Synthesis of MWNTs using nebulized spray pyrolysis

In a typical run, ferrocene (2 g) was mixed with toluene (50 cm³) by stirring with a glass rod in a beaker. The mixture was then nebulized by applying a high frequency ultrasonic signal (1.5 MHz) using a frequency controller. This

formed a spray that was carried through a quartz tube, 65 cm long with an internal diameter of 3 cm by inert argon gas. The carrier gas (argon) flow rate was measured to be 500 cm³ per minute. The temperature of the oven was maintained at 900°C for 45 minutes. After 45 minutes, the oven and the nebulizer were switched off. Carrier gas flow was maintained at a flow rate of 50-60 cm³ per minute until the oven temperature dropped to below 300°C to prevent the nanotubes from being oxidized by air. The synthesized carbon nanotubes were scraped from the walls of the quartz tube. The average yield was 1.7%. **Figure 3.1** shows the experimental set-up for the synthesis of MWNTs using NSP.

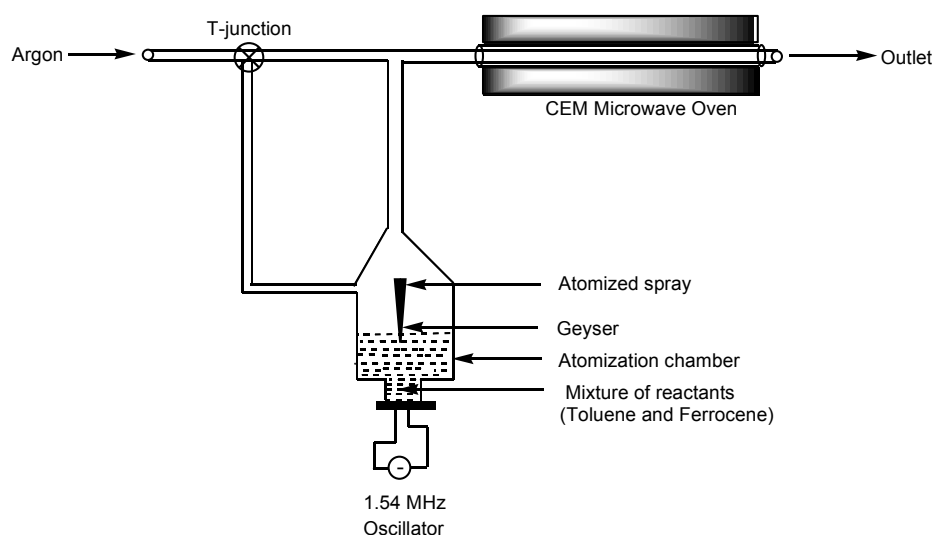


Figure 3.1: Schematic diagram for producing MWNTs NSP

3.3.2 Commercial multiwalled nanotubes

While the procedure used for the synthesis of the commercial nanotubes is not known, it is believed that they were produced by the CVD technique on a silica/alumina support using a metal catalyst.

To confirm the structure of the nanotubes formed, a sample was analysed using transmission electron microscopy (TEM), one of the techniques that is used to view nanotube structures. The principle and characterization procedures using TEM are described in the following section.

3.3.3 Transmission electron microscopy

Transmission electron microscopy (TEM) is a technique that is used to produce images of a sample by illuminating the sample (usually as a thin film) with a beam of electrons. Using TEM, it is possible to study the structure and other characteristics of the compound from the images produced. The beam of electrons is able to pass through the sample because the sample is thin and the transmitted electrons produce an image of the sample. Another advantage of TEM is that it produces a far better resolution compared to light microscopy thereby allowing detailed study and comparison of specimens. TEM is a useful tool and is being extensively used for the characterization of inorganic and organic nanomaterials.⁵⁸

In this study, TEM was used for the determining the general morphology, diameter and length of the MWNTs before and after functionalization.

3.3.3.1 Sample preparation and analysis using TEM

A small quantity of acid functionalised MWNTs[†] (both commercial and NSP MWNTs) was transferred into a plastic vial containing 5 cm³ of ethanol. The mixture was sonicated in a Bransonic ultrasonic bath (model 3510E-MT) for 10 minutes in order to achieve a homogeneous suspension. A drop of the nanotube suspension was spread onto a holey carbon copper grid (200 mesh) and allowed to dry. The grid was then mounted onto the exchange rod and placed into the chamber of the TEM (JEOL 100S) ready for viewing. The sample chamber was evacuated in order to prevent the air molecules from obstructing the movement of the electrons through the chamber to the specimen. Viewing of the specimen was done by following a few work-up procedures, such as the adjustment of the magnification, focus and the contrast. Results of these analyses are presented in **Chapter 4**. Scanning electron microscopy was also used to study the surface characteristics of the nanotubes and details of the procedure are presented in **Section 3.3.8**.

[†] Functionalization discussed in 2.4.5 and 3.3.3

Pristine (as synthesized before purification) CNTs have limited functionality and may not be directly used for various applications such as polymer composites. Modification of their surfaces by means of functionalization with a mixture of acids was employed. The procedure for the acid functionalization is reported below.

3.3.4 Functionalization of MWNTs

Nebulized spray pyrolysis MWNTs (1.00 g) were functionalized in a mixture of nitric acid (10 cm³) and sulphuric acid (30 cm³) at 50⁰C for 24 hrs specifically to introduce hydroxyl and carboxylic acid groups.⁵⁹ The mixture was diluted with distilled water (about 500 cm³) and carbon nanotubes (CNTs) were filtered off using Teflon or Nylon filter paper (pore size 0.45 μm, diameter 47 mm). This was followed by subsequent washing with distilled water until the pH was almost 7.0. The CNTs were later dried under vacuum at room temperature followed by characterization using infrared (IR) spectroscopy, Raman spectroscopy and transmission electron microscopy (TEM). A similar procedure was used to functionalize commercial MWNTs. The functionalized MWNTs were also tested for their solubility in water and organic solvents. The procedure for these tests is given in **Section 3.3.4**.

Carbon nanofibers (CNFs) are similar to carbon nanotubes but they are not carbon nanotubes. They are both hollow and are prepared by changing some conditions used in MWNTs synthesis.⁶⁰ However, the difference is that CNFs have one layer of graphite which is coated by a layer of amorphous carbon. **Figure 3.2** illustrates the structure of carbon nanofibers.

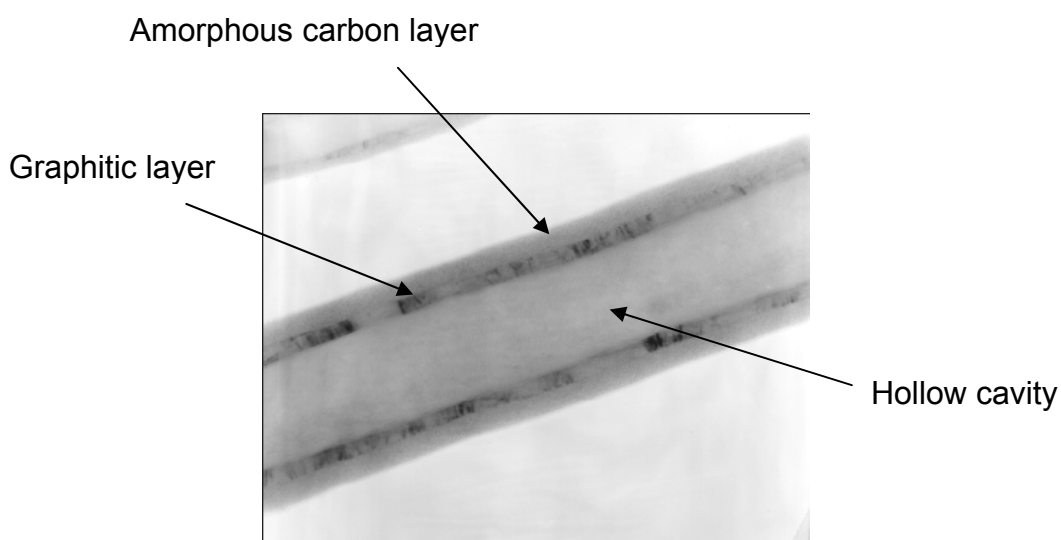


Figure 3.2: Structure of carbon nanofiber

Carbon nanofibers (HTF-150FF-HHT), purchased from Electrovac, Austria were functionalized in a mixture of nitric (10 cm^3) and sulphuric acid (30 cm^3) in order to introduce carboxylic groups to the walls of the nanofibres (CNF). 1.00 g of sample was oxidized at 50°C for 24 hrs. The acid was diluted with distilled water and nanofibres were filtered off using Teflon or Nylon filter paper (pore size $0.45 \mu\text{m}$, diameter 47 mm). This was followed by washing with distilled water until the pH was almost seven.

3.3.5 Solubility tests of functionalized MWNTS

Solubility of MWNTs in water and organic solvents is a desired property because it enhances homogeneous dispersion of MWNTs in a polymer. Solubility tests were performed on MWNTs (commercial and NSP MWNTs) before and after functionalization using water and DMF. In this study, DMF was used as solvent for polymerization reactions.

Raw MWNTs (0.05 g) were placed in a vial containing water (10 cm^3). Similarly, functionalized MWNTs (0.05 g) were charged in a vial containing DMF (10 cm^3). The vials were put in the ultrasonic bath for 15 minutes after which the mixture was allowed to stand on the bench for up to five months. Functionalized MWNTs were found to be soluble in water and DMF. In order

to confirm if the CNTs had dissolved, the mixtures were centrifuged for ten minutes at 10000 revolutions per minute (rpm) using a Jouan BR 4 centrifuge. The temperature during centrifugation was maintained at 20⁰C. Detailed results are presented in **Chapter 4**.

3.3.6 Infrared spectroscopy

Infrared spectroscopy is one of the important tools used to identify functional groups that are present in a molecule or compound.^{61,62} Unlike ultra-violet (UV) visible radiation that cause excitation of valence electrons in the molecule, infra-red radiation, because of its low energy, only causes electrons (bonds) within the molecule to vibrate. These vibrations, depending on the type of atoms may be symmetrical or asymmetrical about a central point. The asymmetrical vibrations usually create a dipole within the molecule. Molecules with these types of vibrations absorb IR radiation and are therefore called IR active. Due to differences in bond energies, different functional groups will absorb IR radiation at different wavelengths (energies). This makes it possible to identify various functional groups present in the system as each functional group would absorb at a particular wavelength. IR spectroscopy was used to confirm the introduction of functional groups onto the CNTs and to further verify if polymerization between the MWNTs, CDs and the bifunctional linkers had occurred.

One percent by weight of unfunctionalized and functionalized MWNTs (for both commercial and NSP MWNTs) were thoroughly mixed with potassium bromide (KBr) in a porcelain mortar. The mixture was pressed using a mechanical press to form a transparent pellet, which was then mounted in the sample holder of a MIDAC FT-IR (model 4000). The spectrum was collected as percent transmittance of the IR radiation. Sixteen scans were collected per spectrum and the resolution was 4 cm⁻¹. Results of this characterization are presented in **Chapter 4**.

3.3.7 Raman spectroscopy

This is a spectroscopic technique similar to Infrared Spectroscopy. However, in this technique, the change in vibrational motion must change the polarizability of the molecule if the molecule is to be Raman active. Raman spectroscopy is commonly used in chemistry and other branches of science to study vibrational, rotational and other low frequency modes in a sample.⁶³ It takes advantage of the differences in vibrational modes and energies of molecular bonds. Upon illuminating the sample with a laser beam, usually in the visible, near infrared or near ultraviolet range, some monochromatic radiation is scattered. The scattered light has different energies depending on the types of molecular vibrations present in the sample. This backscattering allows one to determine structure and quality of the sample.

Raman spectroscopy of functionalized and unfunctionalized MWNTs (for both commercial and NSP MWNTs) was performed at University of Witwatersrand, in the School of Physics, at the Raman and Luminescence Laboratory, using a Jobin-Yvon T64000 Raman spectrometer. It was operated in a single spectrograph mode with 600 lines/mm grating. A 514.5 nm line of the argon ion laser was used as the excitation source. Laser light was focused onto the sample using 20x objective lens of an Olympus microscope. Laser power at the sample was kept at 1.2 mW or less in order to avoid local heating. The scattered light was collected in a backscattering configuration and was detected using a nitrogen cooled charge coupled detector (CCD) detector. A discussion of the results is given in **Chapter 4**.

After confirming the introduction of –COOH and –OH which are required for the polymerization process, the functionalized MWNTs were polymerized with β -CDs.

3.3.8 Polymerization of functionalized MWNTs with CD

β -CD (2.00 g) was dissolved in DMF (18 cm³) by stirring. To the solution of β -CD was added functionalized MWNTs (0.02 g, 0.04 g, 0.06 g, 0.08 g and 0.10 g). These masses represented a 1, 2, 3, 4 and 5 percent nanotube

composition with respect to the mass of CD, respectively. The nanotubes were previously suspended in DMF (2 cm³) by sonication for 15 minutes using a Selecta ultrasonic bath. The mixture of the cyclodextrin and carbon nanotubes was heated to about 70⁰C at constant stirring. This was followed by drop-wise addition of the bifunctional linkers such as HMDI and TDI. The amount of linker used for polymerization was 7.5 mole equivalents to CD. The temperature for the reaction was maintained at 70⁰C under an inert atmosphere for 24 hrs. The polymer formed was precipitated by addition of acetone (~100 cm³) and then filtered off to remove the solvent. This was followed by subsequent washing to remove residual DMF and the remaining acetone was removed under vacuum. The polymers produced were characterized by IR spectroscopy. IR ν (cm⁻¹): C-H (2930), C=C (1616), C=O (1703), O-H (3397), C-O (1030). IR results gave an insight into the functional groups that were present in the polymers and the information obtained helped to determine whether the intended reaction had been achieved. The procedure for obtaining the IR spectrum of the polymers has been described in **Section 3.3.5**. These polymers were further characterized using SEM, BET, DSC and TGA in order to elucidate their surface and thermal properties.

3.3.9 Scanning electron microscopy

Scanning Electron Microscopy (SEM) is a technique that is used to study the surface morphology or physical nature of solids.⁶⁴ SEM uses a beam of electrons to scan the surface of the sample. As the surface is being scanned, a variation in electron current which is dependent on the surface properties occurs. This variation is depicted as a map showing the surface morphology of the sample.

Unfunctionalized and functionalized MWNTs (for both commercial and NSP MWNTs) were mounted on aluminium stubs with carbon tape or cadmium graphite as a support. The samples were then coated with gold in order to make the surface conductive. Viewing of the specimen was performed by mounting the sample into a SEM (JEOL, JSM-840 Scanning microscope) and irradiating the specimen with a beam of electrons. This was followed by

proper magnification and focussing for better viewing of the specimen's surface.

3.3.10 Brunauer-Emmett-Teller analysis

Branauer-Emmett-Teller (BET) is a technique that is used to measure the surface area and pore volume of a sample. These parameters are important, for example, when studying absorption properties of polymers because they may have an effect on the absorption efficiency of the polymers. BET analysis of the synthesized polymers was performed at the School of Chemistry, at the University of Witwatersrand using an automated gas adsorption analyzer (Trister 3000 V6.05).

Samples were degassed with N₂ gas using Micromeritics Degassing System at 150⁰C prior to the determination of their surface areas and pore volumes. Degassing was done for twelve hours at the N₂ flow rate of 60 cm³/min. Analysis was performed under liquid nitrogen.

3.3.11 Differential scanning calorimetry

Differential scanning calorimetry (DSC) is an instrumental technique that measures the amount of heat absorbed or released by the sample as it is heated, cooled or kept isothermal.⁶⁵ It is also used to determine melting point, crystallization time and temperature, glass transitions and thermal stability of a sample. DSC is therefore widely used in polymer science for characterization of melting, crystallization and glass transitions temperatures of the polymers. Hence, it was used in this application to determine the above physical properties.

A Mettler Toledo (DSC 822^e) was used to analyze the polymers. 1% MWNT (β -CD/HMDI) polymer (5.210 mg) was weighed using an aluminium pan (40 μ L). The sample was then heated from 30⁰C to 400⁰C at a heating rate of 5⁰C per minute. Nitrogen was used as the purge gas at a flow rate of approximately 30 cm³/min. Native β -CD/HMDI and 5% MWNT (β -CD/HMDI)

polymers (4.2500 mg and 5.2000 mg, respectively) were comparatively analysed using the same parameters and procedure.

3.3.12 Thermal gravimetric analysis

Thermal gravimetric analysis (TGA) is an instrumental technique that is used to study the changes in a sample with variations in heating temperature.⁶⁶ The changes are often associated with weight loss resulting from the dehydration or decomposition of the sample with increase in temperature. The weight loss can also arise from the formation of physical and chemical bonds that may lead to the release of volatile compounds. TGA comprises an automatic balance onto which the sample is loaded. The pan containing the sample is encapsulated by a furnace, which is heated from room temperature to about 1000⁰C at a heating rate of 5 – 10⁰C per minute. The sample is continuously weighed while being heated to higher temperatures and the mass loss is recorded as a function of temperature.

About 0.01 g of polymers were analyzed using a Pyris 1 Thermal gravimetric analyzer. Samples were heated from ambient temperature to 1000⁰C under nitrogen to provide inert conditions. The heating rate was set at 10⁰C per minute. The weight loss with increase in temperature was automatically recorded. With reference to the graphs from the different polymer compositions, a comparative study on the stability was made and results are presented in chapter 4.

After characterization, the polymers were tested for their ability to remove selected organic pollutants in water. Techniques and procedures used in these absorption tests are discussed in the next sections of this chapter.

3.3.13. Trichloroethylene absorption tests

Trichloroethylene (TCE) was selected as one of the organic pollutants for the absorption tests of the polymers because it is one of the priority organic pollutants. It is also known to affect the endocrine system. Trichloroethylene

(6.84 μl) was transferred into a volumetric flask (100 cm^3) containing 10 cm^3 dichloromethane. The volume was then made up to the mark with further addition of dichloromethane. This solution had a concentration of 100 mg/dm^3 . Serial dilutions were then performed in order to prepare standard solutions with the following concentrations: 10, 1.00, 0.10, 0.01 and 0.001 mg/dm^3 . These standards were used in determining residual TCE in the spiked water samples. Dichloromethane was used as a solvent because TCE is soluble in DCM. In addition DCM is insoluble in water; hence it was used to extract the residual TCE after passing through the polymer. Calculation procedures used in the preparation of these standards are shown in the **Appendix A**. Trichloroethylene concentrations of 10 mg/dm^3 and $50\text{ }\mu\text{g/L}$ in water were used as working concentrations in this study.

Polymers (0.03 g) were packed into an empty C8 solid phase cartridge whose measurements were 6 cm long and 1 cm wide. The cartridge was then connected to a filtering unit comprising a separating funnel and a receiving flask. The receiving flask was connected to a water aspirator in order to create a vacuum that would enhance steady and controlled flow of the water samples through the polymer. The polymers were conditioned by passing through distilled water (5 cm^3) after which spiked water samples (30 cm^3 , 10 mg/dm^3 and $10\text{ }\mu\text{g/L}$ TCE) were passed through the polymers. The water sample flow rate was maintained at between 3 and 5 cm^3 per minute. Residual TCE was extracted from the eluent with dichloromethane (15 cm^3) using the liquid-liquid extraction technique. **Figure 3.3** shows the set-up for the solid phase extraction technique that was employed.

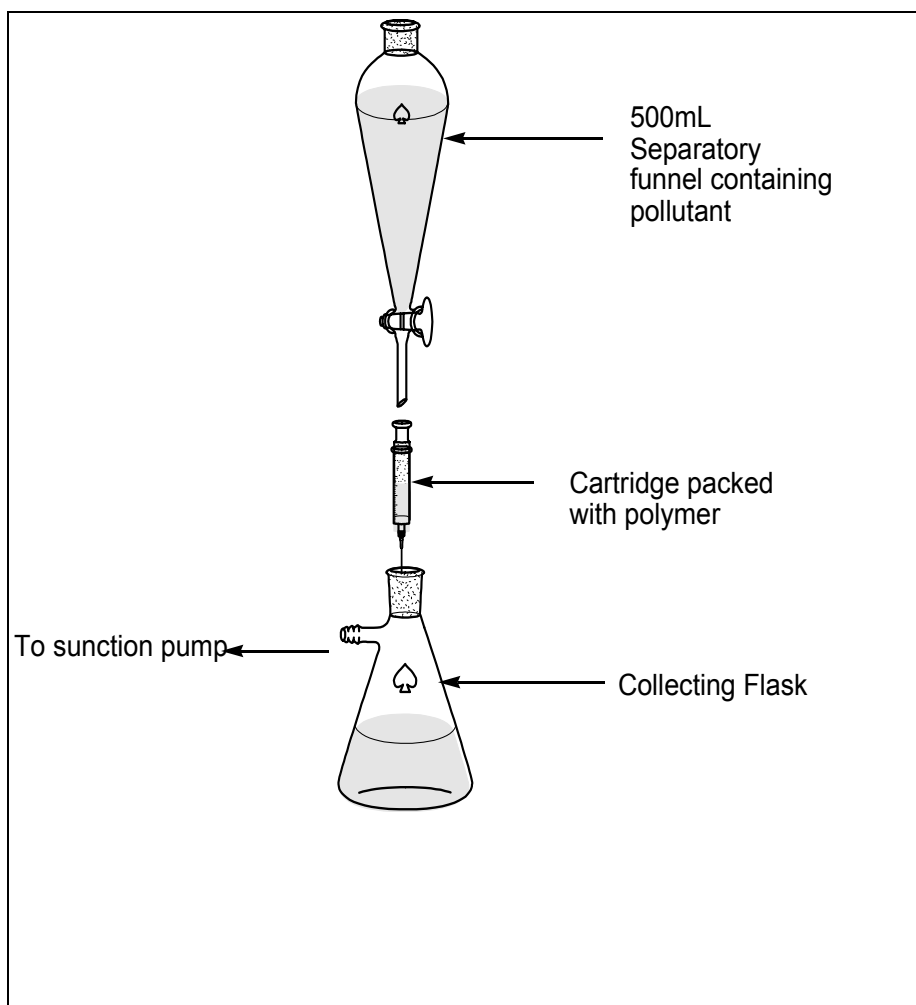


Figure 3.3: Demonstration of SPE technique⁶⁷

Samples were then analyzed using GC-MS as described in the following section.

3.3.14 GC-MS analysis

The popularity of GC-MS comes as a result of its ability to separate mixtures into individual components while identify them and even providing qualitative and quantitative information.⁶⁸ This is possible because of the combination of the two principle components of this instrument namely the Gas Chromatography (GC) and the Mass Spectrometry (MS). The GC separates a mixture of compounds into individual components while the MS identifies and quantifies them based on their mass to charge ratios. It also has an

advantage in that colourless samples that cannot be analysed by other techniques such as UV-Visible spectroscopy, whose principle technique is based on colour absorption can be easily analyzed. The GC-MS also has lower detection limits compared to UV-Visible spectroscopy, which allows this technique to quantify even smaller concentrations in samples.

Upon injection, the sample is vaporised and then swept through the column by the mobile phase. Components of the sample are separated based on their interaction with the stationary phase which is normally a liquid coated on a solid support. These separated components are ionised into charged molecules or fragments. These fragments move on to the detector where they are recorded as mass to charge ratios.

DCM extract (1 μL) was injected into the GC-MS in order to determine the residual TCE in the sample after passing through the polymer. Similarly 1 μL of a standard sample solution (30 cm^3 , 10 mg/L and extracted with DCM (15 cm^3) but not passed through the polymers was also injected into the GC-MS. The instrumental technique was adapted from the analysis of semi-volatiles from the Environmental Protection Agency (EPA 8270). The analyses were carried out using a Varian 3800 capillary Gas Chromatography (GC) coupled with a Saturn 2000 ion-trap mass spectrometer. The GC was equipped with a Chrompack CP Sil 8 CB, 30 $\text{m} \times 0.25$ mm capillary column with an internal diameter of 0.25 μm . The chromatographic conditions were 1 μL splitless injection at 75 $^{\circ}\text{C}$ using helium (He) as a carrier gas at 0.9 cm^3/min constant gas flow. The oven temperature settings were: 30 $^{\circ}\text{C}$ (held for 2 min) to 75 $^{\circ}\text{C}$ at 10 $^{\circ}\text{C}/\text{min}$, to 100 $^{\circ}\text{C}$ at 20 $^{\circ}\text{C}/\text{min}$ (held for 4 min).

3.3.15 Procedure for removal of *p*-nitrophenol using polymers

p-Nitrophenol (0.01 g) was transferred into a volumetric flask (1000 cm^3) containing a little water. The mixture was shaken until the *p*-nitrophenol was dissolved and the volume was made up to 1000 cm^3 with distilled water. This preparation had a concentration of 10 mg/dm^3 . *p*-Nitrophenol (30 cm^3 , 10 mg/dm^3) was passed through the polymers (0.30 g) that were packed in a

small cartridge. The column was previously conditioned by passing through water (5 cm^3). The flow rate for *p*-nitrophenol was approximately 3 to 5 cm^3 per minute. The eluent was collected and absorbances were measured using a UV-Visible spectrophotometer. The extraction technique is demonstrated in **Figure 3.2**.

p-Nitrophenol (0.05g,) was then dissolved in water (100 cm^3). This was quantitatively transferred to a one litre volumetric flask and then made up to the mark with distilled water. The concentration of this solution was 50 mg/dm^3 . From this solution, a series of standards (5, 10, 15 and 20 mg/dm^3 *p*-nitrophenol in water) were prepared. These standards were used to calculate residual *p*-nitrophenol concentration before and after passing through polymer.

3.3.16 Analysis of *p*-nitrophenol using UV-Visible spectroscopy

UV-Visible spectroscopy is an instrumental technique used for qualitative and quantitative determination of some organic and inorganic compounds in a solution. Compounds analyzed by this technique must have chromophores (covalently bonded but unsaturated groups such as NO_2 , $\text{C}=\text{C}$ and $\text{C}=\text{O}$) that absorb electromagnetic radiation in the ultraviolet and visible regions of the spectrum.⁶⁹ The amount of energy absorbed by the compound is directly related to concentration of the compound in the solution. For instance, *p*-nitrophenol has a characteristic yellow colour and absorbs electromagnetic radiation in the visible range. It was therefore easy to even visually monitor the colour of the polymer before and after passing its solution through the polymer, using this technique.

Samples of *p*-nitrophenol and standards were analyzed using a Cary UV (50 Scan). Samples were placed in sample holders (cuvettes) that were 1 cm wide and 4.5 cm long. The cuvette was then placed in the instrument and absorbances were recorded at 318 nm. Water was used as a reference sample to zero the instrument. All measurements were taken at room temperature.

3.3.17 Recycling tests for polymers

The ability to regenerate a polymer when saturation is reached was an important attribute of our study. If the regeneration step is cheaper than the cost of replacing the polymer, this would then make the polymer economical for water treatment applications.

Recycling studies for 1% MWNT (β -CD/HMDI) polymers were performed using *p*-nitrophenol as the test pollutant. It was chosen as a pollutant in these studies because of its characteristic yellow colour that made it easy for monitoring absorption using UV-Visible spectroscopy. *p*-Nitrophenol (30 cm^3 , 10 mg/dm^3) was passed through the polymer (0.30 g in a column). The flow rate was maintained at between 3 and 5 cm^3 per minute just like in the normal absorption tests. The eluent was collected and residual *p*-nitrophenol was measured using a UV-Visible spectrometer as described in section 3.3.16. The polymers were regenerated by passing 35 cm^3 of ethanol (70%) followed by washing with water (5 cm^3). Diluted ethanol (70%) was used for the regeneration studies because absolute ethanol did not appear to remove the *p*-nitrophenol from the polymers as the yellow colour persisted even after passing 35 cm^3 of absolute ethanol. The process of loading and washing was repeated for twenty-five times. Similarly, native β -CD/HMDI polymers (i.e. those without carbon nanotubes) were recycled in order to compare their absorption efficiency and structural stability of the two types of polymers during and after recycling.

CHAPTER FOUR

RESULTS AND DISCUSSION

4.1 Introduction

Results obtained from this study are presented and discussed in this chapter. These include characterization of the CNTs and polymers incorporating the CNTs using the various techniques that have been discussed in the previous chapter. Absorption tests of these polymers using *p*-nitrophenol and trichloroethylene as test organic pollutants are also discussed. Finally, results for the recycling tests of the polymers to determine their absorption efficiency and structural integrity after prolonged recycling are also expounded.

4.2 Synthesis of MWNTs by nebulized spray pyrolysis

A comparison amongst MWNTs synthesized by the nebulized spray pyrolysis (NSP), arc-discharge and CVD (commercial nanotubes) was made. Multiwalled nanotubes made by the nebulized spray pyrolysis were found to be superior over those produced by CVD and arc discharge methods because they were well aligned with very little amorphous carbon. In addition, the NSP uses a homogeneous catalyst and the size of the CNTs can be controlled by varying the synthetic parameters. On the contrary, TEM pictures of carbon nanotubes produced from the arc-discharge showed a lot of amorphous carbon and were therefore not used in this study, as they would require extensive purification. Instead, MWNTs from the nebulized spray pyrolysis and CVD (commercial) CNTs from Sunnano were used. A discussion on their synthesis and characterization is presented in the sections that follow.

MWNTs were synthesized *via* nebulized spray pyrolysis of a mixture of toluene (50 cm³) and ferrocene (2.00 g). The carrier flow rate was 500 cm³/min while the oven temperature was 900⁰C as per the method described in **Chapter 3**. Results of the synthesis are presented in **Table 4.1**.

Table 4.1: Mass of NSP MWNTS from the four runs

Run Number	Mass of MWNTs (g)
1	0.70
2	0.85
3	0.60
4	0.87

Results in the table above show a mass range of 0.60 g to 0.87 g with an average of 0.76 g. The nanotubes were then functionalized and characterized.

4.3 Functionalization of MWNTs

Masses of the MWNTs before and after functionalization using the two functionalization modes are shown in **Tables 4.2a** and **4.2b**.

Table 4.2a: Yield of MWNTs after reflux for 30 minutes at 95⁰C

Source of MWNTs	Mass before reflux (g)	Mass after reflux (g)	Yield (%)
Commercial MWNTs	1.0580	0.3010	28
NSP MWNTs	0.0530	0.0088	16

Table 4.2b: Yield of MWNTs oxidized at 45-50⁰C for 24 hrs

Source of MWNTs	Mass before oxidation (g)	Mass after oxidation (g)	Yield (%)
Commercial MWNTs	2.150	1.921	89
NSP MWNTs	0.590	0.450	76

A comparison of the yields from the two functionalization modes show that there was tremendous mass loss when MWNTs were heated under reflux for 30 minutes (**Table 4.2a**) compared to when the MWNTs were functionalized at 50⁰C for 24 hours (**Table 4.2b**). Under reflux the yield from commercial

MWNTs was 28% while that for NSP was 16%. These yields were low compared to 70% reported by Esumi *et al.*⁵⁹ and Saito *et al.*⁷⁰ This suggests that most of the nanotubes were destroyed by the mixture of the strong acids. Because of this limitation, the method was therefore adjusted to functionalizing the nanotubes using a similar mixture of the acids but at between 45-50⁰C for 24 hrs. The yield was 89% and 76% for the commercial and NSP MWNTs, respectively and IR results showed that the revised method successfully introduced carboxylic groups to the CNTs. The section that follows presents characterization of these CNTs by TEM.

4.4 Transmission electron micrographs of raw commercial and NSP MWNTs

Transmission electron micrographs of raw commercial and NSP- MWNTS are given in **Figures 4.1a** and **4.1b**, and they show the different morphologies present in the samples.



Figure 4.1a: Raw Commercial MWNTs

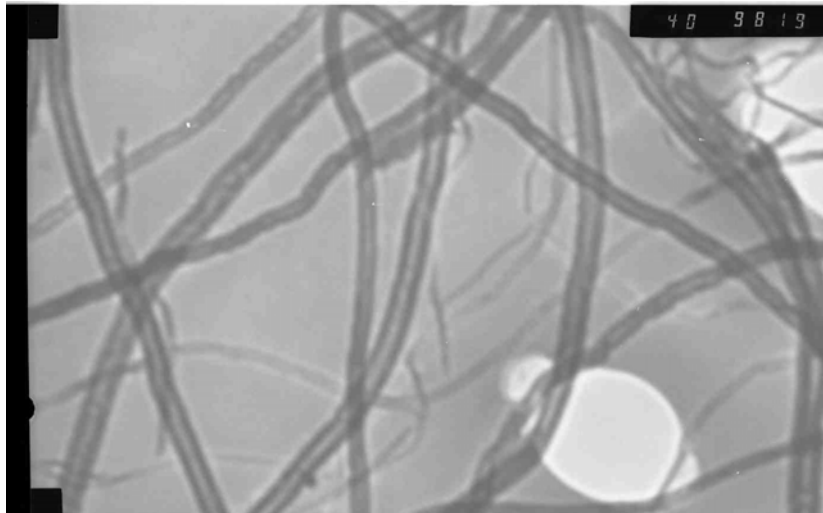


Figure 4.1b: Raw NSP MWNTs

It was observed that raw commercial MWNTs (purchased from Sunnano) (**Figure 4.1a**) had some impurities which were suspected to be amorphous carbon (seen as dark irregular spots). A further observation of the Raman data showed that the ratio of area for the G/D bands was 1.03. This is close to 1.00 indicating that the area of the disordered band (D) was almost equal to that of graphitic band G. This suggests that the commercial MWNTs were more disordered (as can be seen in the TEM picture in **Figure 4.1a**) even before functionalization or had impurities. Discussion on Raman results is presented in **section 4.5**. The TEM images also showed that the nanotubes were not uniform in shape and length. Although some non-uniformity was observed for the NSP MWNTs (**Figure. 4.1b**) these MWNTs appeared to have no amorphous carbon. These observations prompted further studies to compare characteristics of polymers prepared from the NSP MWNTs to those from commercial MWNTs. The characteristics would hopefully have a bearing on the performance of these polymers when used in water treatment.

4.5 Transmission electron micrographs of functionalized commercial and synthesized nanotubes

MWNTs were functionalized in a mixture of acids for the purpose of introducing hydroxyl and carboxylic acid functional groups that would react with the isocyanate groups during polymerization with the cyclodextrin monomers. **Figure 4.1c and 4.1d** show TEM images of NSP MWNTs functionalized for 24hrs at 45-50⁰C (**Figure 4.1c**) and those functionalized under reflux in a mixture of nitric and sulphuric acids for 30 minutes at 95⁰C (**Figure 4.1d**).

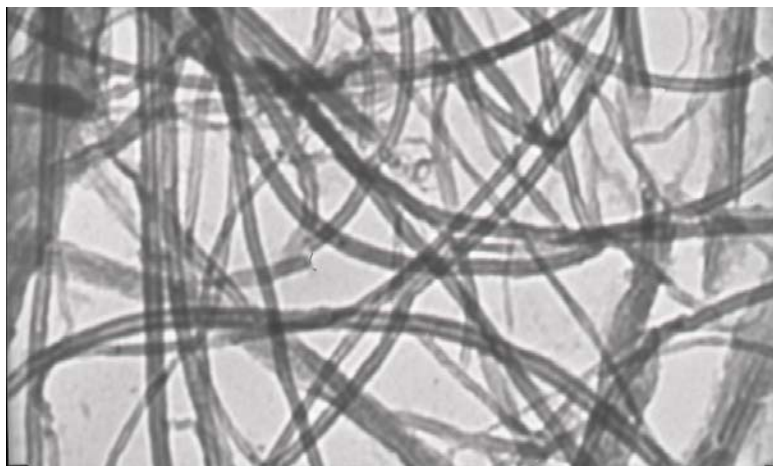


Figure 4.1c: NSP MWNTs functionalized by a mixture of HNO₃ and H₂SO₄ at 45-50⁰C for 24 hrs

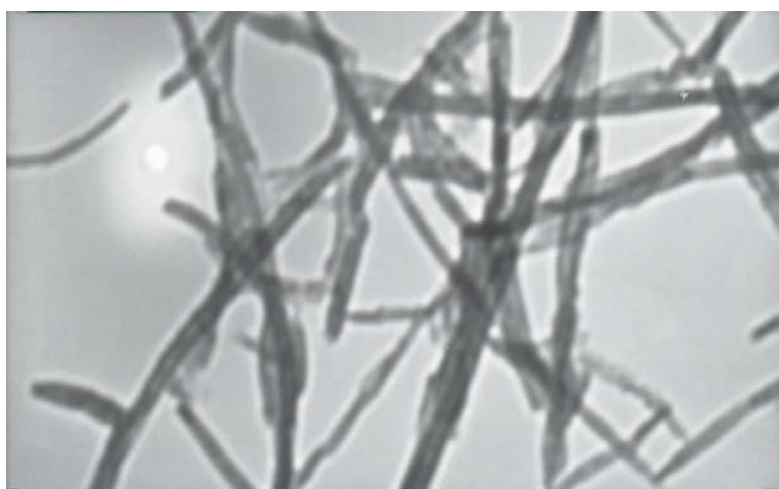


Figure 4.1d: NSP MWNTs functionalized by reflux in HNO₃ and H₂SO₄ at 95⁰C

Functionalization of the carbon nanotubes in a mixture of HNO_3 and H_2SO_4 at 50°C appeared to have slightly degraded the surface of the nanotubes, producing much smaller “pieces” than the original sample (**Figure 4.1c**). The degree of surface damage was, however, more pronounced for nanotubes functionalized under reflux 95°C in a similar acid mixture (**Figure 4.1d**). One drawback with functionalization under reflux was the tremendous mass loss for both commercial and NSP nanotubes. Taking these limitations into account, it was decided that MWNTs functionalized at 50°C be used in this study.

4.6 Solubility tests of functionalized MWNTs

Solubility test results for the functionalized and raw (unfunctionalized) MWNTs are presented in **Figure 4.2a**.

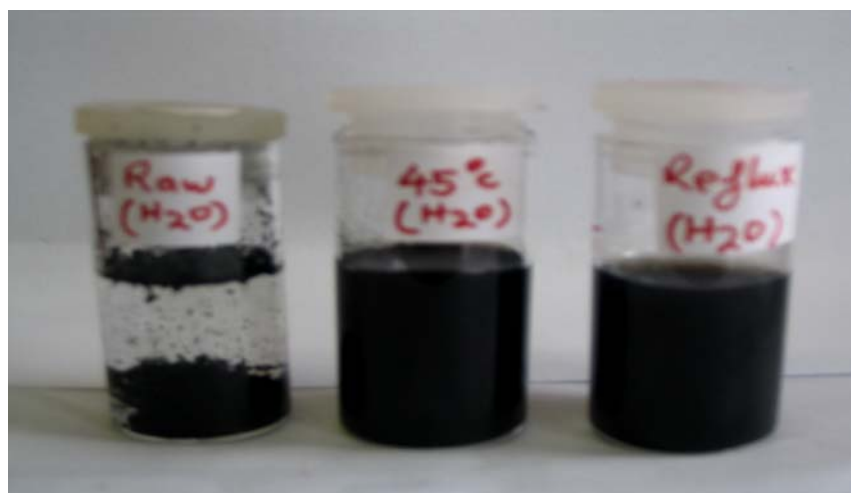


Figure 4.2a: Pictures of functionalized and raw MWNTs mixed with water (H_2O)

Figure 4.2a shows three vials containing approximately 0.5 g each of raw (unfunctionalized) NSP MWNTs, those functionalized at $45\text{--}50^\circ\text{C}$, and those functionalized under reflux for 30 minutes at 95°C . These MWNTs were mixed with distilled water (10 cm^3) followed by sonication for 15 minutes after which the mixtures were allowed to stand for up to five months. It can be observed in this figure that functionalization of carbon nanotubes with a mixture of nitric

and sulphuric acid changed the dispersion or solubility properties of the nanotubes. Functionalization made the nanotubes soluble in water even before sonication and they remained soluble for over five months. Raw MWNTs could not dissolve in water. Instead they aggregated and settled at the bottom or were suspended at the top of the solvent. In order to ascertain whether functionalized and unfunctionalized MWNTs were soluble in organic solvents, solubility tests were also performed in DMF and results are shown in **Figure 4.2b**.

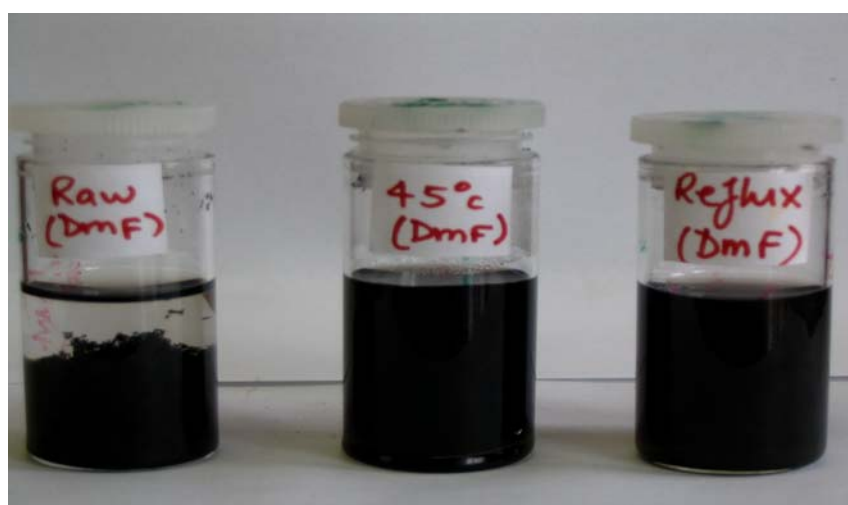


Figure 4.2b: Pictures of functionalized and unfunctionalized NSP MWNTs mixed with DMF

A similar trend as that in water (**Figure 4.2a**) was observed in DMF (**Figure 4.2b**) where unfunctionalized MWNTs aggregated and settled at the bottom of the vial while functionalized CNTs remained soluble in the solvent. To further ascertain if the functionalized MWNTs were finely suspended or if they had actually dissolved in water or DMF, samples were centrifuged at 10000 rpm for ten minutes using a Jouan BR 4 centrifuge. Functionalized nanotubes in either water or DMF did not settle out but remained in solution. This confirmed that the MWNTs were not finely dispersed, as they would have settled out by gravity but that functionalization had made the MWNTs soluble.

This physical property can only come about when functional groups like O-H and -COOH are introduced to the walls of the nanotubes, as these groups change the hydrophobic properties of the MWNTs. These results are in agreement with reports by Kuzmany *et al*⁷¹ and Saito *et al* and suggests that O-H and -COOH groups were introduced to the walls of MWNTs. Further characterization to support this hypothesis was performed by techniques such as Infrared spectroscopy (IR) and Raman spectroscopy.

4.7 Characterization of MWNTs by IR spectroscopy

MWNTS were characterized by IR spectroscopy in order to confirm if the hydroxyl and carboxyl groups had been successfully attached onto the walls of the nanotubes. **Figure 4.3a** and **4.3b** show IR spectra for the unfunctionalized and functionalized nanotubes, respectively. These figures clearly indicate the changes in functional groups on the two samples.

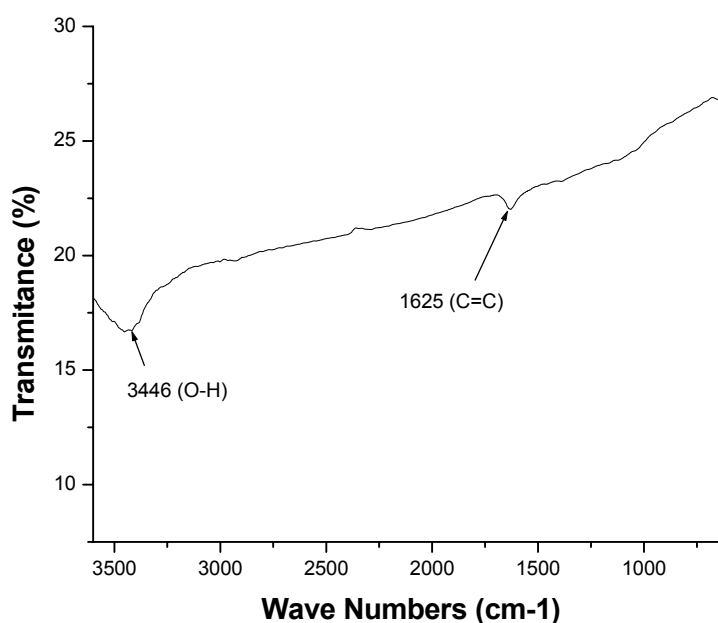


Figure 4.3a: IR spectrum of NSP MWNTs before functionalization

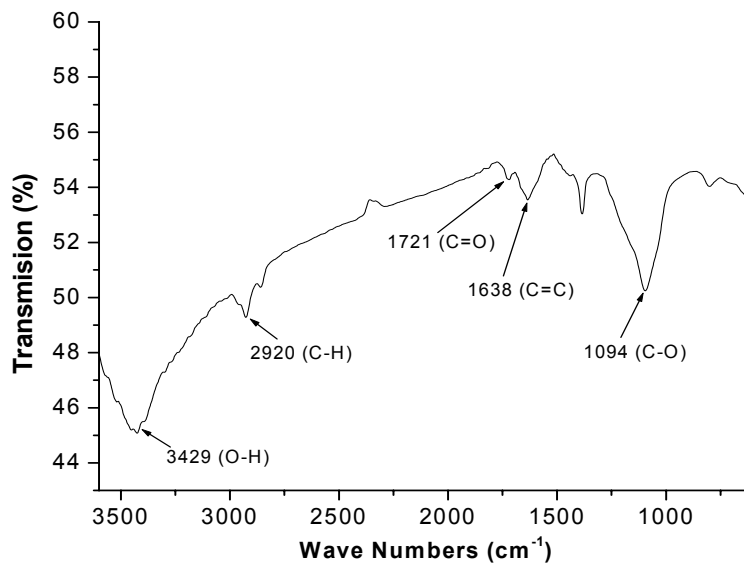


Figure 4.3b: IR spectrum of NSP MWNTs after functionalization

It can be observed from **Figure 4.3a** that unfunctionalized MWNTs had limited functional groups already. The O-H (3446 cm^{-1}) functional groups were probably due to the oxidation of CNTs during synthesis. Care was taken to ensure that the KBr used in making the sample pellets was dry to exclude any possibility of moisture being introduced. The C=C (1625 cm^{-1}) functionality was derived from the nanotubes. After functionalizing with a mixture of HNO_3 and H_2SO_4 , peaks corresponding to O-H (3429 cm^{-1}), C-H (2929 cm^{-1}), C=O (1721 cm^{-1}), C=C (1638 cm^{-1}) and C-O (1094 cm^{-1}) emerged or intensified (**Figures 4.3b**). Comparison of the peak intensities before and after functionalization (**Figures 4.3a** and **4.3b**) clearly shows that the intensity for the O-H peak increased after functionalization. This was not purely a concentration effect as the amount of sample was carefully controlled. It is also noted that new peaks corresponding to C-H, C-O, and C=O appeared after functionalizing the nanotubes. The increase in intensity of the O-H peak after functionalization and the appearance of C-H, C=O and C-O bonds suggests that oxidation of the MWNTs successfully introduced carboxyl groups (COOH) onto the walls of the nanotubes. The C-H signals in the IR spectrum further confirms that carbon atoms of the functionalized carbon nanotubes were now sp^3 hybridized instead of being sp^2 hybridized, which is the hybridization state of raw carbon CNTs.

A similar trend was observed for the commercial nanotubes, and **Figure 4.4a** and **4.4b** show IR spectra for raw and functionalized commercial MWNTs.

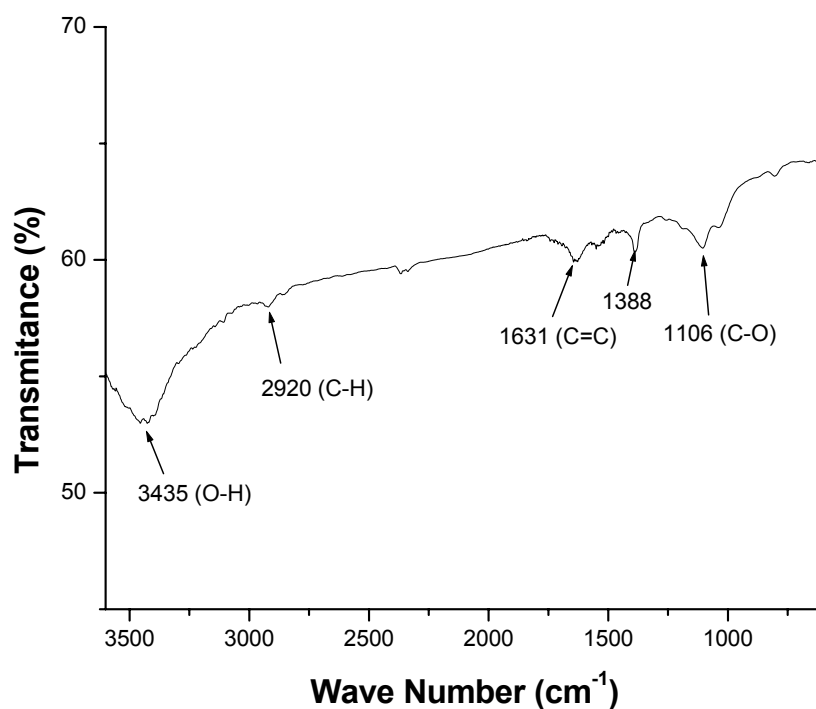


Figure 4.4a: IR spectrum of raw commercial MWNTs

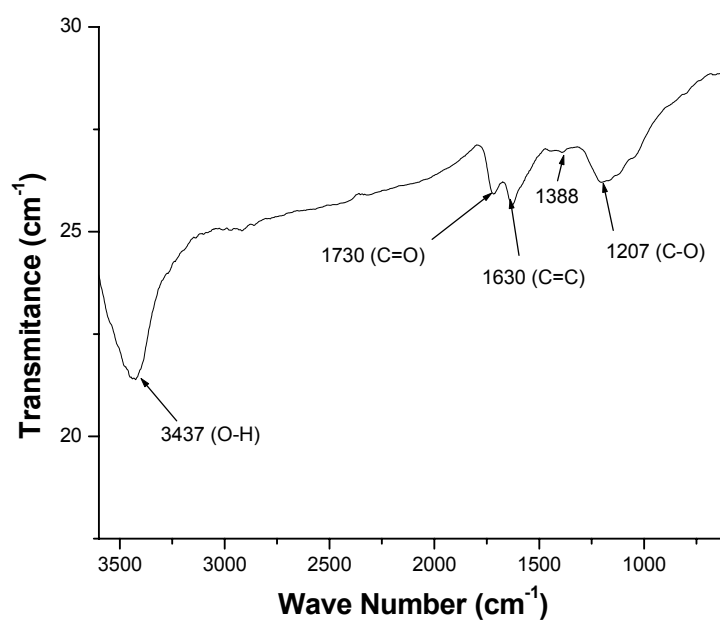


Figure 4.4b: IR spectrum of functionalized commercial MWNTs

A comparison of infrared absorption spectra for the NSP MWNTs (**Figure 4.3a**) and commercial MWNTs (**Figure 4.4a**) showed that the raw MWNTs in both cases had limited functional groups. However, the raw commercial MWNTs had C-H and C-O functional groups in addition to O-H and C=C which were observed in the NSP MWNTs. This could also suggest the reason for the higher disorder in the raw commercial nanotubes as compared to the NSP MWNTs as was observed by the Raman data in **Figure 4.5a** and **Figure 4.5b**. This added functionality is probably as a result of the amorphous carbon fragments present. Functionalization of commercial MWNTs increased the O-H and C-O peak intensities as can be seen in **Figure 4.4b**. A peak at 1730 cm^{-1} corresponding to C=O was also introduced. This suggested COOH groups had been introduced to the nanotubes. The peak appearing at 1388 cm^{-1} in both spectra could not be identified.

4.8 Raman spectroscopy

Raman spectra of the NSP and commercial MWNTs showing the D and G band are presented in **Figure 4.5a** and **4.5b**.

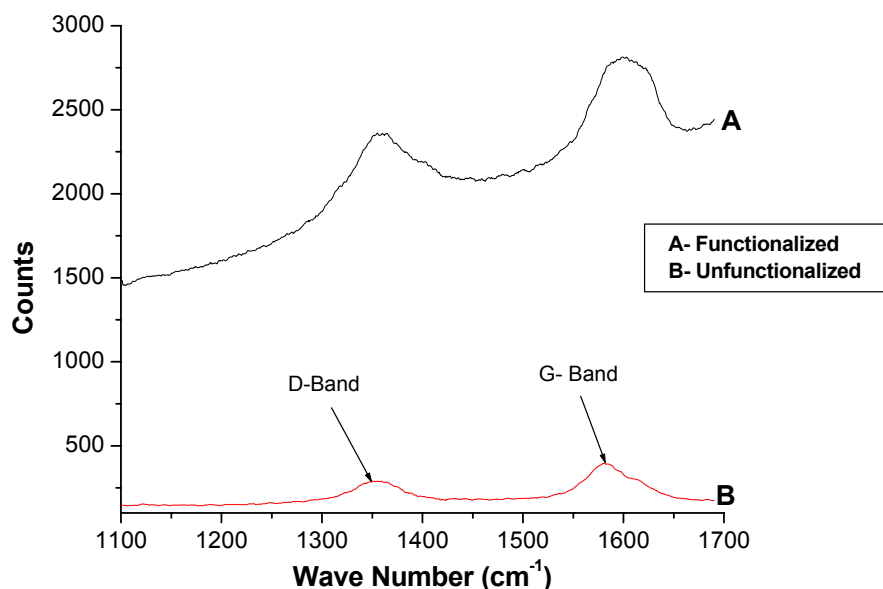


Figure 4.5a: Comparison of Raman spectra of functionalized and unfunctionalized NSP MWNTs

The interpretation of Raman analyses of MWNT is primarily dependent on two bands. The first is the D-band (the defect peak), which arises due to the amorphous or non-crystalline carbon present in the material.⁷² The second is the G-band which corresponds to a splitting of the E_{2g} stretching mode of graphite, which arises due to the tangential vibrations of the carbon atoms.⁷³ The intensity ratio of these bands (I_G/I_D) or the ratio of their areas supplies crucial information of the “graphicity” or lack of defects on the MWNTs. Raman spectra of NSP MWNTs are presented in **Figure 4.5a**. The ratio of the areas of G/D for the unfunctionalized and the functionalized NSP MWNTs were found to be 2.20 and 0.72 respectively. Initially the unfunctionalized MWNTs showed a high G/D area ratio because these tubes were highly graphitic (**Figure 4.1b**). However, this ratio decreased for the functionalized MWNTs. This was clearly an indication that the structures of the functionalized nanotubes were more disordered as compared to those of the unfunctionalized MWNTs i.e. there was a relative increase in the D-band. This was most probably due to the introduction of the functional groups such as O-H, C-O and -COOH on the walls of the nanotubes as earlier confirmed by IR spectroscopy. These functional groups on the MWNTs changed some of the carbon atoms from the sp^2 hybridized state to sp^3 . **Figure 4.5b** shows the Raman spectra of raw and functionalized commercial MWNTs.

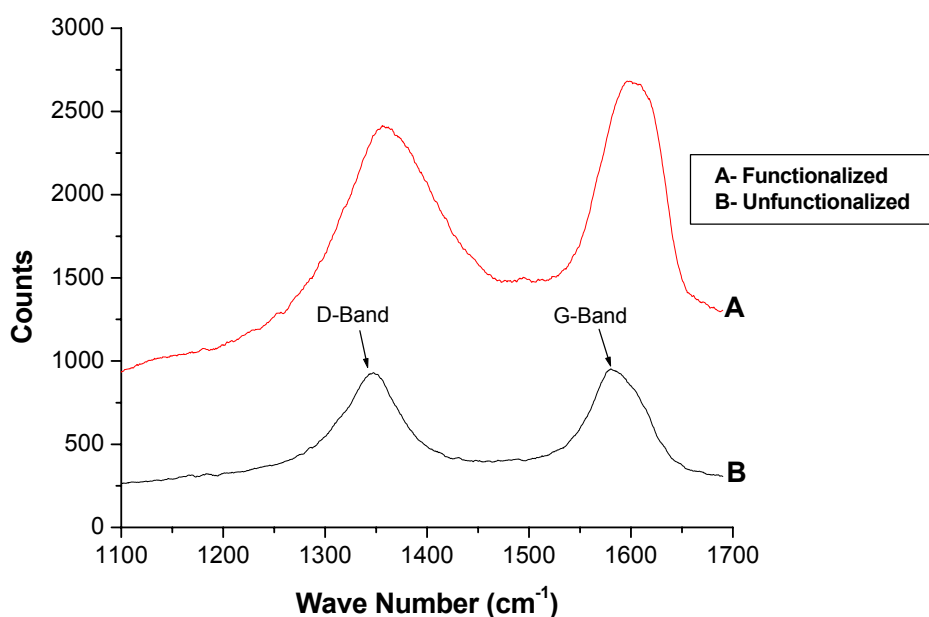


Figure 4.5b: Raman spectra of raw and functionalized commercial MWNTs

A comparison of the unfunctionalized and functionalized commercial MWNTs nanotubes (**Figure 4.5b**) shows a similar trend to that of the NSP MWNTs (**Figure 4.5a**). However, the ratio of the areas of G/D for the unfunctionalized and the functionalized commercial MWNTs were found to be 1.03 and 0.83, respectively. Comparing the ratio of the unfunctionalized for the NSP MWNT and that of commercial MWNTs show a large area ratio of 2.20 for the NSP MWNT compared to 1.03 for the commercial MWNT. This could mean that the commercial MWNTs were more disordered probably because of the purification processes to which these nanotubes were subjected and the presence of highly disordered amorphous carbon. Characterization by IR showed that unfunctionalized commercial MWNTs had some functionality while TEM revealed the presence of amorphous carbon. These might have contributed to the increase in D peak, hence low G/D ratio.

4.9 Polymerization of β -CD with carbon nanotubes

Polymerization reactions were performed as per the method described in **Chapter 3** and were monitored using infrared spectroscopy. **Figures 4.6a** and **4.6b** show the disappearance of the isocyanate peak for the HMDI at about 2700 cm^{-1} as the polymerization reaction proceeded. As discussed in **Chapter 3**, the isocyanate is a group on the HMDI which combines with the $-\text{COOH}$ or $-\text{OH}$ groups on the walls of functionalized MWNTs during polymerization reaction. Thus monitoring its disappearance indicated that the nanotubes polymerized with the HMDI.

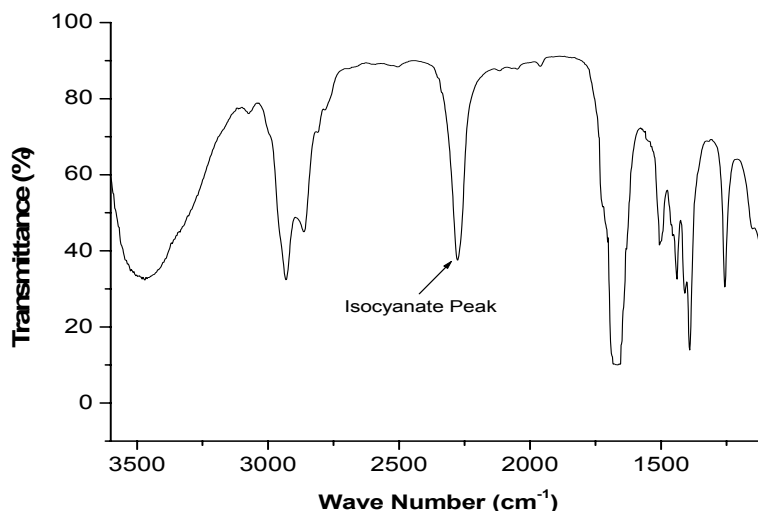


Figure 4.6a: IR spectrum showing isocyanate peak at the start of reaction

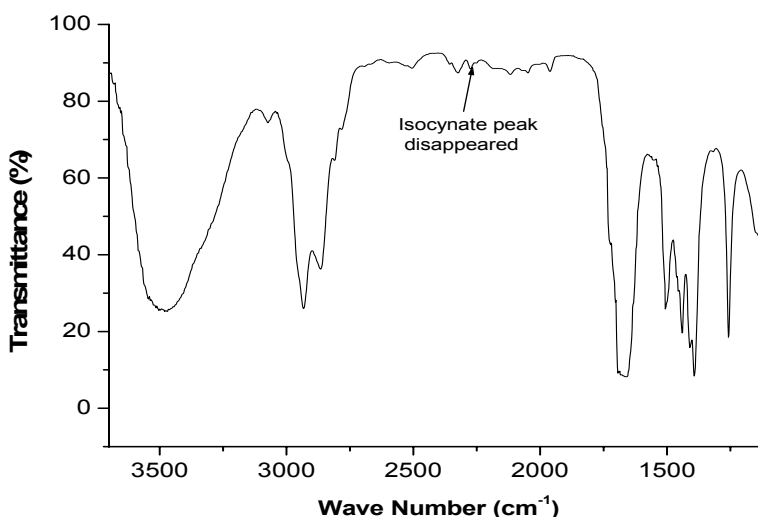


Figure 4.6b: IR spectrum showing the disappearance of isocyanate peak at the end of the reaction.

In a separate experiment it was further confirmed that the NSP MWNTs had polymerized with the linker, whereby the carbon nanotubes, using their functional groups reacted with the diisocyanate in the absence of any CD. The isocyanate peak disappeared and a completely new product was formed. **Figures 4.7a** shows the reduction of the isocyanate peak. The peak completely disappeared after twenty-four hours (**Figure 4.7b**). The fact that

these reactions were carried out using dried solvents and under inert conditions confirms that the disappearance of the diisocyanate peak was solely due to the reaction of the isocyanate group with the -COOH and -OH of the MWNTs. For this particular study, this finding was very important as it confirmed that there was indeed participation of all the three monomers (CD, MWNTs and the linker) in the polymerization reaction.

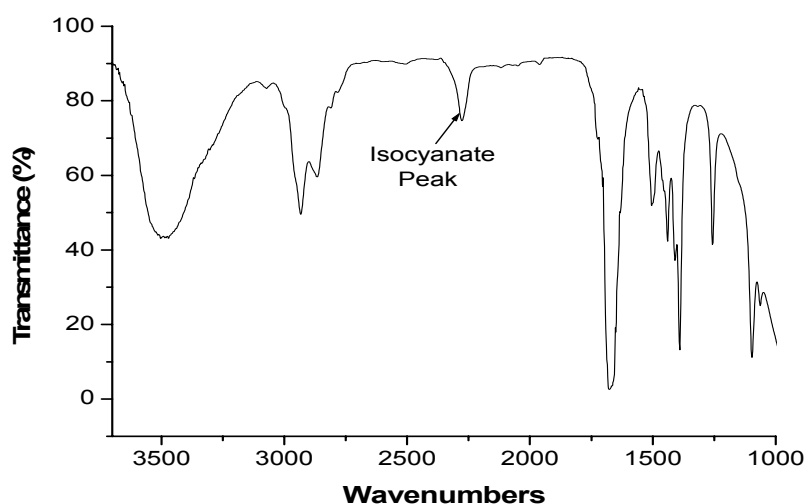


Figure 4.7a: IR spectrum showing the reduction of isocyanate peak during MWNTs polymerization

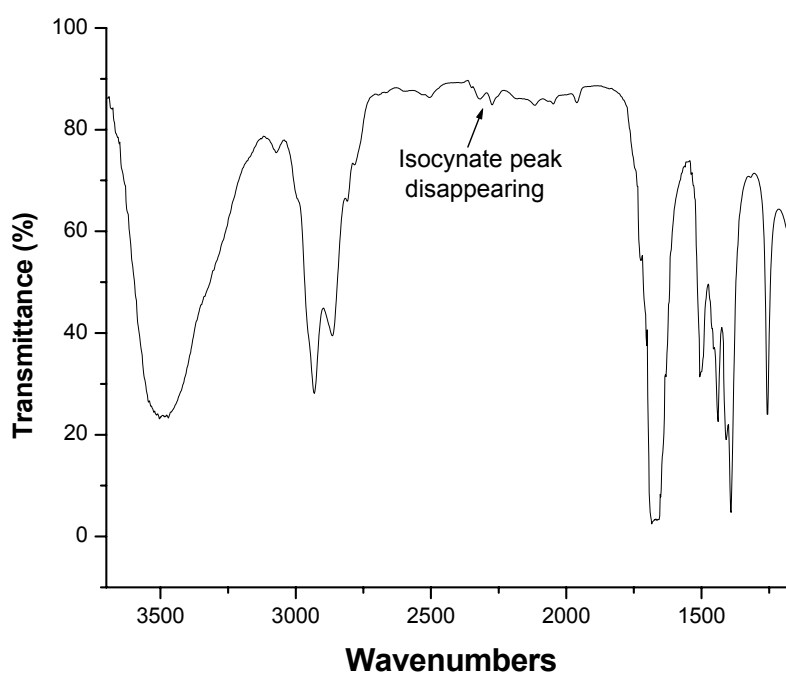


Figure 4.7b: IR spectrum showing the disappearance of the isocyanate peak during MWNTs polymerization

Solubility tests of the polymerized carbon nanotubes (without any CD) showed that these nanotubes were now insoluble in water, DMF and ethanol, while they had been soluble before polymerisation. A similar result was obtained when water soluble cyclodextrins were polymerized with diisocyanate linkers; the resultant polymer was water insoluble. The IR spectrum of the polymerized nanotubes (**Figure 4.8**) also showed enhanced C-H and C=O peaks. The enhanced C=O peak resulted from the reaction of the OH groups of the carbon nanotubes and the diisocyanate groups.

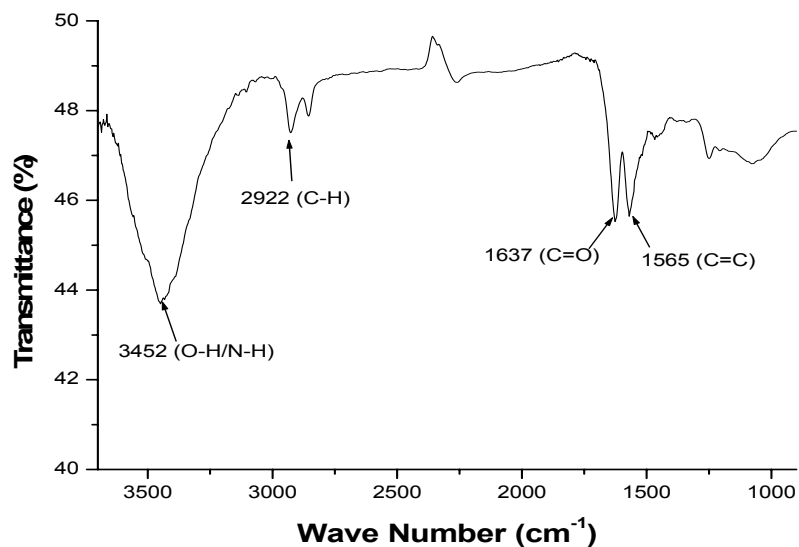


Figure 4.8: IR spectrum of polymerized nanotubes

4.10 Physical properties of the native β -CD and nanotube included polymers

Table 4.3 shows some of the physical properties of the prepared native β -CD polymers and the polymers that were incorporated with various percentages of carbon nanotubes.

Table 4.3: Physical properties of β -CD polymers

Polymer	Colour	Texture	Yield(%)
β -CD/HMDI	White	Mixture of granules and powder	100
1% f-CNT (β -CD/HMDI)	Whitish grey	Soft, powdery with some granules	75
2% f-CNT (β -CD/HMDI)	Grey to black	Powdery with few granules	66
3% f-CNT (β -CD/HMDI)	Grey to black	Granulated	70
5% f-CNT (β CD-HMDI)	Grey to black	Granulated and soft	78

All the polymers were obtained in high yields and were insoluble in water and organic solvents. Insolubility of these polymers is an important physical property for applications in water treatment. Characterization of the polymers was performed by using IR spectroscopy and SEM among others.

4.11 Characterization of polymers using infrared spectroscopy (IR)

The prepared polymers were characterized using IR and the spectra are represented in **Figures 4.9a** and **4.9b**. Examination of the spectrum of a 1% MWNT (β CD-HMDI) (**Figure 4.9a**) shows characteristic absorption bands. These absorption bands correspond to O-H (3382 cm^{-1}), C-H (2938 cm^{-1}), C=O (1714 cm^{-1}), C=C (1631 cm^{-1}) and C-O (1034 cm^{-1}). A similar interpretation is also given in **Figure 4.9b** for 1% MWNT (β -CD/TDI) where corresponding O-H and, C-H, C=O, C=C and C-O absorption bands are observed at 3355 cm^{-1} , 2930 cm^{-1} , 1655 cm^{-1} , 1602 cm^{-1} and 1029 cm^{-1} respectively.

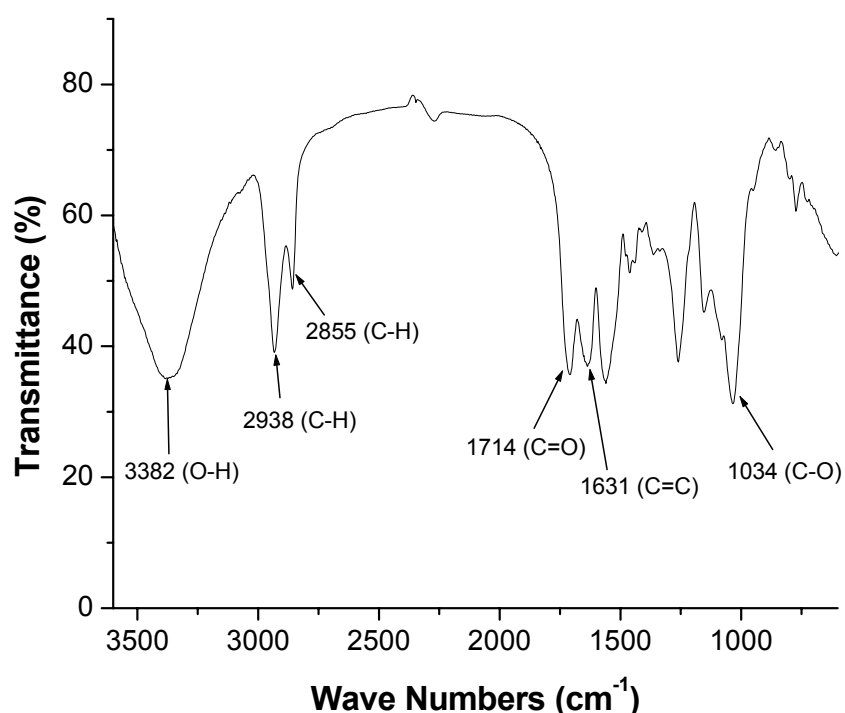


Figure 4.9a: IR spectra of a 1% MWNT (β -CD/HMDI) polymer

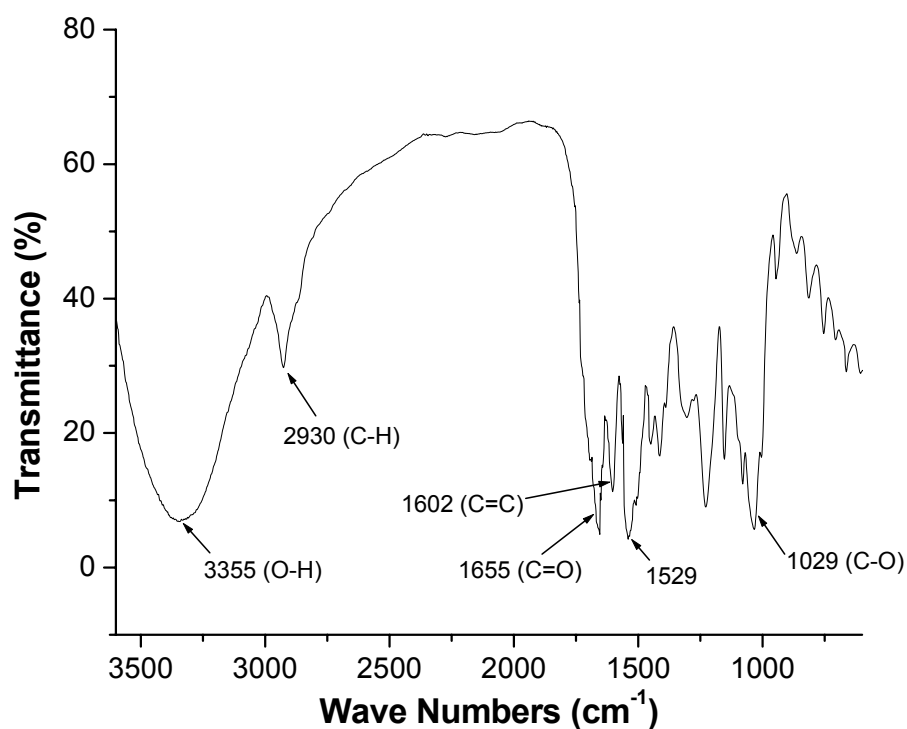


Figure 4.9b: IR spectra of a 1% MWNT (β -CD/TDI) polymer

IR spectra for a 3 and 5% CNT (β -CD/HMDI) polymer and a 5% CNT (β -CD/TDI) polymer showed a similar trend to the ones incorporated with 1% MWNTs. These spectra are shown in **Appendix C**. There were, however, some differences in the absorption bands between HMDI and TDI linked polymers. For example, there were two C-H peaks for HMDI polymers at 2932 cm^{-1} and 2855 cm^{-1} (**Figure 4.10a**) while there was only one peak at 2930 cm^{-1} for TDI linked polymers (**Figure 4.10b**). This suggests that HMDI linked polymers have two different C-H environments, while TDI polymers have only one IR active C-H bond.

4.12 Characterization of polymers by scanning electron microscopy.

Both native and nanotube incorporated polymers were analyzed using SEM in order to determine their surface features. All the micrographs were taken at a

magnification of 190000x. It can be observed that the surface of native β CD-HMDI polymer (**Figure 4.10a**) and that incorporated with 1 percent MWNT (**Figure 4.10b**) resembled that of a sponge. However, as the percentage nanotubes was increased to 5 percent, the spongy appearance diminished as can be seen in **Figure 4.10c, 4.10d** and **4.10e**. It is not clear at this stage whether this could be attributed to the processing of the polymer or was just a function of the increase in the amount of nanotubes. Further work needs to be done in order to account for these properties.

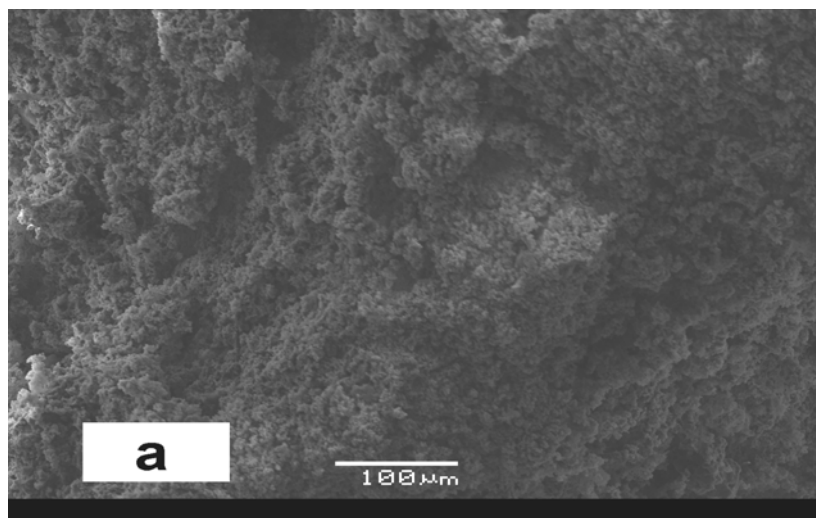


Figure 4.10a: SEM of native β -CD/HMDI polymer

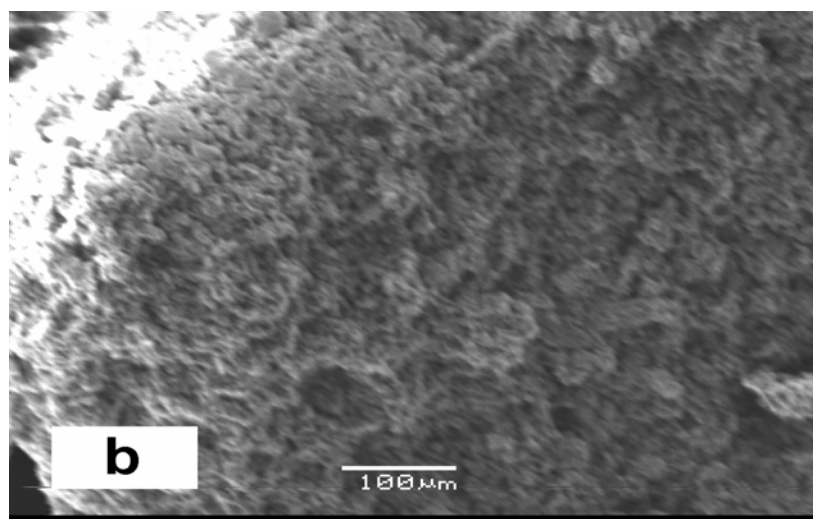


Fig. 4.10b: SEM of 1% MWNT (β -CD/HMDI) polymer

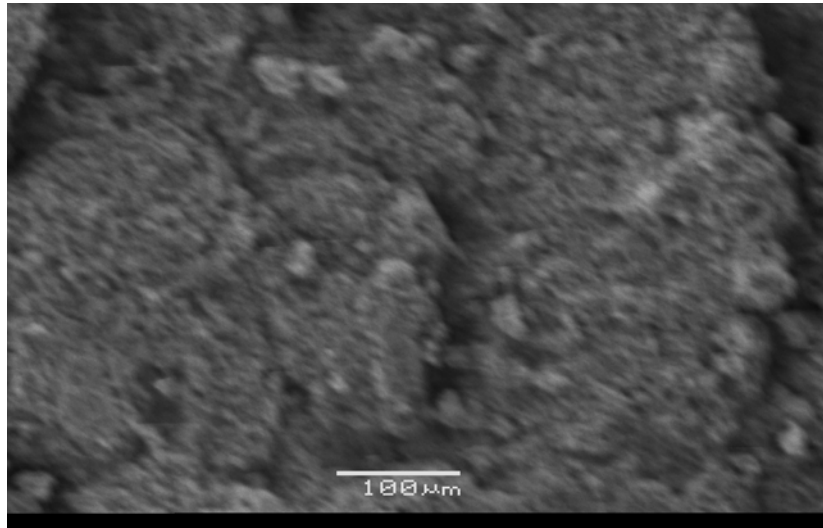


Fig. 4.10c: SEM of 3% MWCNT (β -CD/HMDI) polymer

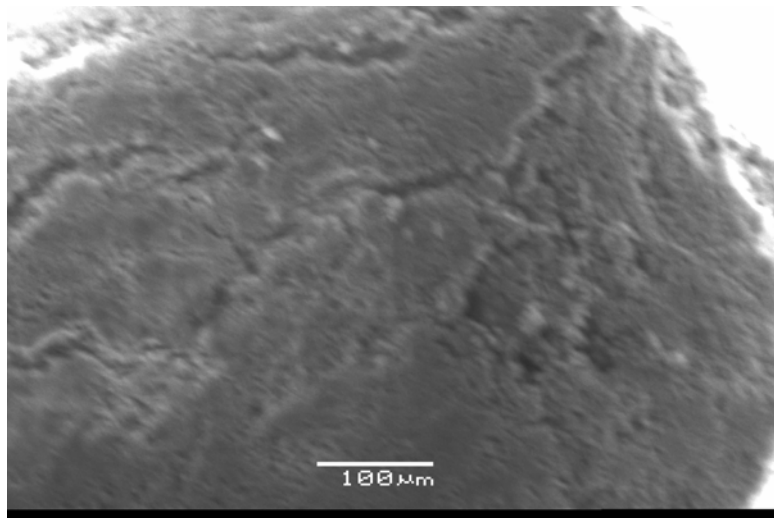


Fig. 4.10d: SEM of 4% MWCNT (β -CD/HMDI) polymer

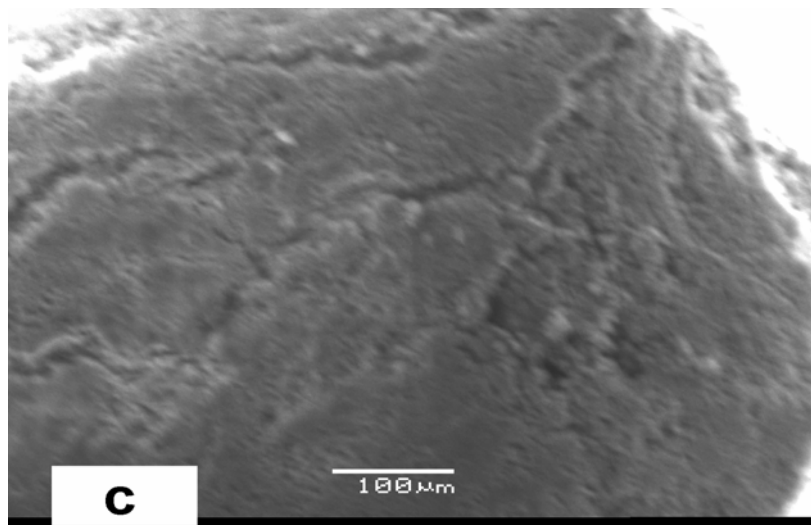


Fig. 4.10e: SEM of 5% MWCNT (β -CD/HMDI) polymer

Polymers made from TDI, however, did not display any spongy appearance as compared to those of native β -CD/HMDI, 1% CNT (β -CD/HMDI) and 2% CNT (β -CD/HMDI). Just like the HMDI linked polymers, it is not clear whether this was a processing phenomenon. However, the physical properties of these polymers will further be investigated by techniques such as BET. **Figures 4.11a, 4.11b and 4.11c** show SEM images of TDI linked polymers.

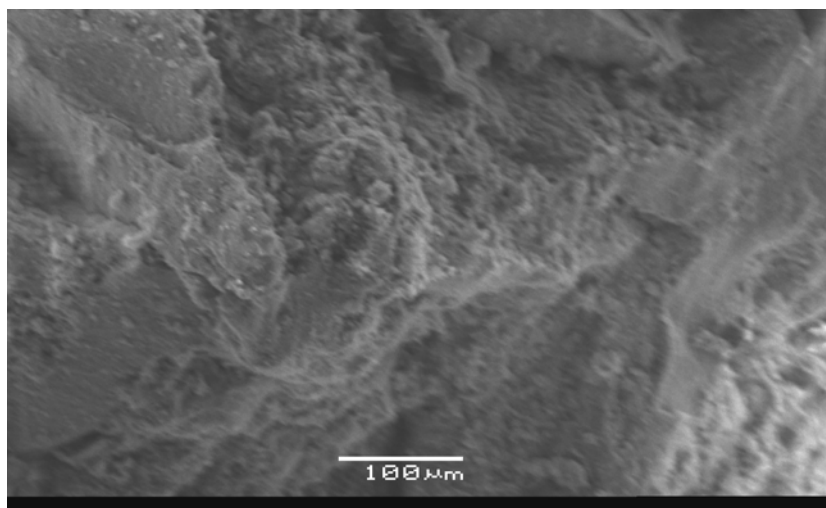


Figure 4.11a: SEM of a 1% CNT (β -CD/TDI) polymer

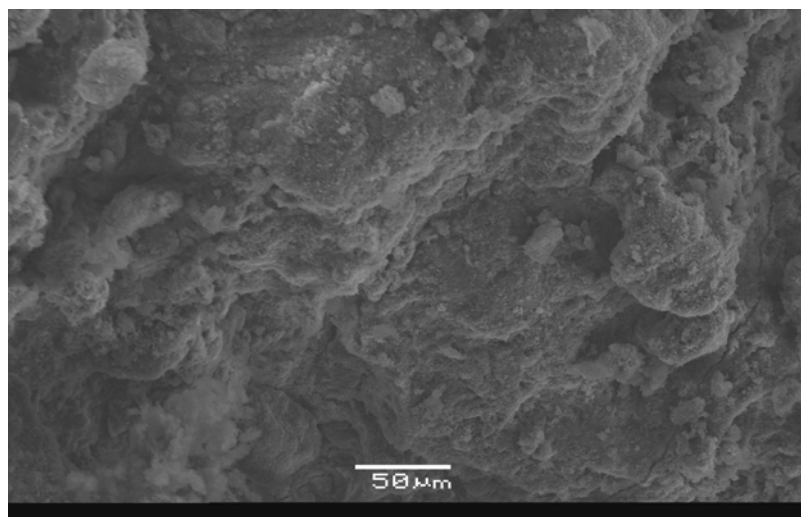


Figure 4.11b: SEM of a 2% MWCNT (β -CD/TDI) polymer

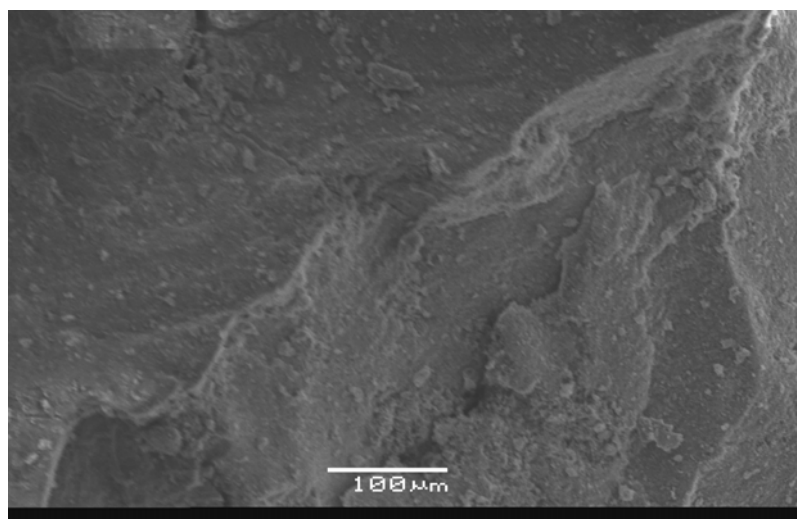


Figure 4.11c: SEM of a 3% MWCNT (β -CD/TDI) polymer

4.13 BET analysis of the polymers

Table 4.2 presents BET measurements for native polymers and those containing varying percentages of carbon nanotubes. Linkers used in the synthesis of these polymers were HMDI and TDI.

Table 4.4: BET results for native and MWNT included polymers

MWNT Composition	β -CD/HMDI		β -CD/TDI	
	Surface area (m ² /g)	Pore Volume (cm ³ /g)	Surface area (m ² /g)	Pore Volume (cm ³ /g)
Native	2.52	0.009	1.704	0.009
1% f-CNT	8.65	0.038	14.064	0.072
2% f-CNT	6.82	0.026	17.356	0.059
3% f-CNT	6.46	0.027	20.740	0.079
4% f-CNT	2.40	0.008	9.946	0.063
5% f-CNT	3.92	0.013	10.112	0.037

It can be seen from these results that surface area of the polymers dramatically increased with addition of MWNT for TDI linked polymers. Surface area for HMDI polymers also increased but not considerably. The

results also show a general increase in the pore volumes for the TDI and HMDI polymers with increase in MWNTs although there was no direct relationship. These observations suggest that the inclusion of functionalized MWNTs to the native β -CD/HMDI polymers generally caused the surface area to increase. A comparison of the surface area and the amount of pollutant absorbed by polymers is made in **Table 4.5**

Table 4.5: Comparison of surface area versus percent *p*-nitrophenol Absorbed (10 mg/dm³)

MWNT Composition	β -CD/HMDI		β -CD/TDI	
	Surface area (m ² /g)	% <i>p</i> - Nitrophenol absorbed	Surface area (m ² /g)	% <i>p</i> - Nitrophenol absorbed
Native	2.52	62	1.70	72
1% f-CNT	8.65	99	14.06	80
2% f-CNT	6.82	95	17.37	97
3% f-CNT	6.46	96	20.74	82
4% f-CNT	2.40	98	9.95	90
5% f-CNT	3.92	97	10.11	97

These results show that there was no direct relationship between the surface area and the amount of pollutant absorbed. However, further studies need to be done in order to make it absolutely certain that there is indeed no direct relationship.

Thermal properties of the native and polymers containing MWNTs were also investigated and results are presented in the following section.

4.14 Thermal analysis of the polymers

Thermal analyses of the polymers to determine their stability, melting and decomposition temperatures were performed using DSC and TGA.

4.14.1 Differential scanning calorimetry analysis of polymers

Figure 4.12 shows DSC curves of the native β -CD/HMDI polymer, a 1% MWNT (β -CD/HMDI) polymer and a 5% MWNT (β -CD/HMDI) polymer.

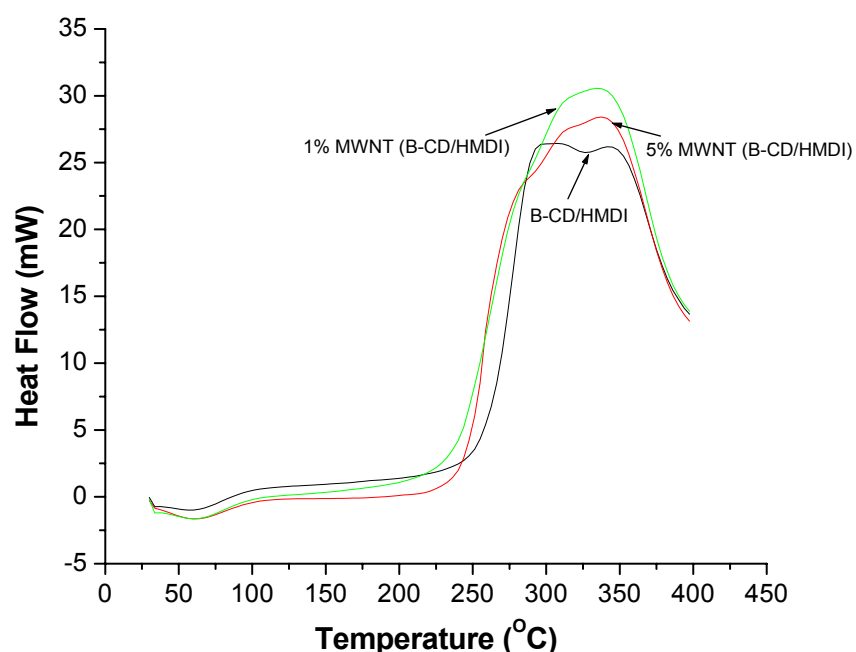


Figure 4.12: DSC curves of native and nanotube included polymers

It can be observed in **Figure 4.12** that the native and nanotubes included polymers displayed a similar trend. They showed an endothermic peak from about 60°C to 95°C. This peak depicted the loss of water from the polymers. The region between 218°C and 287°C showed the melting range of the polymers. However, some differences were observed at around 327°C where the native β -CD polymer showed a second endothermic peak which is associated with the melting of the polymer. Polymers incorporated with MWNTs did not show this endothermic peak; instead they showed an exothermic peak which was associated with curing of the polymer. This

observation confirms high cross-linking of the polymers incorporated with functionalized MWNTs. All of the polymers began decomposing at about 340°C. A conclusion on the stability of the polymers could not be drawn from these results alone, hence, further characterisation of the thermal properties of the polymers were carried out using TGA and results of these analyses are presented below.

4.14.2 Thermal gravimetric analysis (TGA)

Thermal gravimetric analyses of the native β -CD/HMDI polymer and those incorporated with one and five percent MWNTs were performed in order to compare the thermal stability of the polymers before and after inclusion of MWNTs. **Figure 4.13** shows the TGA thermographs of these polymers.

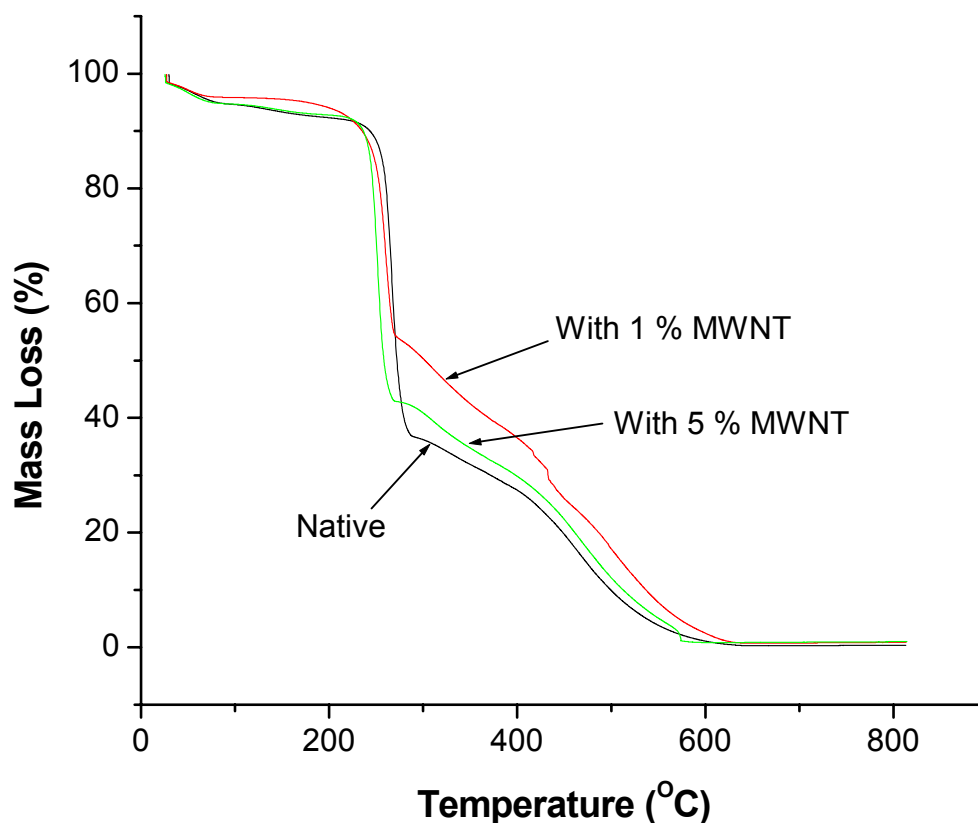


Figure 4.13: Superimposed TGA thermographs of native β -CD/HMDI polymer, 1% MWNT (β -CD/HMDI) polymer and 5% MWNT (β -CD/HMDI) polymer

A comparison of the thermographs for the native β -CD/HMDI polymer and those incorporated with MWNTs in **Figure 4.13** showed a similar trend for all three polymers, which were characterized by the loss of moisture and then the decomposition of the polymers at about 235⁰C. However, it was observed that the polymers with 1 and 5% MWNTs incorporated in them degraded at a slower pace than that of the native β -CD/HMDI polymer. This showed that the polymers which had MWNTs incorporated in them had slightly higher thermal stability than the native polymers. These results agree with the observation made by DSC and it is possible that the high degree of cross-linking of the polymer by addition of functionalized MWNTs could be a contributing factor to the increased stability.

4.15 Comparison of polymers on the absorption of *p*-nitrophenol

p-Nitrophenol was chosen as a model pollutant because it is one of the priority pollutants and because it has been used previously in our laboratory in this capacity, in similar systems. In addition, *p*-nitrophenol is yellow in colour and this makes it easy to monitor by UV-Visible spectroscopy. Two types of polymers formed from the linkers HMDI and TDI, containing various percentages of functionalized MWNTs, were compared for their ability to absorb *p*-nitrophenol. *p*-Nitrophenol (30 cm³, 10 mg/dm³) was passed through each polymer (0.30 g) that was packed in a cartridge as has been explained in **Chapter 3**. Triplicate measurements were performed and absorbances were recorded at room temperature. Results of these analyses are recorded in **Tables 4.6a, 4.6b and 4.6c**. Granular activated carbon and native polymers were used for comparison purposes.

Table 4.6a: Average *p*-nitrophenol removed by HMDI polymers

Sample	Amount of <i>p</i>-nitrophenol removed (%)
GAC	49
β CD-HMDI	62
1% f-MWNT (β -CD/HMDI)	99
2% f-MWNT (β -CD/HMDI)	95
3% f-MWNT (β -CD/HMDI)	96
4% f-MWNT (β -CD/HMDI)	98
5% f-MWNT (β -CD/HMDI)	97

Table 4.6b: Average *p*-nitrophenol absorbed by TDI polymers

Sample ID	Amount of <i>p</i>-nitrophenol removed (%)
GAC	49
B-CD/TDI polymer	72
1% f-MWNT (β -CD/TDI) polymer	80
2% f-MWNT (β -CD/TDI) polymer	97
3% f-MWNT (β -CD/TDI) polymer	82
4% f-MWNT (β -CD/TDI) polymer	90
5% f-MWNT (β -CD/TDI) polymer	97

A comparison of the absorption efficiencies for GAC and the native polymers with those incorporated with functionalized commercial MWNTs (**Table 4.6a and 4.6b**) showed that the incorporation of MWNTs to native polymers enhanced the absorption of *p*-nitrophenol. For example, 1% CNT (β -CD/HMDI) and 2% CNT (β -CD/TDI) polymers removed 99% and 97% of *p*-nitrophenol, respectively. These absorptions are far greater than those observed for native polymers, which were 62% and 72% for HMDI and TDI respectively. Further interrogation of the results show that polymers made from HMDI linkers had better absorption efficiency compared to TDI linked polymers. Variations in absorption of the TDI polymers could possibly be attributed to the texture. Nevertheless, it has been demonstrated that such polymers can absorb *p*-nitrophenol effectively especially in polymers where 2% and 5% MWNTs are incorporated as these composites now absorbed as high as 97% of the pollutant.

When taking into consideration the surface area and pore volume, and the amount of pollutant absorbed by these polymers (**Table 4.6c**), it can be observed that the absorption pattern was independent of the surface area and pore volume. Hence it was difficult to correlate the surface area and the absorption efficiency of the polymers. **Table 4.6c** shows a comparison of the surface area and the percentage of *p*-nitrophenol absorbed by the polymers.

Table 4.6c: Comparison of surface area and absorption efficiency of the polymers

MWNT Composition	β -CD/HMDI		β -CD/TDI	
	Surface area (m ² /g)	% <i>p</i> - Nitrophenol absorbed	Surface area (m ² /g)	% <i>p</i> - Nitrophenol absorbed
Native	2.52	62	1.70	72
1% f-MWNT	8.65	99	14.06	80
2% f-MWNT	6.82	95	17.36	97
3% f-MWNT	6.46	96	20.74	82
4% f-MWNT	2.40	98	9.95	90
5% f-MWNT	3.92	97	10.11	97

4.16 Comparison of absorption efficiencies of polymers prepared from commercial and NSP MWNTs

Absorption efficiencies of polymers made from commercial and NSP MWNTs were compared. This was done by passing *p*-nitrophenol (30 cm³, 10 mg/dm³) through 0.30 g of polymers containing commercial and synthesized nanotubes and measuring absorbances using the UV-Visible spectrophotometer according to the procedure discussed in the preceding sections. Results are shown in **Table 4.7**.

Table 4.7: Absorption efficiencies of polymers containing commercial and NSP MWNTs

Polymer composition	Incorporating Commercial MWNT	Incorporating NSP MWNT
	% <i>p</i> -Nitrophenol absorbed	% <i>p</i> -Nitrophenol absorbed
1 % f-MWNT (β -CD/HMDI) polymer	99	97
3% f-MWNT (β -CD/HMDI) polymer	96	94

Results in **Table 4.7** show that polymers made from synthesized nanotubes also had a good absorption efficiency of the *p*-nitrophenol and there was no significant difference in absorption from polymers incorporated with commercial MWNTs. It would seem like the original source and state of the nanotubes (being either graphitic or not) had no bearing in the absorption efficiency of the polymers incorporated with nanotubes.

4.17 Absorption tests of polymers incorporated with carbon nanofibers.

Carbon nanofibers (CNFs) are similar to carbon nanotubes but they are not carbon nanotubes. They are usually both hollow and are prepared by changing some conditions used in MWNTs synthesis.⁷⁴ However, the difference is that CNFs have one layer of graphite which is coated by a layer of amorphous carbon. After observing some important attributes of MWNTs especially in the removal of organic pollutants, it was decided to compare polymers incorporated with MWNTs and CNFs to see if the two polymers have similar absorption properties of the model organic pollutant. This would give us an indication of whether the actual structure of the nanotubes is most important factor in the absorption process. The nanofibers used in this study had diameters of 150 nm and were functionalized in a similar way to the

MWNTs used in the CD polymers previously mentioned. Polymers containing CNFs were synthesized and tested for their ability to remove *p*-nitrophenol from water just like the polymers containing CNTs. **Table 4.8** shows a comparison of absorption efficiencies for a 1% f-MWNT (β -CD/HMDI) polymer, a 1% f-CNFs (β -CD/HMDI) polymer and the native polymer.

Table 4.8: Comparison of absorption efficiencies between MWNT included polymers and CNFs included polymers

Polymer	% Absorption of <i>p</i> -nitrophenol
1% f-MWNT (β -CD/HMDI)	99
1% f-CNFs (β -CD/HMDI)	92
β -CD/HMDI	62

Results in **Table 4.8** show that polymers incorporated with MWNTs had a slightly higher absorption efficiency compared to those containing CNFs. It is also observed that incorporation of CNTs increased the absorption efficiency of the native β -CD/HMDI polymers by about 30%. It is difficult to correlate the high absorption efficiencies for the polymers containing MWNTs and CNFs and further research still needs to be done to elucidate this property.

4.18 Comparison of *p*-nitrophenol absorption with time.

Absorption tests to compare the amount of *p*-nitrophenol removed by different polymer compositions with time were performed by adding *p*-nitrophenol (30 cm³, 10 mg/dm³) to 0.30 g of polymer in a beaker. A residual concentration of *p*-nitrophenol in solution was monitored by UV-Visible spectroscopy at room temperature for a period of about two hundred hours. These tests were also

used to check the possibility of the pollutant leaching out when saturation was reached. **Figure 4.14** displays results from this study.

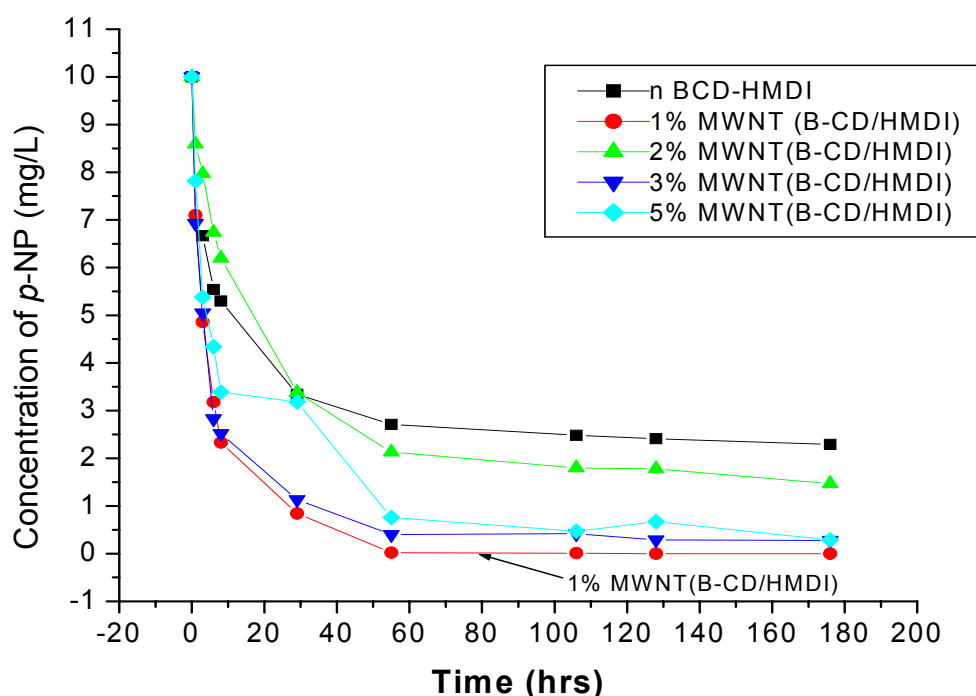


Figure 4.14: Removal of *p*-nitrophenol from water by HMDI polymers with time

Polymers with a one percent composition of MWNTs demonstrated the highest and fastest absorption capacity, with about eighty percent being absorbed within the first ten hours (**Figure 4.14**). The results also show that the rate of absorption appeared to decrease as the polymers became saturated with pollutant. Except for a 1% CNT (β -CD/HMDI) polymer, the other polymers were saturated or the organic pollutant was leaching out. This is demonstrated by the non-zero residual concentration, which remained almost constant after sixty hours. These results call for the call for the synthesis and testing of polymers with less than 1% CNTs incorporated (see chapter 5.2)

4.19 Gas Chromatography-Mass Spectrometry (GC-MS) analysis for trichloroethylene (TCE) absorption

Being an endocrine disrupting chemical and one of the priority organic pollutants found in many South African river water systems, TCE was used as a test pollutant. The GC-MS experiments were performed in spiked water samples whose TCE concentrations were 50 $\mu\text{g/L}$ and 10 mg/dm^3 . These concentrations were selected in order to determine the absorption efficiency of polymers at very low and medium concentrations. Residual TCE in water was extracted by liquid-liquid extraction with dichloromethane as has been described in **Section 3.16**. GC-MS conditions that were used in this study are also mentioned in **Section 3.18**. **Figures 4.15a-4.15c** show results of GC-MS analysis of a 50 $\mu\text{g/L}$ TCE passed through the native polymer and polymers containing MWNTs.

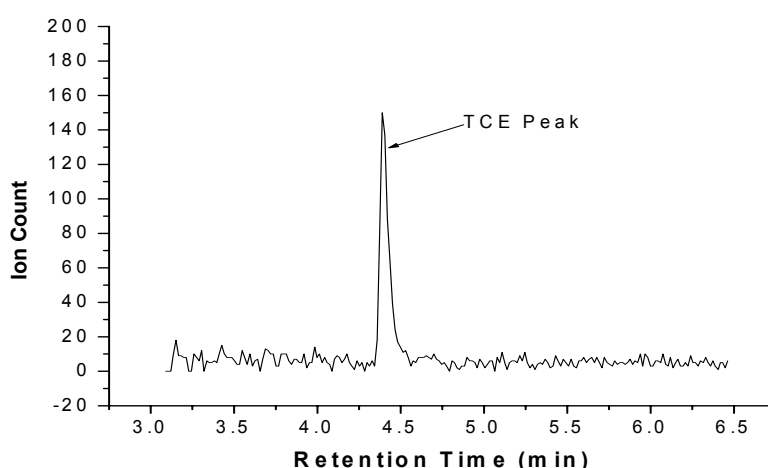


Figure 4.15a: GC-MS chromatogram of 50 $\mu\text{g/L}$ TCE before contact with polymer

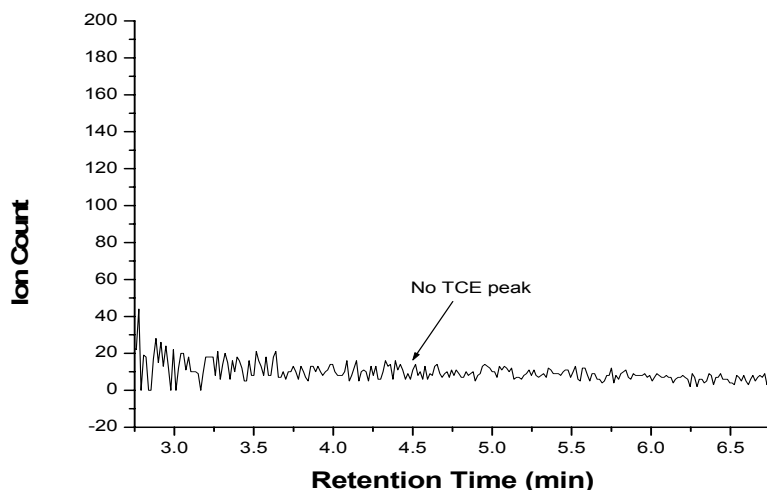


Figure 4.15b: GC-MS chromatogram of 50 µg/L TCE after passing through a 1% MWNT (β -CD/HMDI) polymer

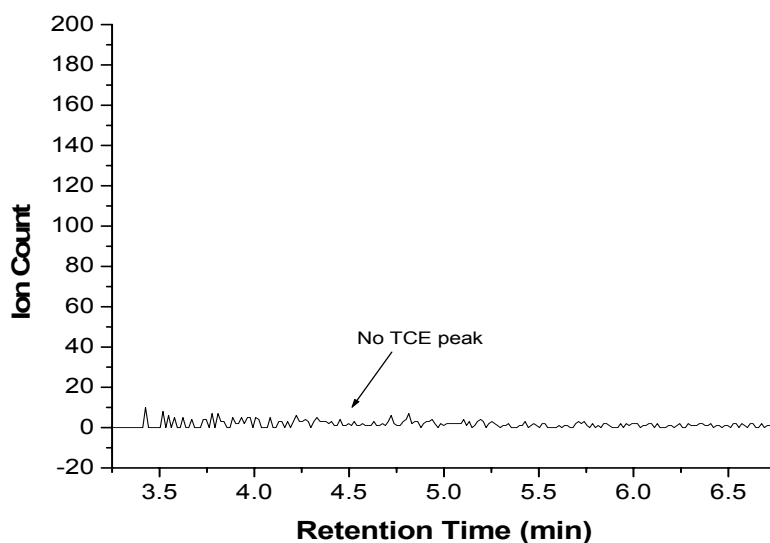


Figure 4.15c: GC-MS chromatogram of 50 µg/L TCE after passing through a 5% MWNT (β -CD/HMDI) polymer

Chromatograms **4.15b** and **4.15c** clearly show that polymers containing MWNTs were very effective in removing the TCE from the samples. In fact the absorption efficiency was almost 100%. This gives credence to the assertion

that CD based polymers generally perform better at very low levels of organic pollutant concentration.

Further tests were performed to ascertain if the polymers would be effective at a medium TCE concentration (10 mg/dm^3). Results of these analyses are displayed in **Figures 4.16a-4.16c**.

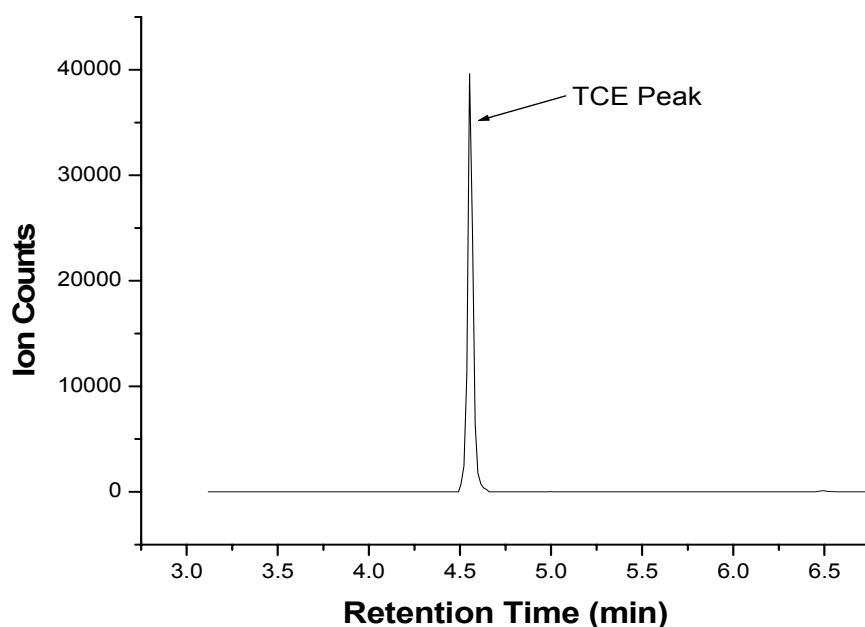


Figure 4.16a: GC-MS chromatogram of TCE before contact with the polymers

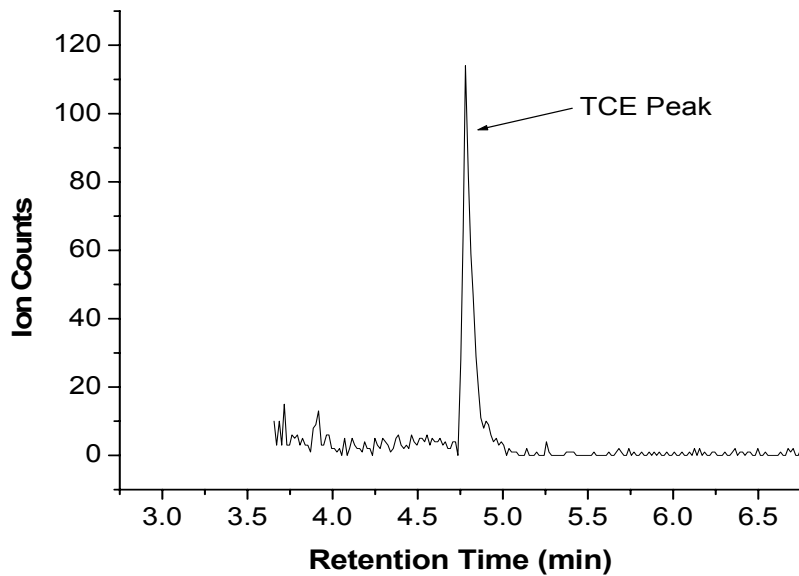


Figure 4.16b: GC-MS chromatogram of residual TCE after passing through β -CD polymer

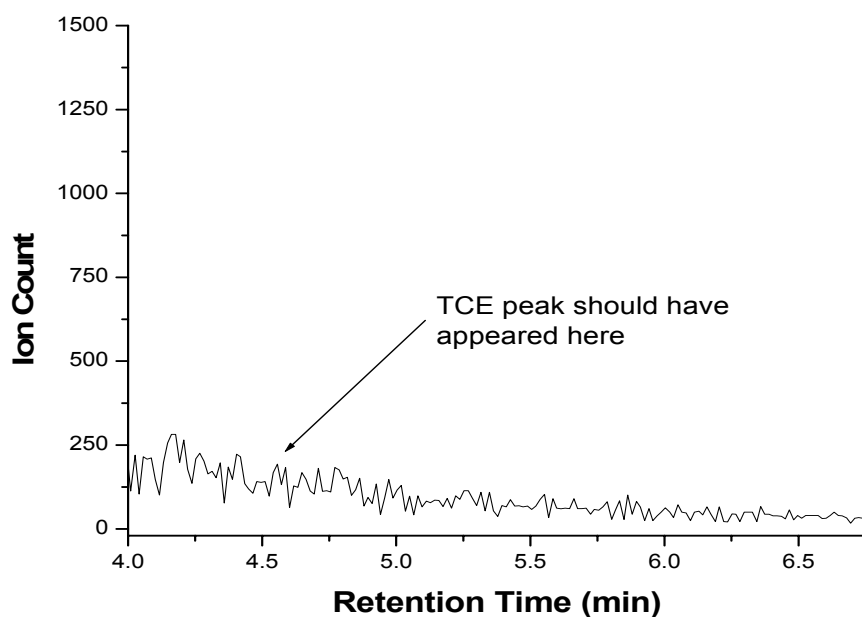


Figure 4.16c: GC-MS Chromatogram after passing through 5% MWNT (β -CD/HMDI) polymer

It is observed that the polymers containing nanotubes were better at removing TCE from spiked water samples. For example, polymers containing 5%

MWNTs (**Figure 4.16c**) removed almost all the TCE from water while the native polymers still had the residual TCE peak in the chromatogram. These results show that incorporation of MWNTs to the polymers enhanced the polymer's ability to remove TCE in water even at high pollutant concentrations.

4.20 Recycling tests of polymers

The ability of a polymer to be regenerated when saturation is reached is an important attribute. Such polymers are economical because the regeneration step is cheaper than the cost of replacing the polymer. Both 1% MWNT (β -CD/HMDI) and native β -CD/HMDI polymers were tested for their ability to be regenerated using a 10 mg/dm^3 *p*-nitrophenol as the test pollutant. Results of these analyses are shown in **Figures 4.17a** and **4.17b**.

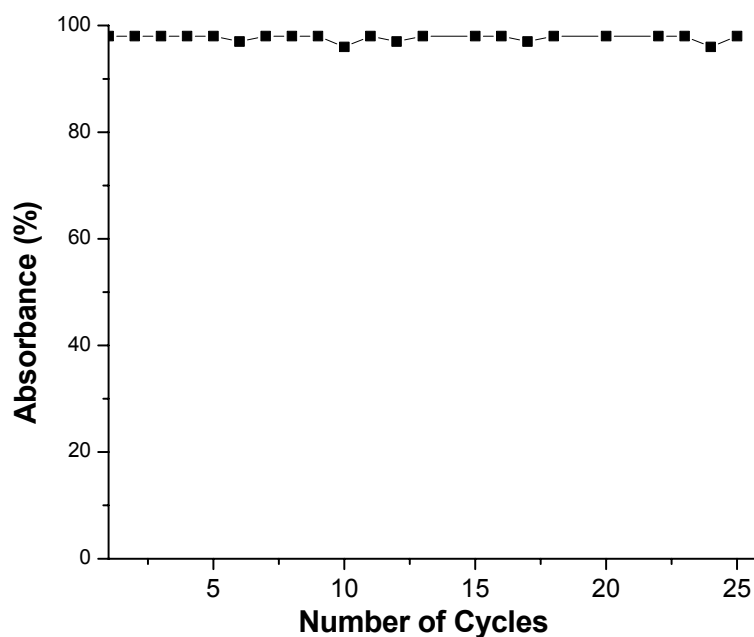


Figure 4.17a: Results of recycling of a 1% MWNT (β -CD/HMDI) polymer

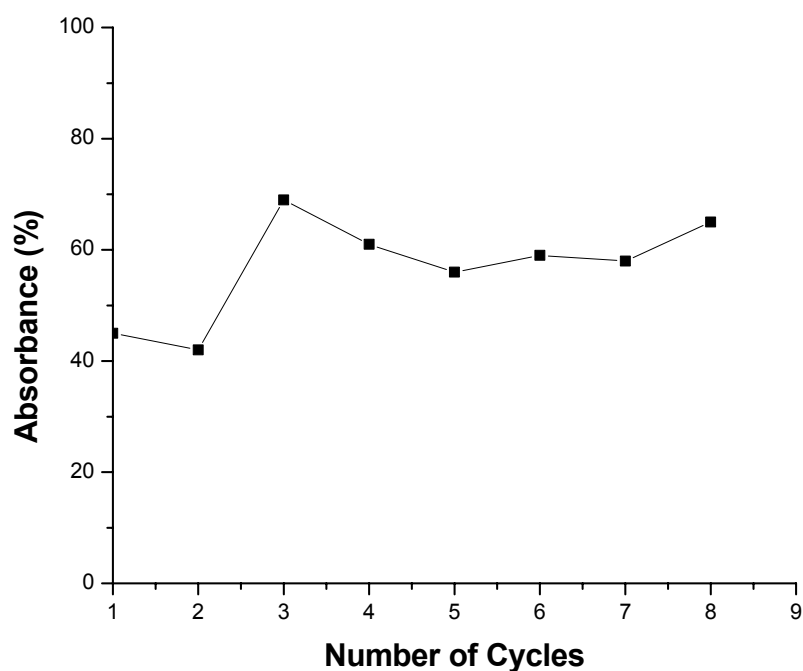


Figure 4.17b: Results of recycling using β -CD/HMDI polymer

It can be observed from **Figure 4.17a** that β -CD/HMDI polymers containing MWNTs had better absorption efficiency with an average absorption of greater than 98% over the twenty-five cycles. These polymers showed an outstanding performance when compared to the native β -CD/HMDI polymers whose average absorbance for the nine cycles was 56%. Comparison of SEM of the 1% MWNT (β -CD/HMDI) polymer before and after recycling (**Figures 4.18a** and **4.18b**) shows that the polymer maintained its spongy appearance and did not appear to have significantly lost its structural integrity.

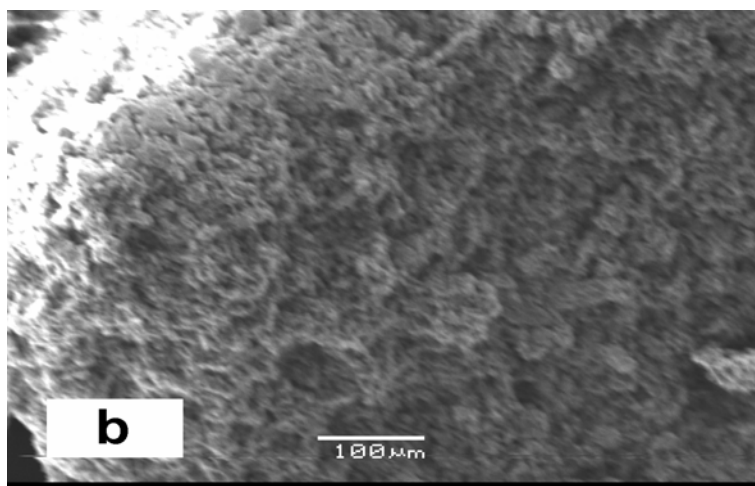


Figure 4.18a: SEM of 1% MWCNT (β -CD/HMDI) polymer before recycling

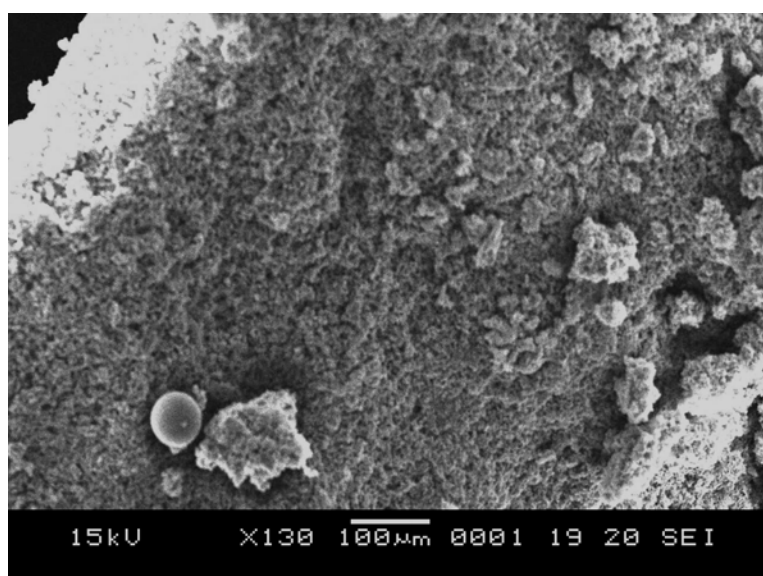


Figure 4.18b: SEM of 1% MWCNT (β -CD/HMDI) polymer after recycling

However, the 1% MWCNT (β -CD/HMDI) polymer lost only 5% of its mass after the nine cycles. IR spectroscopy of the recycled polymer (**Figure 4.19a**) shows that there was no change in absorption peaks when compared to IR spectrum of the pre-used polymer (**Figure 4.19b**) which further suggests that the chemical properties of the polymer were maintained.

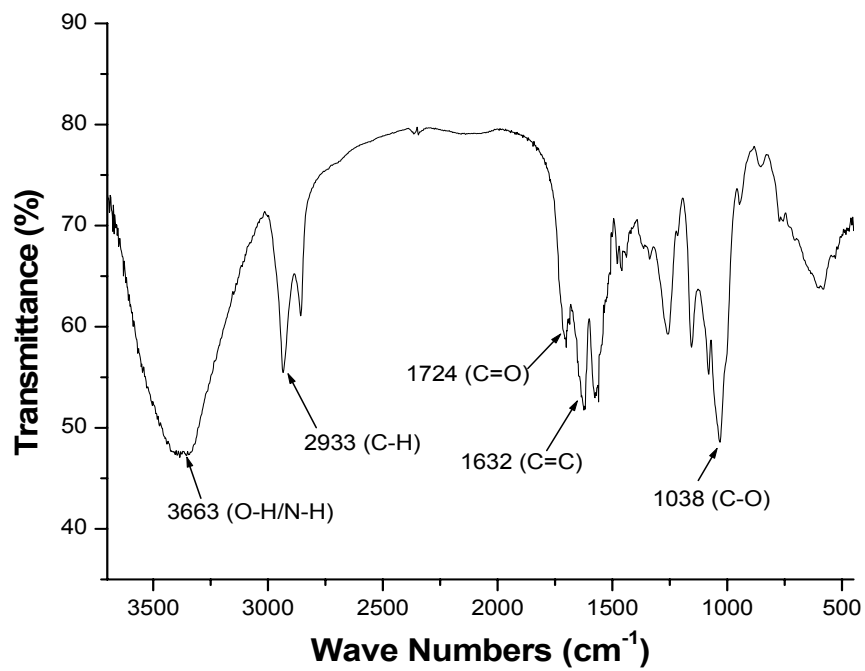


Figure 4.19a: IR spectrum of a 1% MWNT (β -CD/HMDI) polymer after recycling

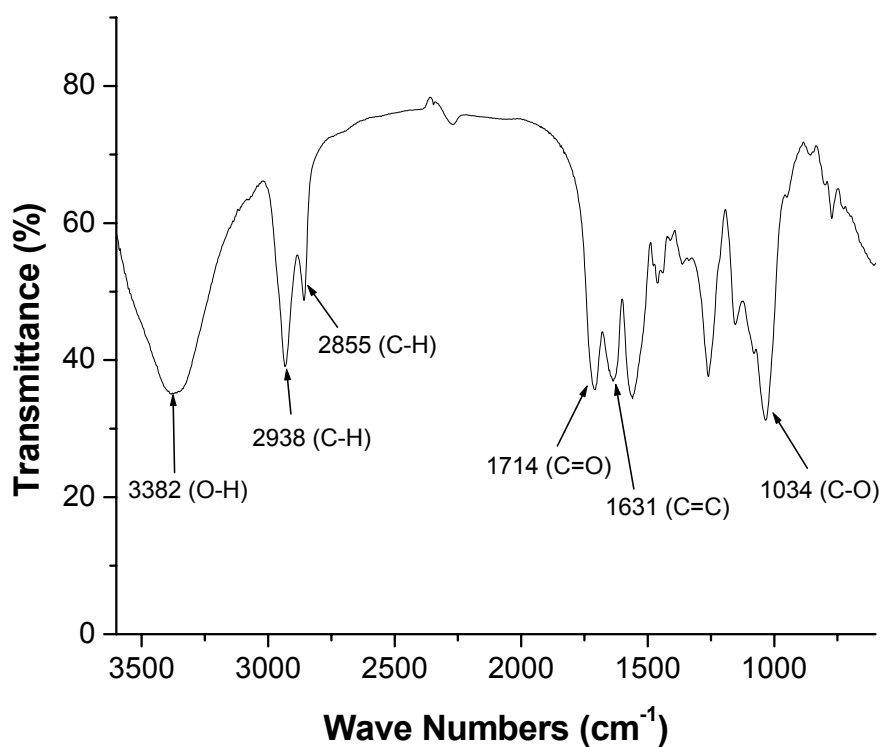


Figure 4.19b: IR spectrum of a 1% MWNT (β -CD/HMDI) polymer before recycling

The native β -CD/HMDI polymers (**Figure 4.17b**) showed some inconsistency in absorption when compared to the polymers that contained nanotubes (**Figure 4.17a**). The average absorption for these polymers was 56%, which is far lower when compared to 98% for the 1% MWNT (β -CD/HMDI) polymers. Furthermore, the native polymers lost 17% of the initial mass after only nine cycles. Comparing the 5% loss after nine cycles and the 17% loss after the nine cycles, it can be inferred that inclusion of carbon nanotubes to the native polymers increased the polymer stability.

CHAPTER FIVE

CONCLUSIONS AND RECOMMENDATIONS

5.1 Conclusions

The objectives of this investigation were to synthesize cyclodextrin polymers containing a small percentage of multiwalled carbon nanotubes (MWNTs), characterize them using IR spectroscopy, BET, TEM, SEM, DSC and TGA, and finally test these polymers for their ability to remove model organic compounds such as trichloroethylene (TCE) and *p*-nitrophenol in water. This study was successfully done and the following conclusions were drawn from this research project.

- ❖ Multiwalled carbon nanotubes with well aligned and very little amorphous carbon were synthesized using the nebulized spray pyrolysis (NSP) technique. In this technique, toluene or benzene were used as carbon sources while ferrocene was used both as a carbon source and a catalyst.
- ❖ NSP MWNTs, commercial MWNTs and carbon nanofibers were functionalised by acid treatment in order to introduce hydroxyl and carboxyl groups onto the walls of the nanotubes. Success of the functionalization was confirmed by IR spectroscopy, which confirmed the presence of the C=O, O-H and C-O functional groups after functionalization.
- ❖ Analysis of the functionalized and unfunctionalized MWNTs using Raman spectroscopy showed an increase in the relative size of the disorder peak, D, after functionalization. This type of disorder usually arises when there is a change on the MWNT structure, of which the introduction of the functional groups was the most likely reason.

These results therefore further confirm the attachment of the functional groups onto the nanotubes.

- ❖ Novel polymers containing cyclodextrins and functionalized MWNTs were successfully synthesized by polymerizing hexamethylene diisocyanates or toluene 2,4-diisocyanate with β -CD and functionalized MWNTs. These polymers were obtained in high yields.
- ❖ Characterization of the polymers by IR spectroscopy confirmed the presence of functional groups such as C=O, C=C, C-H and C-O. Furthermore, the disappearance of the isocyanate peak even when MWNTs were polymerized in the *absence* of cyclodextrins provided a clear indication that the carbon nanotubes indeed took part in the polymerization reaction.
- ❖ Characterization of the polymers using SEM revealed that the polymers had a spongy appearance. The sponginess however diminished as the percentage loading of the MWNTs was increased from 1 to 5%. It is not clear at this stage if this was a processing phenomenon or a function of the incorporated MWNTs. BET results, on the other hand, showed a general increase in surface area and pore volume with the addition of MWNTs. However, a relationship between the surface appearance and surface area of the polymers was not conclusive. It would be worthwhile to further investigate how surface area and porosity varies with increase in percent loading of MWNTs (**see 5.2 for future work**).
- ❖ Thermal gravimetric analysis of the polymers has demonstrated that the incorporation of the MWNTs to the native polymers increased their thermal stability slightly. This was confirmed by the lag in decomposition for the polymers containing MWNTs (1 and 5%) as compared to the native β -CD/HMDI polymers. A similar observation was also made when these polymers were analysed using DSC. The

native polymer showed an endothermic peak at about 327°C. This was contrary to the MWNTs incorporated polymers that showed an increase in heat flow associated with the curing of the polymers.

- ❖ One of the objectives of this research was to test these novel MWNT polymers for their ability to remove organic pollutants from water. Trichloroethylene and *p*-nitrophenol were used as model pollutants for these studies. Generally, β -CD/HMDI polymers are effective at removing organic pollutants at very low concentrations. This was also demonstrated when both the native β -CD/HMDI polymers and those incorporated with MWNTs removed almost 100% of the TCE (30 cm³, 50 μ g/L) when passed through the polymer. However, only polymers incorporated with carbon nanotubes were seen to be effective at removing TCE (close to 100% for a 5% MWNTs (β -CD/HMDI) polymers) when a moderately high concentration of TCE (30 cm³, 10 mg/dm³) was used. Similar results were also observed when *p*-nitrophenol (30 cm³, 10 mg/dm³) was passed through the polymers where polymers containing MWNTs removed about 99% compared to 62% by the native β -CD/HMDI polymers. These results show that incorporation of MWNTs enhanced the absorption efficiency of the selected organic pollutants especially at parts per million levels where the native polymers did not demonstrate a greater absorption capacity.
- ❖ The ability of these polymers to be regenerated a number of times when saturation point is reached has obvious economical advantages. The native β -CD/HMDI polymer and the 1% MWNT (β -CD/HMDI) polymer were tested for their ability to be regenerated. Results showed that polymers containing 1% MWNTs could be recycled at least twenty-five times while still maintaining a high absorption efficiency (98%). The average absorption efficiency for the native β -CD/HMDI polymer was only 56%. Comparison of the mass loss after nine recycles showed that the polymer containing MWNTs lost 5% while the native polymers lost 17% after nine cycles.

It can be concluded from these results that apart from improving absorption efficiency, incorporating the MWNTs also improves the stability of the native polymers.

5.2 Recommendations for further work

- ❖ While it has been demonstrated that with incorporation of only 1% MWNT to the native polymers promotes the absorption efficiency to as high as almost 100%, lower nanotube concentrations could probably produce a similar effect. This would be economical when large scale tests are to be carried out. It is therefore recommended that studies on absorption efficiency when much less MWNT, e.g. 0.1 to 0.5% are incorporated be carried out. Other physical properties of such polymers such as stability, strength, surface area and pore volume analysis can also be investigated.
- ❖ Effectiveness of these novel polymers have only been demonstrated on two model pollutants, TCE and *p*-nitrophenol. It would be necessary to test these polymers on a wider range of priority organic pollutants such as geosmin and 2-MIB.
- ❖ Absorption test experiments were only carried out at a laboratory scale. It would be necessary to investigate the performance of these polymers on a larger system with real water samples.
- ❖ Preliminary studies in our laboratory have demonstrated that zero valent nanoparticles such as iron and palladium could convert TCE to non toxic hydrocarbons. Efforts to incorporate these bimetallic particles into carbon nanotube cavities were not that successful because the particles were big.⁷⁵ It would be worth to produce nanoparticles of smaller diameters, incorporate these nanoparticles to the functionalized MWNTs and subsequently polymerize these MWNTs with cyclodextrins. This would

hopefully result in both the degradation of TCE into non toxic organic compounds while at the same time residual TCE would be absorbed within the cyclodextrin moiety.

APPENDICES

Appendix A

Preparation of trichloroethylene standards

$$100 \text{ mg/L} = 100 \text{ ppm}$$

$$100 \text{ mg} = 0.1 \text{ g}$$

$$\text{Density of TCE} = 1.46 \text{ g/cm}^3$$

$$\begin{aligned} \text{Therefore } \frac{0.1 \text{ g}}{1.46 \text{ g/cm}^3} &= 0.06848 \text{ cm}^3 \\ &= 68.5 \text{ } \mu\text{L} \end{aligned}$$

Therefore 68.5 μL in a 1000 cm^3 of dichloromethane made a TCE solution with a concentration of 100 mg/dm^3 .

For only a 100 cm^3 solution of 100 mg/dm^3 , 6.8 μL of TCE were transferred into a 100 cm^3 volumetric flask and then diluted to the mark with dichloromethane

Standards of lower concentration were prepared from the 100 mg/dm^3 TCE stock solution as per example below.

For a 20 mg/dm^3 TCE standard in a 100 cm^3 volumetric flask

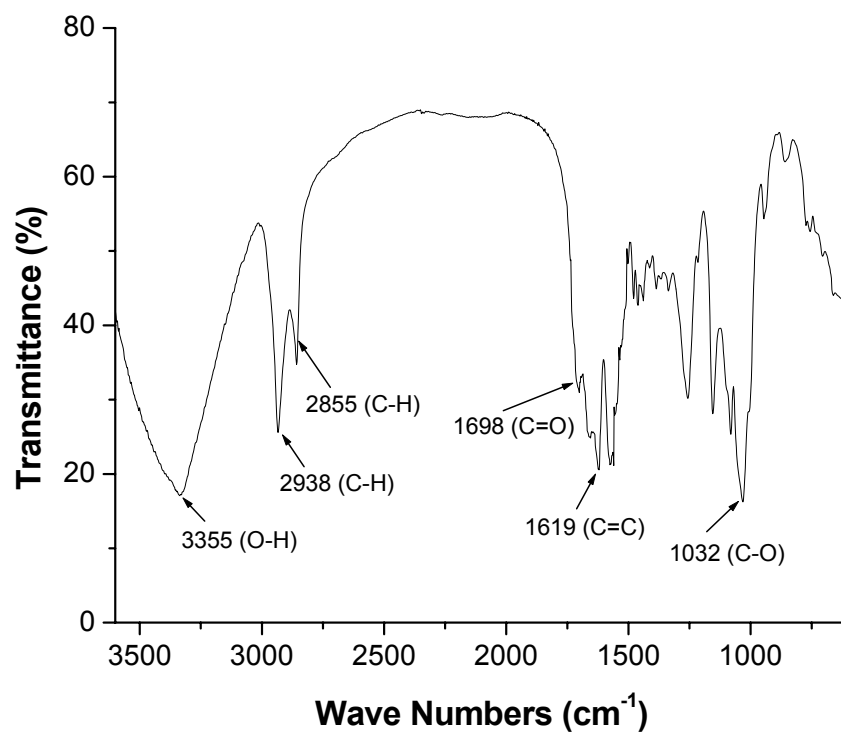
$$\begin{aligned} C_1 V_1 &= C_2 V_2, \quad 100 \text{ mg/dm}^3 \times V_1 = \frac{20 \text{ mg/L} \times 100 \text{ cm}^3}{100 \text{ mg/L}} \\ &= 20 \text{ cm}^3 \text{ of a } 100 \text{ mg/cm}^3 \text{ TCE diluted to} \\ &100 \text{ cm}^3 \text{ with DCM to make a } 20 \text{ mg/dm}^3 \\ &\text{TCE standard} \end{aligned}$$

Appendix B
List of selected priority organic pollutants as per European Union
Directive, 2006

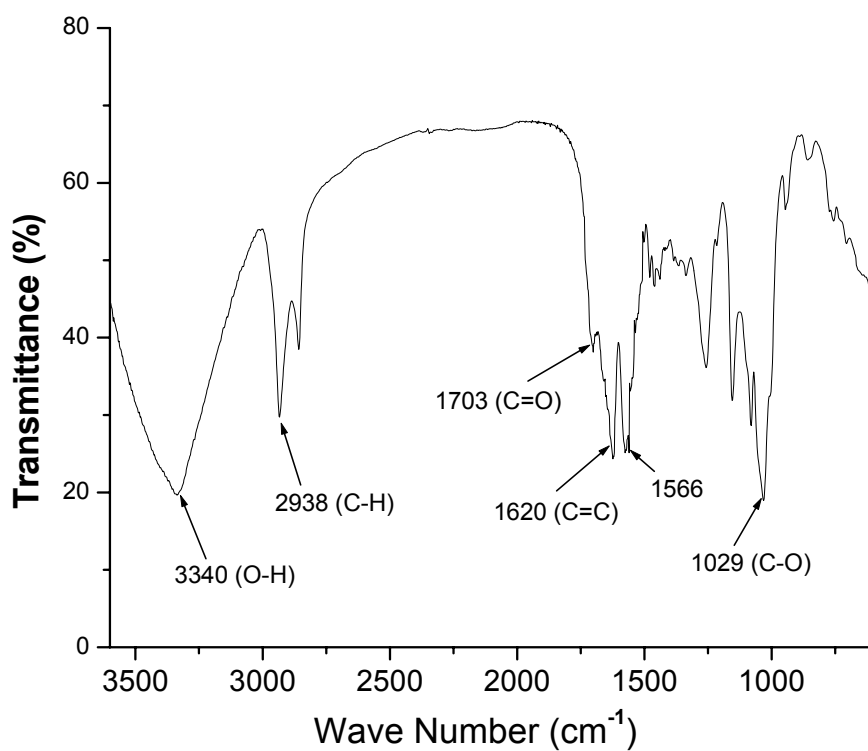
Dichloromethane
Anthracene
Benzene
Chloroalkanes
Endosulfane
Atrazine
Fluorathene
Hexachlorobenzene
Hexachlorobutadine
Benzo(a)pyrene
Polycyclic aromatic hydrocarbons
Pentachlorophenol
Naphthalene
Octylphenol
Benzo(b)fluorathene
Pentachlorobenzene
Trichloroethylene
Trichloromethane

Appendix C

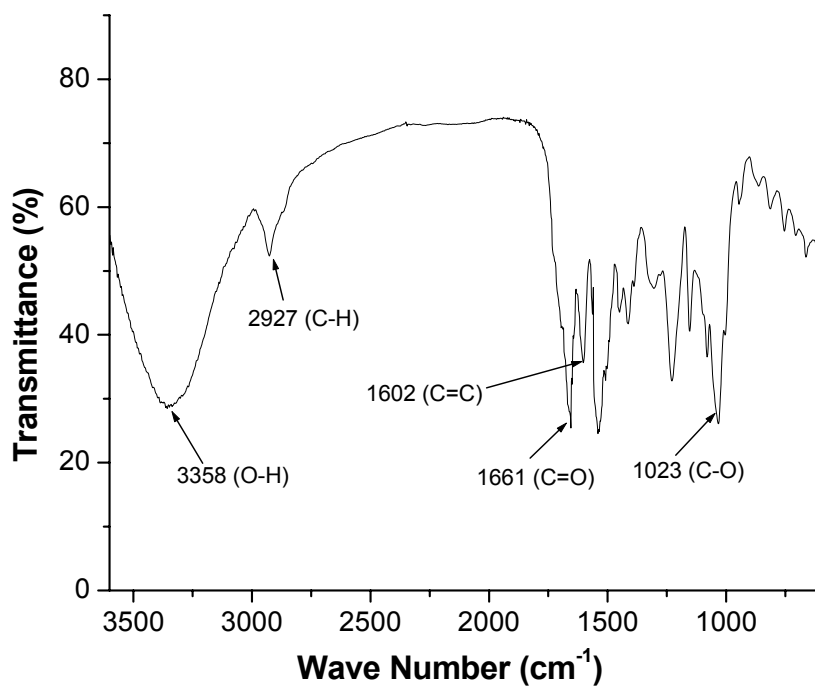
IR spectra of MWNT incorporated β -CD polymers



Appendix C1: IR spectrum of a 3% MWNT (β -CD/HMDI) polymer



Appendix C2: IR spectrum of a 5% MWNT (β -CD/HMDI) polymer



Appendix C3: IR spectrum of a 5% MWCNT (β -CD/TDI) polymer

References

- 1 Margiloff I. B. *Chem. Eng. Proceedings* **93** (1997) 10
- 2 Li D.Q., Ma M. *Chemtech* **35** (1999) 31
- 3 Mhlanga S. D., M Tech Dissertation (2005), University of Johannesburg.
- 4 Long R., Young R. *J. Am. Chem. Soc* **123** (2001) 2058
- 5 Ryan K. P., Cadek M., Nicolosi V., Walker S., Ruether M., Fonseca A., Nagy J. B., Blau W. J., Coleman J. N. *Synthetic Metals* **156** (2006) 332
- 6 Vasseur P., Cossu-Leguille C., *Chemosphere* **62** (2006) 1033
- 7 Paris F., Jeandel C., Servant N. *Environmental Research* **100** (2006) 39
- 8 Petkewich R. Cleaning up Dioxin with Nanotubes. Technology news, April 10, 2001, http://pubs.acs.org/subscribe/journals/esthag-w/2001/apr/tech/rp_cleandioxin.html (09/03/2005)
- 9 Morrison, D., Sunlight Converts Common Antibacterial Agent to Dioxin. <http://www.sciteclibrary.ru/eng/catalo/pages/5063.html> (03/09/2005)
- 10 Eljarrat E., Barcelo D. *Trac Trends in Analytical Chemistry* **22** (2003) 655
- 11 Walker C. H. (2001) Organic Pollutants, an Ecotoxicological Perspective. Taylor and Francis, New York, p 138-147
- 12 Paris F., Jeandel C., Servant N. *Environmental Research* **100** (2006) 39
- 13 Problems with toxics: EDCs. http://www.panda.org/about_wwf/what_do_we_do/toxic/problems/pops.cfm. (08/04/2005)
- 14 Richardson D.R.S. *Anal. Chem.* **76** (2004) 3337
- 15 Vidaeff A.C., Sever, L.E. *Reproductive toxicology* **20** (2005) 5
- 16 Directive of the European Parliament on and of the Council on Environmental Quality Standards in the Field of Water Policy and Amending Directives 2000/60/EC. <http://ec.europa.eu/environment/water/water> (30 /10/2006)

-
- 17 Burger A.E.B., Moolman A.P.M. *Water Practice and Technology* **1** (2006) 1
- 18 Macalady D. L., Ranville J. F. (1998). The Chemistry and Geochemistry of Natural Organic Matter (NOM). In: Macalady D. L. ed. *Perspectives in Environmental Chemistry*. Oxford University Press, New York, p 95-130
- 19 Connell D. W. (1997) Basic concepts of Environmental Chemistry. Lewis Publishers, New York, p 317-338
- 20 Aoustin A., Schafer A. I., Fane A. G., Waite T. D. *Separation and Filtration Technology* **22-23** (2001) 63
- 21 Gibbons J., Laha S. *Environmental Pollution* **106** (1999) 425
- 22 Connell D. W. (1997) Basic Concepts of Environmental Chemistry. Lewis Publishers, New York, p 205-216
- 23 Walker C. H. (2001) Organic Pollutants, an Ecotoxicological Perspective. Taylor and Francis, New York, p 165-176
- 24 Jacques R. J. S., Santos E. C., Bento, F.M., Peralba, M. C. R., Selbach P. A., Sa E. L. S., Camargo F. A. O. *International Biodeterioration and Biodegradation* **56** (2005) 143
- 25 Connell D. W. (1997). Basic Concepts of Environmental Chemistry. Lewis Publishers, New York, p 125
- 26 Schwarz M., Appel K. *Regulatory Toxicology and Pharmacology* **43** (2005) 19
- 27 Xie M., Zgang C. *Reproductive toxicology* **19** (2004) 79
- 28 Gale A. J. Water Shedss Organics.
<http://www.water.ncsu.edu/watershedss/info/organics.html>.
(11/03/2005)
- 29 Urynowicz M., Siegrist R. *Journal of Contaminant Hydrology* **80** (2005) 93
- 30 Bhattacharyya J., Read D., Amos S., Dooley S., Killham K., Paton G. I. *Environmental Pollution* **134** (2005) 485
- 31 Kamon M., Endo K., Kawabata J., Inui T., Katsumi T. *Journal of Hazardous Materials* **110** (2004) 1

-
- 32 Trichloroethylene. <http://www.atsdr.cdc.gov/toxicpro2.html>.
(04/07/2005)
- 33 Poh-Gek F., Lash L. H., Nandean V., Tardif R., Simons A. *Toxicology and Applied Pharmacology* **182** (2002) 244
- 34 Watson R. E., Jacobson C. F., Williams A. L., Howard W. B., DeSesso J. M. *Reproductive Toxicology* **21** (2006) 117
- 35 Barton H. A., Lipscomb F. J. C. *Toxicology* **111** (1996) 271
- 36 Jones E. Use of non invasive techniques to investigate partitioning tracer theory in NAPL contaminated porous media.
<http://www.cwr.uwa.edu.au/news/seminars>. (11/04/2005)
- 37 Iijima S. *Nature* **354** (1991) 56
- 38 Weldon D. N., Blau W. J., Zandbergen H. W. *Chemical Physics Letters* **241** (1995) 365
- 39 Kuzmany H., Kukovecz A., Simon F., Holzweber M., Kramberger C., Pichler T. *Synthetic Metals* **141** (2004) 113
- 40 Multidisciplinary Project Wondrous World of carbon nanotubes.
<http://students.chem.tue.nl/ifp03.synthesis.html>. (20/04/2006)
- 41 Peng X., Luan Z., Ding J., Di Z., Li Y., Tian B. *Materials Letters* **59** (2005) 399
- 42 Cui S., Scharff P., Siegmund S., Schneider D., Risch K., Klötzer S., Spiess L., Romanus H., Schawohl J. *Carbon* **42** (2004) 931.
- 43 Durbach S., Coville N.J., Witcomb M.J. *Fullerenes, Nanotubes and Carbon Nanotubes* **13** (2005) 155
- 44 Tapasztó L., Kertész K., Vertesy Z., Horváth Z. E., Koos A. A., Osvath Z., Sarkózi Zs., Darabont Al., Biro L. P. *Carbon* **43** (2005) 970
- 45 Vivekchad S. R. C., Cele L. M., Deepack F. L., Raju A. R., Govindaraj A. *Chem. Phys. Lett.* **386** (2004) 313
- 46 Dettlaff-Weglikowska U., Benoit J. M., Chiu P. W., Graupner R., Lebedkin S., Roth S. *Current Applied Physics* **2** (2002) 497
- 47 Strong K. L., Anderson D. P., Lafdi K., Kuhn J. N. *Carbon* **41** (2003) 1477
- 48 Konya Z., Vesselenyi I., Niesz K., Kukovecz A., Demortier A. *Chem. Phys. Lett.* **360** (2002) 429

-
- 49 Xu M., Zhang T., Gu B., Wu J., Chen Q. *Macromolecules* **39** (2006) 3540
- 50 Xiong J., Zheng Z., Qin X., Li M., Li H., Wang X. *Carbon* **44** (2006) 2701
- 51 Villiers A. *Comp. Rend. Acad. Sci* **112** (1891) 536
- 52 Croft A.P., Bartsch R. *Tetrahedron* **39** (1983) 1417
- 53 Girek T., Shin D. H., Lim S. T. *Carbohydrate Polymers* **42** (2000) 59
- 54 Easton C. J., Lincoln S. F. (1999) *Modified Cyclodextrins*. Imperial College Press, p 41-52
- 55 Khan A. R., Stine K., Forgo P., D'Souza V. T. *Chemical Reviews* **98** (1998) 1978
- 56 Szejtli J. *Chemistry Review* **98** (1998) 1743
- 57 Szejtli J. (1998) *Cyclodextrin Technology*. Kluwer Academic Publishers, p 79
- 58 Lenhert S. Transmission Electron Microscope. www.nanoworld.net.
- 59 Esumi K., Ishigami M., Nakajima A., Sawada K., Honda H. *Carbon* **34** (1996) 277
- 60 Steigerwalt E, S., Lukehart C. M. *J. nanosci.* **2** (2002) 25
- 61 Wade L. G. (2003). *Organic Chemistry*, 5th ed, Prentice Hall, New Jersey, p490-538
- 62 Kalsi P.S., (1993). *Spectroscopy of Organic Compounds*. Wiley Eastern Limited, New Dehli, p61-164
- 63 Raman spectroscopy, <http://en.wikipedia.org/wiki/Ramanspectroscopy>
- 64 Skoog D. A., Holler E. J., Nieman T. A. *Principles of Instrumental Analysis*, 5th Ed, Brooks/Cole. Australia, p 535-562
- 65 Thermal analysis of materials.
www.npl.co.uk/materials/cog/thermal.html
- 66 Willard H. H., Merritt L. L., Dean J. A., (1974). *Instrumental Methods of Analysis*, 5th ed. D. Van Nostrand Company, New York, p 496-521
- 67 Nxumalo E. N., M Tech Dissertation (2006), University of Johannesburg
- 68 Mc Master M., Mc Master C., (1998). *GC-MS, a practical users guide*. Wiley-VCH, p 4-21

-
- 69 Field L. D., Sternhell S., Kalman J.R., (1995). *Organic Structures from Spectra*, John Wiley and Sons, New York, p 6
- 70 Saito T., Matsushige K., Tanaka K. *Physica B* **323** (2002) 280-283
- 71 Kuzmany H., Kukovecz A., Simon F., Holzweber M., Kramberger C., Pichler T. *Synthetic Metals* **141** (2004) 113-122
- 72 Jorio A., Pimenta M. A., Souza Filho A. G., Saito R. Dresselhaus M. S., Dresselhaus G., Saito R. *New Journal of Physics* **5** (2003) 139.1
- 73 Dresselhaus M. S., Dresselhaus G., Saito R., Jorio A. *Physics Reports* **409** (2005) 47
- 74 Steigerwalt E, S., Lukehart C. M. *J. Nanosci.* **2** (2002) 25
- 75 Molepo K. G. B-Tech report (2006), University of Johannesburg.